Technical Report No. TRL-107

AN ANALYSIS OF THE TURBULENT BUOYANT JET

by

Clifford Bruce Baker

Turbulence Research Laboratory
Faculty of Engineering and Applied Sciences
State University of New York at Buffalo
Buffalo, New York 14214

A Thesis in Aerospace Engineering
Submitted in Partial Fulfillment to
The Pennsylvania State University
for the degree of
Doctor of Philosophy

May 1980

ACKNOWLEDGEMENTS

To Professor William K. George, Jr., teacher, thesis advisor, professional colleague, and friend, the author expresses sincere gratitude for the opportunity to carry out this work under his guidance and encouragement at the State University of New York at Buffalo. The author also wishes to express his appreciation to Professor Dale B. Taulbee of SUNY at Buffalo for his guidance and advice on numerical techniques and his assistance in the theoretical development of this thesis. In addition the author wishes to thank Professors Barnes W. McCormick and Thomas M. York, who coordinated many of the details of the author's graduate program, and extend a deeply felt thank you to Professor Joseph J. Eisenhuth who has served on the author's graduate committee since the inception of his graduate program.

This research was conducted at the State University of New York at Buffalo and the University of Pittsburgh at Johnstown and supported in part by the National Science Foundation, Atmospheric Sciences Division, Meteorology Program under grants ATM7601257 and ATM7808442 and AFOSR Grant F4962078C0047.

ABSTRACT

Existing theoretical work on axisymmetric turbulent buoyant jets is confined to integral techniques developed by Morton in the early 1950's. From these techniques only centerline velocities and temperatures can be calculated. Experimental data for this type of flow are essentially confined to centerline temperature measurements except for pure jet or pure plume data which constitute the extremes for a buoyant jet. The jet provides initial conditions, and the plume represents the asymptotic state for a buoyant jet flow.

This dissertation addresses the problem of developing a theoretical model for an axisymmetric turbulent buoyant jet. The governing equations for an axisymmetric turbulent buoyant vertical jet are transformed using jet similarity variables. In this transformation a length scale is introduced which controls the buoyancy term in the jet equations. In the limit as this length scale approaches zero, the buoyancy effects vanish and the jet equations are recovered. As this length scale approaches infinity, the plume equations are obtained. The perturbation expansion is developed for the near jet yielding a system of ordinary differential equations. Asymptotic equations are developed from which the plume solution is recovered. Analytical and numerical solutions are carried out using several eddy viscosity models. The solutions compare favorably with available experimental data on the buoyant jet centerline. The off-axis jet data appear to be in error because the mean velocity data fail to satisfy the momentum integral constraint.

TABLE OF CONTENTS

LIST OF TABLES

LIST OF FIGURES

LIST OF SYMBOLS

A, B, C - constants in jet and plume equations

B_1 - constant from fit of jet centerline velocity data

B_2 - constant from fit of jet temperature data

b - width parameter for entrainment function

E - entrainment function

$F(\xi)$ - designates ξ variable of velocity in asymptotic expansion

F_o - rate at which buoyancy is added at source

f - modified velocity function

G - value of integral constraint for density flux

$G(\xi)$ - designates ξ variable of temperature in asymptotic expansion

H_j - buoyant jet turbulent heat flux scale

H_p - plume turbulent heat flux scale

h_1 - radial turbulent heat flux function

h_2 - axial turbulent heat flux function

k - radial velocity function

L - buoyant plume "forced" length scale

ℓ - designates length dimension

M_o - rate at which momentum is added at source

m - exponent in temperature equation

P_T - turbulent Prandtl number

Q - fraction of total buoyancy carried by mean motion

Q_1 - fraction of total momentum carried by mean motion

R_j - buoyant jet turbulent energy scale

R_p - plume turbulent energy scale

R_T - turbulent Reynolds number

r - radial coordinate

S_j - buoyant jet Reynolds stress function

S_p - plume Reynolds stress function

T - mean temperature

T_j - buoyant jet temperature scale

T_p - plume temperature scale

ΔT - difference in flow mean temperature and ambient

t - temperature difference function

U - mean axial velocity

U_j - buoyant jet velocity scale

U_p - plume velocity scale

u - fluctuating vertical velocity

V - mean radial velocity

v - fluctuating radial velocity

W - mean velocity in azimuthal direction

w - fluctuating velocity in azimuthal direction

x - axial coordinate

α - constant

$\alpha(\eta)$ - dimensionless function defining eddy diffusivity

α_e - eddy diffusivity

β - coefficient of thermal expansion

γ - mean specific weight

ε - inverse dimensionless "forced" length scale

η - dimensionless radial coordinate

θ - fluctuating temperature

λ - inverse of Reynolds number

$\nu(\eta)$ - dimensionless function defining eddy viscosity

ν_e - eddy viscosity

ξ - buoyant jet dimensionless "forced" length scale

ρ - density or transformed dimensionless radial coordinate

σ - Prandtl number

τ - designates time dimension

ϕ - designates η variable of velocity in asymptotic expansion

ψ - Stokes stream function

Subscripts

$\mathfrak{L}$ - centerline

j - jet

p - plume

1,2, - designates power of ξ associated with expanded form of function

o - ambient or source

CHAPTER 1

INTRODUCTION

1.1 Flow Description

It is important that the reader distinguish the difference between the terms jet, buoyant jet, and plume.

> A jet is defined as a flow which is driven by the continuous addition of momentum at the source.
>
> A buoyant jet is defined as a flow which is driven by the continuous addition of both bouyancy and momentum at the source.
>
> A plume is defined as a flow which is driven by the continuous addition of buoyancy at the source.

Even if the rate at which momentum is added at the source is sufficiently large to dominate the effect of the buoyancy discharge so that the flow is jet-like, it will eventually evolve into a plume-like flow since the initial buoyancy (no matter how small) continuously produces additional momentum. The principal topic of this dissertation is the study of how a hot axisymmetric turbulent jet evolves into a turbulent plume in a neutrally stable and quiescent environment. Only the case where buoyancy adds to the momentum will be considered.

1.2 Background

At the turn of this century little consideration was given to the

fluid dynamics associated with the discharge of pollutants from municipal and industrial waste. In recent years laws have been enacted which define both the permissible level of pollutants generated by a given process and the permissible concentration of those pollutants in the vicinity of the source. These laws have provided an impetus for a more rapid development of an understanding of buoyant jets since such jets are representative of the techniques by which pollutants are discharged.

The study of turbulent buoyant jets is rather recent. The problem was first addressed by Morton (1) in 1959. This work was an extension of a preceding work by Morton, Taylor, and Turner (2) in which an integral technique was developed to describe buoyant turbulent plumes.

The history of turbulent buoyant plumes precedes that of the buoyant jet by only 20 years. The early plume work included Zel'dovich (3), Schmidt (4), Taylor (5), Rouse, Yih, and Humphreys (6), Batchelor (7) and the aforementioned work of Morton, et al. (2). The data of Rouse, et al. (6) remained the basis for theoretical evaluations until recently.

Studies of axisymmetric turbulent jets, on the other hand, were undertaken in the 1920's. For example, in 1926 Tollmien (8) developed a theoretical analysis for turbulent jet flow using Prandtl's mixing-length theory. Görtler (9) developed the eddy viscosity model for jet flow in 1942. (This analysis will be described in detail later.) Early measurements of the jet mean velocities and temperatures include work by Zimm (10), Ruden (11), Reichardt (12), Hinze and van der Hegge Zignen (13) and Corrsin and Uberoi (14).

From this brief overview it is apparent that theoretical and experimental knowledge of the plume and jet developed along separate

paths. In fact, only integral type solutions were discussed by Turner in his review of plumes in 1969. In the mid 1970's Yih (15), Hamilton and George (16) and Baker, Taulbee, and George (17) applied eddy viscosity techniques to the plume problem. This was after Chen and Rodi (18) and Tamanini (19) had begun to calculate bouyant plume flows using higher order models.

1.3 Experimental Investigation

1.3.1 The Jet

Hinze (20) provides an extensive review of the available data for an axisymmetric jet which will be only briefly summarized here. The velocity data are summarized in Figure 1 adapted from Wygnanski and Fiedler (21) which also includes two theoretical solutions to the jet equations which will be discussed later. The data are presented in terms of the jet similarity variables $\sqrt{M_o}$ and x where ρM_o is the rate at which momentum is added at the source and x is the distance from the source.

The data from all investigations are seen to be in good agreement if plotted in similarity variables. The empirical fit (discussed in detail later) is calculated from

$$U = B_1 \sqrt{M_o}\, x^{-1}[1+A\eta^2]^{-2} \qquad 1.3.1$$

where $B_1 \simeq 5.6$ and $A \simeq 62.5$ represent a reasonable fit for data in the core region. As discussed at the end of this section, the data beyond $\eta \simeq 0.05\text{-}0.1$ are subject to increasing measurement errors and are probably not reliable. In fact, the measured profile will be shown in Chapter 3 to be incorrect.

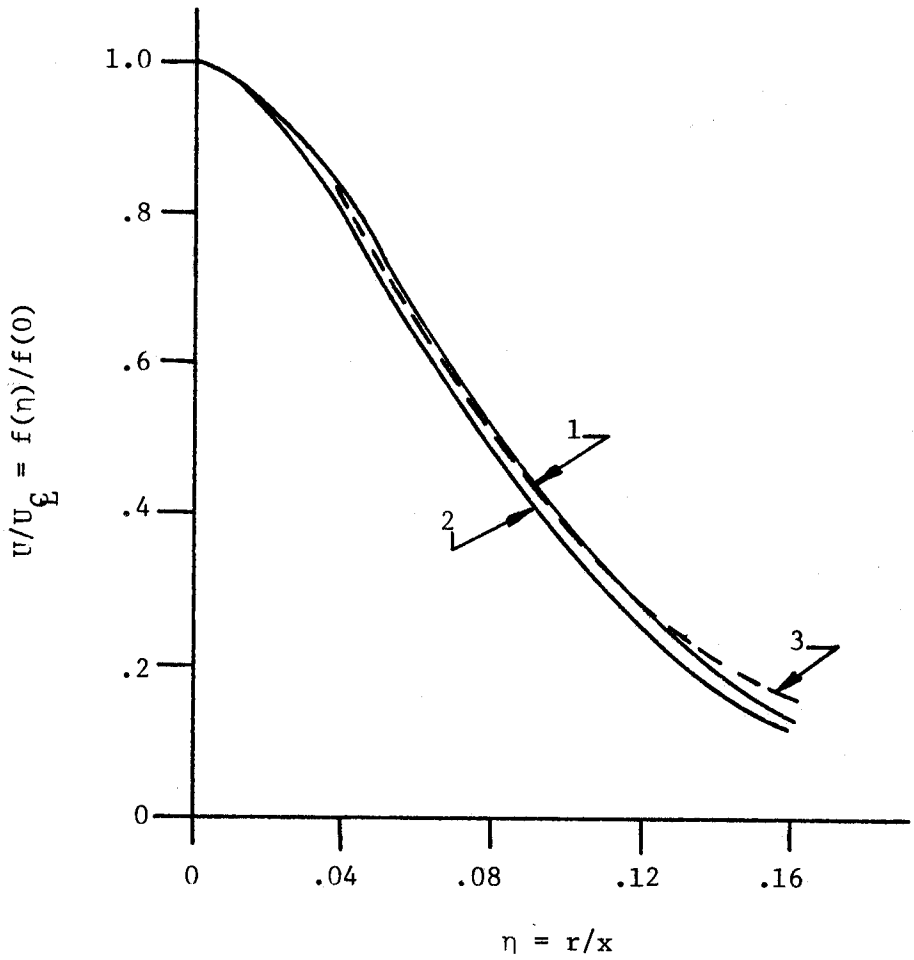

Figure 1. Comparison of jet mean velocity data with theory. 1 - Data fit Wygnanski and Fiedler (21). 2 - Data fit Hinze and van der Hegge Zignen (13). 3 - Theory equation 1.3.1.

The temperature data are summarized in Figure 2. The approximate similarity variable for temperature will be shown to be $F_o x^{-1}/\sqrt{M_o}$ where ρF_o is proportional to the rate at which heat is added at the source.[1] Like the velocity data, the data of different investigators is seen to be in good agreement if plotted in similarity variables. The empirical fit (discussed in detail later) is calculated from

$$g\beta\Delta T = B_2 F_o x^{-1}/\sqrt{M_o}\ [1+A\eta^2]^{-1.5} \qquad 1.3.2$$

where $B_2 = 6.0$ and $A = 62.5$ as before. From these data it is not difficult to see that the width of the temperature profile is greater than that of the velocity profile. (Width can be defined by any convenient measure, e.g., distance from centerline at which variable has dropped to half its centerline value.)

In summary, the extensive data on the turbulent jet appears to be of high quality, at least near the centerline. For reasons which will be addressed in the next section, however, the profiles should be viewed with suspicion for values of $\eta > 0.1$ because of the high local turbulence intensities in this region. In addition, it will be shown that neither the data nor the fit given by Equation 1.3.1 satisfy the momentum integral for this flow.

1.3.2 The Plume

The plume data of Rouse, et al. (6) show that the velocity and temperature profiles are self-preserving when scaled with the rate at

---

[1] $\rho F_o = g\frac{\beta H}{\rho C_p}$ where g is the gravitational acceleration and H is the rate at which heat is added at the source.

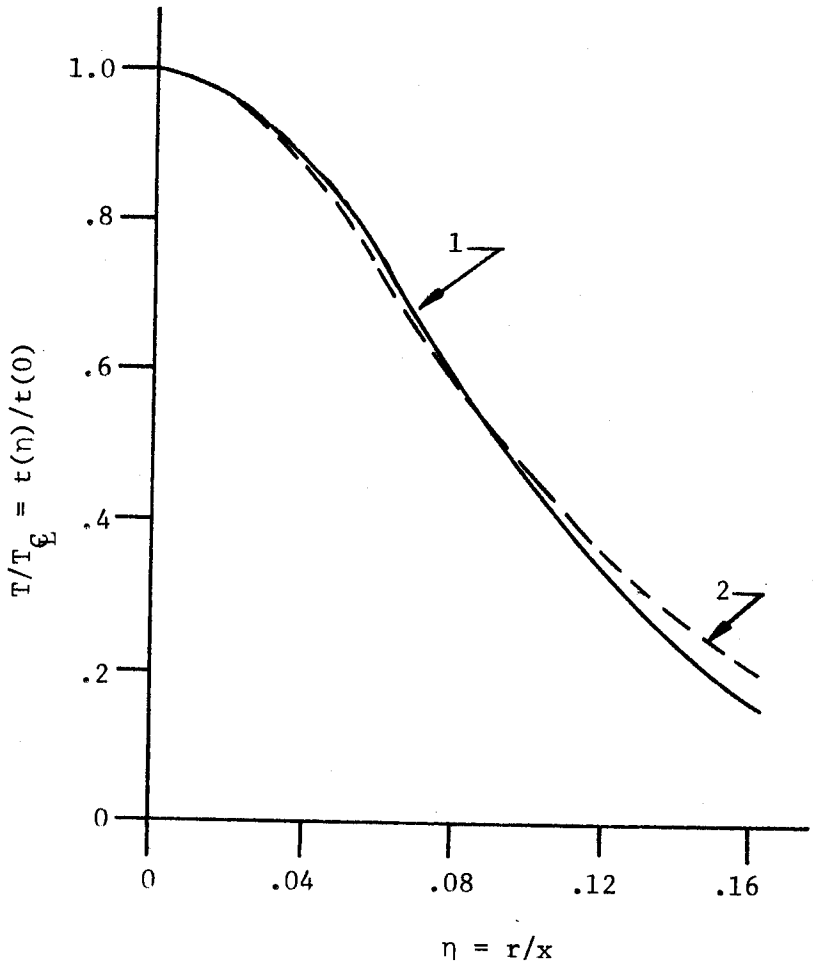

Figure 2. Comparison of jet mean temperature data with theory. 1 - Data fit Hinze and van der Hagge Zignen (13). 2 - Theory equation 1.3.2.

which buoyancy is added at the source and the streamwise distance from the source. For the axisymmetric case empirical fits to the data are given as

$$U = 4.7\ F_o^{1/3}\ x^{-1/3}\ \exp(-96r^2/x^2) \qquad 1.3.3$$

$$g\beta\Delta T = 11\ F_o^{2/3}\ x^{-5/3}\ \exp(-71r^2/x^2) \qquad 1.3.4$$

where

F_o = rate of buoyancy added at source

β = thermal expansion coefficient

r = radial direction

x = height above source.

The mean temperature profile is seen to be wider than the mean velocity profile, the opposite of the jet. These data were obtained using vane anemometers and thermocouples to measure mean velocities and temperatures.

Although the flow measurement techniques have advanced over the years, the data of Rouse, et al. remained the basis for theoretical evaluation until 1974. At that time, George, Alpert, and Tamanini (22, 23) published measurements made in an axisymmetric plume with a parallel hot wire probe. These data include mean velocity and temperature profiles, temperature and velocity fluctuation profiles, and the first measurements of the streamwise turbulent heat flux. The data confirm the self-preserving conclusions of Rouse, et al., but the basic profile shapes do not agree. The empirical data fits recommended by George, et al. are

$$U = 3.4\ F_o^{1/3}\ x^{-1/3}\ \exp(-55r^2/x^2) \qquad 1.3.5$$

$$g\beta\Delta T = 9.1\ F_o^{1/3}\ x^{-5/3}\ \exp(-65r^2/x^2) \qquad 1.3.6$$

The width of the temperature profile for these data is narrower than the velocity profile, this is opposite to the conclusion of Rouse, et al. These profiles of George, et al. are substantiated in a similar (and almost concurrent) experiment of Nakagome and Hirata (24).

The most extensive set of data available are the recent measurements of Beuther, Capp, and George (25) and Beuther (26). These measurements were obtained using a special three-wire probe having two velocity sensors in an X-array and one temperature sensor. Measurements are presented of mean velocity and temperature profiles, mean square velocity and temperature fluctuations, Reynolds stress, axial and radial turbulent heat flux, and mean and fluctuating momentum and energy balances for an axisymmetric turbulent plume.

Profiles of mean velocity and temperature were fitted by the semi-empirical equations

$$U = 3.4\ F_o^{1/3}\ x^{-1/3}[1 + 32r^2/x^2]^{-2} \qquad 1.3.7$$

$$g\beta\Delta T = 9.4\ F_o^{2/3}\ x^{-5/3}[1 + 32r^2/x^2]^{-3} \quad . \qquad 1.3.8$$

Beuther, et al. (25) found Yih's (15) solution, if used as an empirical equation provided a better fit for the velocity data than the Gaussian type fit used by previous investigators. Yih's solution and the Gaussian curves for the temperature are indistinguishable over the range of interest.

A summary of plume mean velocity and temperature data is shown in Figures 3 and 4. The discrepancy in the early data may be attributed to

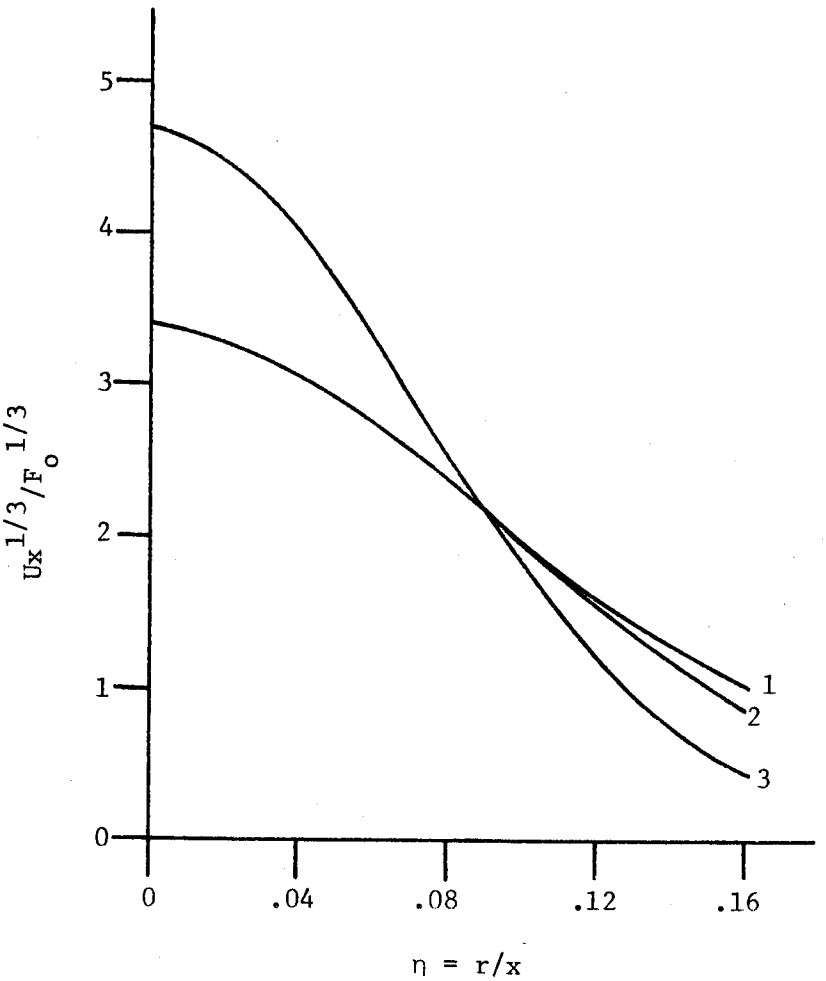

Figure 3. Comparison of plume velocity data. 1 - Data fit Beuther, et al. (25). 2 - Data fit George, et al. (22). 3 - Data fit Rouse, et al. (6).

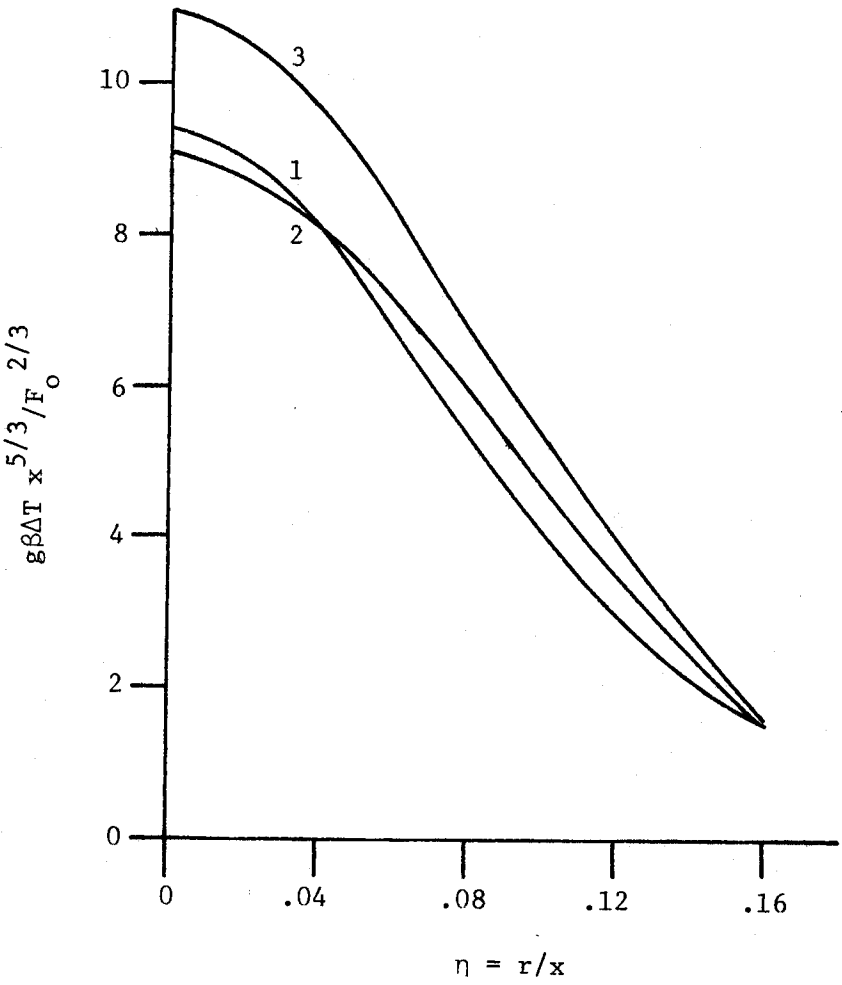

Figure 4. Comparison of plume temperature data. 1 - Data fit Beuther, et al. (25). 2 - Data fit George, et al. (22). 3 - Data fit Rouse, et al. (6).

the instrumentation. The uncertainty in the recent data is smaller but important. This scatter might reflect the difficulty in establishing a pure buoyant plume flow in a uniform ambient which Beuther (26) found to be a critical problem. The differences in the temperature profiles is primarily due to uncertainty in the determination of F_o from the data.

1.3.3 The Buoyant Jet

The data for axisymmetric bouyant jets are scarce, but measurements of centerline temperatures and mean temperature profiles have been reported. These include measurements by Abraham (27), Kotsovinos and List (28), Ryskiewich and Hafetz (29) and Pryputniewicz (30), which are included in Chapter 4, and discussed in Chapter 7. There are no velocity measurements for the buoyant jet region.

1.3.4 Data Reliability

Discrepancies in the recent hot wire measurements have given rise to critical questions concerning the current hot wire probe techniques used in sampling high intensity turbulent flows and in particular, most of the data cited above. Beuther, et al. (25) do not have confidence in the velocity measurements taken for a similarity coordinate value ($\eta=r/x$) greater than 0.10. According to Beuther, et al. (25):

> "The x-wire can only resolve velocities within an angle of 90° with respect to the probe axis, and the calibration functions used to relate the output voltage of the anemometers to a real value of velocity are accurate within an angle of 70°."

Consequently, if the flow direction is at an angle of less than 35° relative to the probe wire, it cannot be measured accurately. This problem is depicted in Figure 5. It is further stated that this problem occurs in approximately 10% of the data at the centerline. The data rapidly deteriorate as the distance from the centerline is increased. This problem cannot be alleviated with laser Doppler anemometer techniques because of the inherent reflective index limitations in heated flows as indicated by Buchhave, George, and Lumley (31). A moving probe technique is presently being developed by George and his co-workers to eliminate this problem, but these results will not be available for some time.

1.4 Theoretical Background

1.4.1 The Jet

The turbulent jet has been the subject of numerous theoretical investigations over the past 50 years. These are reviewed in the recent text of Hinze (20), and only those points relevant to this work will be included here.

The first theoretical treatment of the axisymmetric jet was presented by Tollmien (8) in which the jet flow field was modeled using Prandtl's mixing-length hypothesis. Tollmien was able to obtain an analytical solution which showed good agreement with the data near the outer edge but predicted too large a curvature near the centerline.

Görtler (9) presented an eddy viscosity model for the jet flow and the analytical solution for this model. While this solution is in good agreement near the centerline, the predicted values of velocity and temperature are too large for $\eta > 0.15$. Schlichting (32) extended

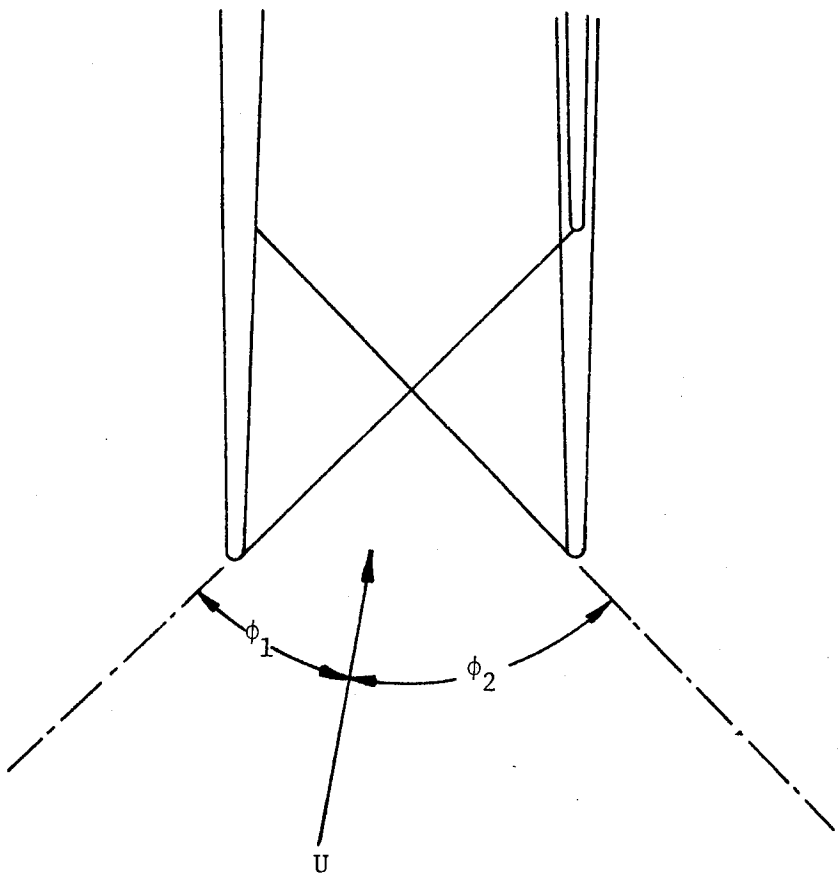

Figure 5. Schematic of two-wire probe in high intensity turbulent flow.

Görtler's solution to include the temperature field. Briefly, these solutions are successful in predicting the proper profile shapes near the axis but cannot satisfy the integral constraints imposed by momentum conservation and provide a reasonable data fit. This fact does not appear to be well-known and led to considerable confusion in the present investigation.

Recent theoretical work has concentrated on higher order turbulence modeling and large eddy simulation techniques. These techniques have encountered problems in modeling the jet using universal constants determined from viscometric experiments. There is reason to believe that the problem may be as much in the experiments as in the model. The large eddy simulation techniques are new and are in a state of development. Both the experiments and the model suffer from the inability to define the large eddy.

1.4.2 The Plume and Buoyant Jet

After the introduction of the similarity analysis developed independently by Zel'dovich (3), Batchelor (7) and Rouse, et al. (6), integral methods were the only techniques used to model buoyant jet and plume flows until the 1970's. The similarity solutions assumed the form

$$U = F_o^{1/3} x^{-1/3} f(r/x) \qquad 1.4.1$$

$$g\beta\Delta T = F_o^{2/3} x^{-5/3} t(r/x) \qquad 1.4.2$$

$$b = Ax \quad . \qquad 1.4.3$$

Morton, et al. (2) used these parameters in the integral forms of the mean flow equations to develop a model to describe plumes. The integral equations take the following forms:

$$\frac{d}{dx}(b^2U) = 2\alpha bU \qquad 1.4.4$$

$$\frac{d}{dx}(b^2U^2) = b^2 g \frac{\rho_o - \rho}{\rho_1} \qquad 1.4.5$$

$$\frac{d}{dx}(b^2 Ug \frac{\rho_o - \rho}{\rho_1}) = b^2 \frac{Ug}{\rho_i} \frac{d\rho_o}{dx} \quad . \qquad 1.4.6$$

Equation 1.4.4 results from the integration of the continuity equation and the so-called "entrainment hypothesis" -- in which it is assumed that the radial velocity V_∞ is proportional to the mean axial velocity U. This assumption results in the appearance of the entrainment coefficient α. Equations 1.4.5 and 1.4.6 are the results of the integration of the momentum and buoyancy (or temperature) equations. A solution of this system of equations requires that the entrainment coefficient be known.

Morton, et al. (2) applied this technique to plumes in neutral and stratified environments. Morton (1) extended this work to include forced plumes (or buoyant jets) by assuming that the entrainment coefficient was the same for both jets and plumes and thus constant throughout the entire flow field. This work remains the standard for most engineering analyses.

The assumption that the entrainment coefficient was constant from jet to plume was shown to be incorrect and inconsistent with experiments by List and Imberger (33). The experimenters developed a first approximation of how the entrainment coefficient α should vary as a buoyant jet

becomes a plume by using an empirical model for α which behaved properly in the limits. Kotsovinos (34) extended the development by List and Imberger (33) by introducing an improved fit for α.

The first departure from the integral techniques for modeling plume flows is due to Yih (15), who used an eddy viscosity model, and Madni and Pletcher (35), who used a mixing-length model. The work of Yih stimulated the work of Hamilton and George (16) and Baker, Taulbee, and George (36). In the present work similarity parameters are used to develop similarity equations for continuity, momentum, and temperature. The momentum and buoyancy integrals used in the integral modeling technique remain as integral constraints for the similarity solutions. An eddy viscosity closure scheme is used together with the similarity analysis to derive a set of similarity equations which can be solved to predict the mean velocity and temperature profiles for assumed values of the turbulent Prandtl number. The solution obtained by Yih is an analytical solution which is valid for Prandtl numbers of 1.1 and 2.0. In reference 36 and Chapter 2 numerical solutions are presented for a large range of Prandtl numbers.

Because of the problems in existing data, it is questionable if higher order modeling is justifiable at this time; however, some work has been published in which higher order models are used to compute the plume flow field parameters. Tamanini (19) and Chen and Rodi (18) present results calculated using algebraic stress modeling (ASM). This model can be used to predict a large number of flow parameters, but the results are questionable for large values of η. This could result from the fact that the model cannot account for the effect of large eddy structures on the turbulence and the resultant intermittency, or it could simply reflect the errors in the measurements.

1.5 The Eddy Viscosity Closure Approximation

Few concepts in turbulence theory are more widely used than the closure of the averaged equations of motion by an eddy viscosity. In the form originally proposed by Boussinesq in 1877 (37), a simple proportionality relationship between turbulent transport and mean gradient is assumed, the constant of proportionality being the eddy viscosity, or diffusivity if concentration or heat are being considered. The turbulent Reynolds stress is written

$$- \overline{uv} = \nu_e \frac{\partial U}{\partial r} \qquad 1.5.1$$

and the turbulent heat flux is written

$$- \overline{vt} = \alpha_e \frac{\partial T}{\partial r} \quad . \qquad 1.5.2$$

The similarity between the two relationships is often referred to as Reynolds' analogy.

The simple eddy viscosity models which utilize only the mean equations have had a variety of successes and failures in modeling turbulent flows. Tennekes and Lumley (38) argue that the eddy viscosity can be expected to be successful when the turbulent flow is characterized by single time and length scales. Thus the presence or absence of dynamically important multiple length or time scales can provide useful clues as to whether an eddy viscosity model might be successful.

Another way to rephrase the thesis of Tennekes and Lumley is to state that eddy viscosity models might be expected to work when the flow is in local scale equilibrium. It will be shown that simple jets and plumes represent such flows; thus an eddy viscosity formed from local

parameters, either assumed or calculated, should provide reasonable solutions.

There have been numerous attempts to model both the turbulent bouyant plume and forced jets involving varying amounts of bouyancy. These attempts have ranged from the integral entrainment velocity models of Morton (1), Morton, et al. (2) and the mixing-length model of Madni and Pletcher (35) to the algebraic stress models of Chen and Rodi (18) and Tamanini (19). It is not the purpose of this study to evaluate these attempts. One of the goals here is to explore in detail the application of the simple eddy viscosity to the plume and jet flows which completely satisfy the conditions for its application. Of particular interest will be the model's ability to accurately predict the profiles, its sensitivity to choice of constants, and the possible importance of the non-negligible vertical turbulent heat and momentum flux.

It will be shown that the bouyant jet, unlike the jet or the plume, has two length and time scales and hence does not absolutely satisfy the criterion for success of the eddy viscosity closure scheme. Since the effect of the second length scale is to continuously transform an initial forced jet into a buoyant plume, an attempt will be made to find an eddy viscosity which can be continuously modified to reflect this evolution. Such solutions would provide a first clue into the dynamics of these poorly understood mixed flows.

The eddy viscosity model to be used in this work can be used to predict only the Reynolds stress and the radial heat flux, but at this time a more complicated model cannot be justified. The experiments are complicated, and the differences between pure forced jets and pure

buoyancy driven plumes are often subtle and within experimental error. This simple model, however, can readily provide estimates of whether the flow region is a buoyant jet or has developed into a pure plume. Furthermore, hot air buoyant jets and plumes are very difficult to isolate from room drafts which cause meandering. While these effects can be minimized by shrouding the experimental configuration in fine mesh screen and isolating the entire facility with solid walls, the walls must be located far enough from the screen to allow sufficient entrainment to sustain the flow field. This model can be used to calculate bounds on the entrainment air required. Because of the model's simplicity it also provides a useful tool for estimating experimental design parameters and for evaluating results.

1.6 Outline of Dissertation

The techniques used in this dissertation have been available for a number of years. These include the eddy viscosity hypothesis, similarity scaling, perturbation and asymptotic expansion techniques. These simply have not been applied to this problem. This work is concerned with the following:

1. Eddy viscosity solutions are presented for an axisymmetric turbulent buoyant plume in a natural environment. These solutions are obtained using numerical techniques and provide complementary results to the analytical results obtained by Yih (15). Yih's solution is valid for Prandtl numbers of 1.1 and 2.0. The numerical solution is more general and provides results for all Prandtl numbers.
2. The eddy viscosity solutions developed by Schlichting (32) for

the buoyant jet are rederived in a more general framework which allows for the transport of momentum by the turbulence fluctuations. These modified solutions are used to provide a critique of the jet experimental data.

3. A set of dimensionless mean flow equations for the buoyant jet are established from first principles in which the jet and plume are recovered in the limits as the buoyancy parameter becomes small and large respectively. This is accomplished by recognizing that the flow field has a "forced length scale" ($L = M^{3/4}/F_o^{1/2}$) which can be combined with the axial coordinate (x) to form a dimensionless length $\xi = x/L$. The dimensionless length ξ controls the bouyancy term in the mean flow momentum equation. Consequently, this parameter dictates the evolution from a jet to a plume. The dimensionless mean flow equations involve two-dimensionless coordinates $\xi = x/L$ and $\eta = r/x$ and represent a universally valid set of equations for arbitrary buoyancy.

4. Perturbation expansions are developed for the two-length scale model of the mean flow equations for the near-jet using an eddy viscosity model. The lowest order solution (pure jet) is developed in detail, and analytical and numerous solutions are developed for higher terms in the expansion for a range of turbulent Prandtl numbers.

5. Plume solutions are shown to be the asymptotic solutions to the buoyant jet equations for large values at ξ.

6. The theoretical developments are used to present a unified theory for the bouyant jet. Results are compared with existing

experimental data and previous theoretical work. Finally, the dependence of the entrainment coefficient in the integral models on $\xi = x/L$ is evaluated.

CHAPTER 2

THE TURBULENT BUOYANT PLUME

2.1 The Equations of Motion

The simple turbulent buoyant plume is shown schematically in Figure 6. A vertical column of fluid is driven by a source of buoyancy at the base and spreads by turbulent entrainment. The plume is assumed to be turbulent and fully developed, stationary in the mean, and to have a sufficiently high turbulent Reynolds number that viscous terms can be neglected in the equations for the mean flow. Making the usual Boussinesq approximations (c.f., Tennekes and Lumley (38)), the mean equations of motion for an axisymmetric flow become[1]

$$U \frac{\partial U}{\partial x} + V \frac{\partial U}{\partial r} = \frac{1}{r} \frac{\partial}{\partial r} (-r\overline{uv}) + g\beta\Delta T$$

$$U \frac{\partial T}{\partial x} + V \frac{\partial T}{\partial r} = \frac{1}{r} \frac{\partial}{\partial r} (-r\overline{v\theta}) + \{\frac{\partial}{\partial x} (-\overline{u\theta})\} \qquad 2.1.1$$

$$\frac{\partial U}{\partial x} + \frac{1}{r} \frac{\partial (Vr)}{\partial r} = 0$$

where ΔT is the difference between the local temperature and the temperature at infinity and β represents the thermal expansion coefficient. Lower case letters have been used to represent the fluctuation velocities and the fluctuating temperature. The mean

---

[1] Complete details on the development of the plume equations are contained in Appendix A.

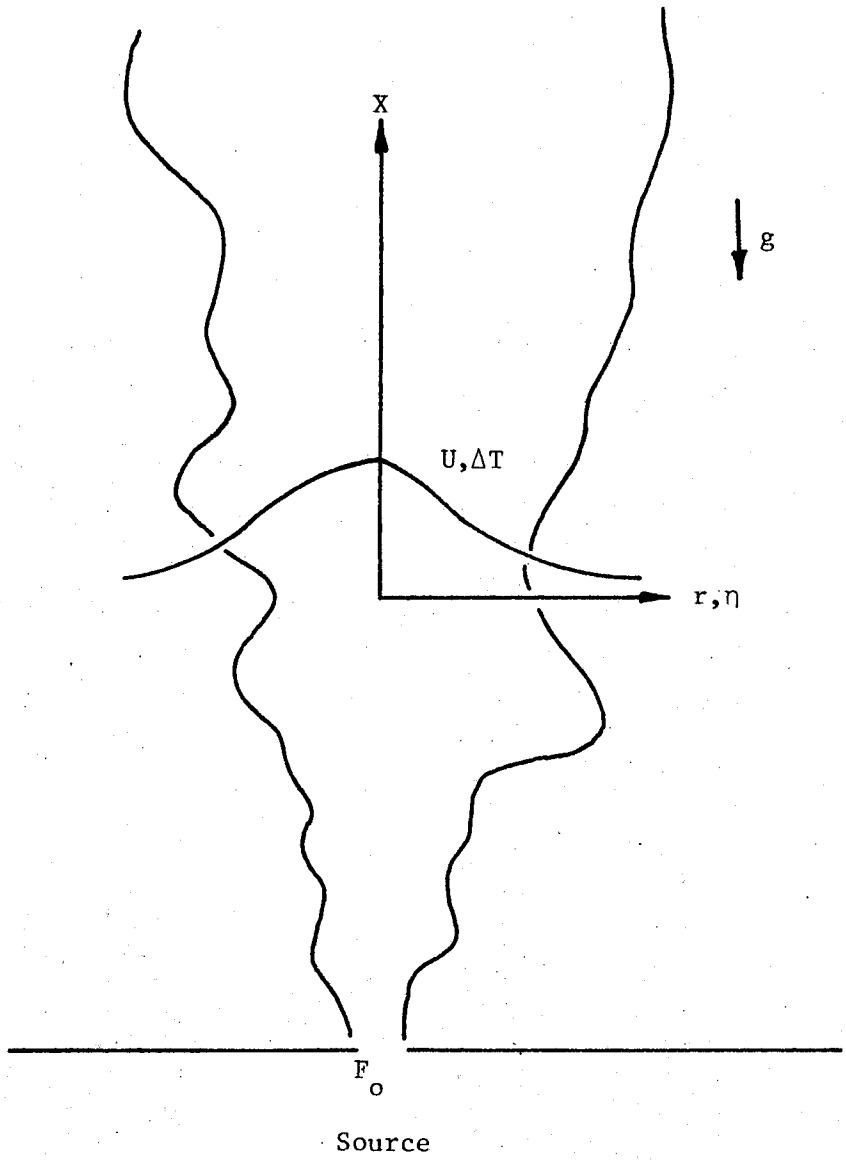

Figure 6. Schematic of plume and coordinates.

pressure gradient term has been eliminated using the r-momentum equation, and the streamwise gradient of the turbulent normal stress gradient has been neglected. The streamwise gradient of the turbulent heat (temperature) flux which is usually neglected has been retained.

For later use the temperature equation is integrated across the flow to obtain

$$2\pi \int_o^\infty g\beta[\Delta TU+\overline{u\theta}]rdr = F_o \qquad 2.1.2$$

where ρF_o can be identified as the rate at which weight deficiency or buoyancy is added to the source. For the neutrally stable environment assumed here, ρF_o is also the rate at which buoyancy crosses any horizontal plane.

It is appropriate to note at this time that the turbulent contribution to the integral above may <u>not</u> be negligible. For the axisymmetric case, the contribution of the turbulence has been estimated as high as 15% by George, Alpert, and Tamanini (23). This question and its significance will be discussed later.

Assuming that the ambient fluid is of uniform density (or neutrally stable), the flow is entirely characterized by the rate at which bouyancy is added at the source and the distance from the source. A set of similarity solutions are sought of the form

$$\eta = r/x \qquad \overline{uv} = R_p s\ (\eta)$$

$$U = U_p f\ (\eta) \qquad g\beta\overline{vt} = H_p h_1(\eta)$$

$$V = U_p k\ (\eta) \qquad g\beta\overline{ut} = H_p h_2(\eta)$$

$$g\beta\Delta T = T_p t\ (\eta) \qquad 2.1.3$$

Substituting into the equations of motion, demanding that the coefficients of terms in the equations be independent of x, and applying the integral condition for a neutral environment that F_o be independent of x, yield the following functional relationships (Zel'dovich (3), Batchelor (7), and Rouse, Yih, and Humphreys (6)):

$$U_p = F_o^{1/3} x^{-1/3}$$

$$T_p = F_o^{2/3} x^{-5/3}$$

$$R_p = F_o^{2/3} x^{-2/3}$$

$$H_p = F_o x^{-2} \quad . \qquad 2.1.4$$

Using these, the equations of motion reduce to

$$-\frac{1}{3} f^2 - \eta ff' + kf' = -\frac{1}{\eta}\frac{d}{d\eta}(\eta s) + t$$

$$-\frac{5}{3} ft - \eta ft' + kt' = -\frac{1}{\eta}\frac{d}{d\eta}(\eta h_1) - \{2h_2 + \eta h_2'\}$$

$$-\frac{1}{3} f - \eta f' + k' + \frac{k}{\eta} = 0 \quad . \qquad 2.1.5$$

The dependence of the set of equations above on k (the cross-stream velocity component) can easily be removed by integrating the continuity equation and substituting for k in the momentum and temperature equations. The results are

$$-\frac{1}{3} f^2 - \frac{5}{3}\frac{f'}{\eta}\int_o^\eta f\eta d\eta = -\frac{1}{\eta}\frac{d}{d\eta}(\eta s) + t \qquad 2.1.6$$

$$-\frac{5}{3} ft - \frac{5}{3}\frac{t'}{\eta}\int_o^\eta f\eta d\eta = \frac{1}{\eta}\frac{d}{d\eta}(\eta h_1) - \{2h_2 + \eta h_2'\} \quad . \qquad 2.1.7$$

2.2 The Eddy Viscosity Model for the Plume

It is clear that these equations (and therefore the flow) are completely characterized by single length and time scales since all lengths are proportional to x, and all time scales to x/U_s. From the previous discussion, it is expected that an eddy viscosity model will be successful in predicting the evolution of this flow.

On dimensional grounds

$$\nu_e = U_p x\ \nu(\eta)$$

$$\alpha_e = U_p x\ \alpha(\eta) \quad . \qquad 2.2.1$$

There is no reason to expect that the eddy viscosity should be the same for both the axial and cross-stream heat flux or momentum flux. For reasons which shall be presented later in the discussion, it is not necessary to include the axial gradients of the turbulent heat flux in the calculation even though the turbulent fluctuations may contribute a significant fraction of the total heat flux. Therefore the bracketed term of equation 2.1.7, which represents the turbulence contribution to the vertical heat transport, will be ignored. This contribution will be accounted for in the integrated energy balance or the bouyancy integral.

The flow being modeled is a free shear flow. Townsend (39) has indicated that flows of this type may be assumed to be well-mixed, since the dynamics will be dominated by a single large eddy structure. Therefore, an eddy viscosity and eddy diffusivity which are independent of radial position are assumed to be of the form

$$\nu(\eta) = \text{constant}\ \frac{1}{R_T}$$

$$\alpha(\eta) = \text{constant}\ \frac{1}{P_T R_T} \qquad 2.2.2$$

where R_T and P_T will be referred to as the turbulent Reynolds' and Prandtl numbers, respectively. Thus

$$\nu_e = \frac{1}{R_T} F_o^{1/3} x^{2/3}$$

$$\alpha_e = \frac{1}{P_T R_T} F_o^{1/3} x^{2/3} \quad . \qquad 2.2.3$$

Substitution into the equations of motion yields

$$-\frac{1}{3} f^2 - \frac{5}{3}\frac{f'}{\eta}\int_o^\eta f\eta d\eta = \frac{1}{R_T} \cdot \frac{1}{\eta}\frac{d}{d\eta}(\eta f') + t \qquad 2.2.4$$

$$-\frac{5}{3} ft - \frac{5}{3}\frac{t'}{\eta}\int_o^\eta f\eta d\eta = \frac{1}{P_T R_T} \cdot \frac{1}{\eta}\frac{d}{d\eta}(\eta t) \quad . \qquad 2.2.5$$

These are ordinary differential equations for the two fuctions f and t that can be solved directly if R_T, P_T and the boundary conditions are specified.

The appropriate boundary conditions are

$$f'(0) = 0, \qquad f(\infty) = f'(\infty) = 0$$
$$t'(0) = 0, \qquad t(\infty) = t'(\infty) = 0 \quad . \qquad 2.2.6$$

These simply state that the flow is symmetric about the axis and vanishes at infinity.

The solutions to these equations must satisfy some form of the integral constraint of equation 2.1.2. Denoting the fraction of the bouyancy which is carried by the mean flow as Q, the appropriate constraint in dimensionless form is

$$2\pi \int_o^\infty f \cdot t \cdot \eta d\eta = Q \quad . \qquad 2.2.7$$

The factor Q can take any value between zero and unity, the latter corresponding to a negligible turbulent contribution to the vertical heat transport. Note that this is the only place where the (unknown) turbulent contribution to the bouyancy integral enters the problem, and the magnitude of this contribution in this formulation must be specified.

2.3 The Dependence on the Parameters R_T, P_T, and Q

The dependence of these equations on the coupled parameters can be illustrated by first carrying out the following transformation on equations 2.2.4 and 2.2.5

$$\rho = \sqrt{R_T}\,\eta$$

$$f(\eta) \to f(\rho), \quad t(\eta) \to t(\rho), \quad k(\eta) \to R_T^{-1/2}\, k(\rho) \quad . \qquad 2.3.1$$

The governing equations can easily be shown to reduce to

$$\frac{1}{2} f^2(\rho) - \frac{5}{3} \frac{f'(\rho)}{\rho} \int_o^\rho f(\rho)\rho d\rho = \frac{1}{\rho} \frac{d}{d\rho} (\rho f'(\rho)) + t(\rho) \qquad 2.3.2$$

$$- \frac{5}{3} t(\rho) \cdot f(\rho) = \frac{5}{3} \frac{t(\rho)}{\rho} \int_o^\rho f(\rho)\rho d\rho = \frac{1}{P_T} \cdot \frac{1}{\rho} \frac{d}{d\rho} (\rho t'(\rho)) \qquad 2.3.3$$

and the integral constraint is now given by

$$\int_0^\infty f(\rho)\ t(\rho)\rho d\rho = QR_T/2\pi \quad . \qquad 2.3.4$$

In this form it is clear that the solutions to equations 2.3.2 and 2.3.3 depend only on the parameter P_T and are independent of R_T and Q. These latter dependencies enter only when the integral constraint of equation 2.3.4 is applied, and then only in the combination R_TQ. Thus an entire family of possible solutions is generated for each value of R_TQ. It is not until the solution is mapped back to physical coordinates by reversing the transformation of equations 2.3.2 and 2.3.3 that the actual dependence on R_T (or Q) enters. The choice of Q is limited by the physical constraints of $0 < Q < 1$.

From the above it is clear that the magnitude and basic shape of the profiles are determined only by the product R_TQ. In particular, the centerline values are uniquely determined. From equation 2.3.1, it is also clear that the actual physical width (or spreading rate) is determined by R_T alone. If the centerline values are assumed to be determined by the data, then the profile width determines Q, the fraction of the total vertical heat (or buoyancy) transport due to the turbulent fluctuations. The reverse is also true.

2.4 The Exact Solution of Yih

Yih (15) found exact solutions[2] satisfying the equations, boundary conditions, and integral constraints for the particular cases $P_T = 1.1$ and 2.0. The profiles are

---

[2]Modified forms of Yih's solutions are presented to include the Q-factor and the development of Yih's exact solutions is given in Appendix B.

$$f(\eta) = f_o/(1+A\eta^2)^2 \qquad 2.4.1$$

$$t(\eta) = t_o/(1+A\eta^2)^m \qquad 2.4.2$$

where $P_T = 1.1$, $m = 3$, or $P_T = 2.0$, $m = 4$. As illustrated in the previous sections the parameters f_o, t_o, A, P_T, R_T must be interrelated. These relationships are summarized in Table 1.

2.5 Numerical Solution for Arbitrary Prandtl Number

The coupled nonlinear second order ordinary differential equations given by equations 2.3.2 and 2.3.3 are solved numerically to give $f(\rho)$ and $t(\rho)$.

The numerical solution involves an iterative process in which for each iteration step the solutions to linearized versions of equations 2.3.2 and 2.3.3 are found. The linearization of equation 2.3.2 is accomplished by specifying that $f(\rho)$ and $\int_o^\rho f(\rho)\rho d\rho$ are known and given by the previous iteration. The linearized equations are central differenced, yielding a system of algebraic equations with a tridiagonal matrix for which a solution is easily accomplished by an elimination process.

The solution is initiated using simple geometric functions to approximate $t(\eta)$ and $f(\eta)$ over the range of interest. The program iterates upon the functions $t(\eta)$ and $f(\eta)$ until convergence is attained. The solution provides the functional relations $t(\eta)$ and $f(\eta)$ for a given R_T and P_T, and computes R_TQ, the value of the mean bouyancy integral.

Two hundred grid points were found to provide an increment in η, which insured accuracy with reasonably fast convergence. The boundary

Table 1. Summary of parameters in buoyant plume equations.

Prandtl No.	$P_T = 1.1$	$P_T = 2.0$
Exponent	m = 3	m = 4
f_o^2/R_TQ	$11/16\pi$	$25/36\pi$
t_o/R_TQ	$11/18\pi$	$125/240\pi$
f_o^2/t_o	9/8	3/4
Af_o/t_oR_T	10/64	11/64
$A/R_T^{3/2}Q^{1/2}$	0.065	0.057

conditions at infinity are known from the physics of the problem, and experimental data are used to bound values at f(o) and t(o). Infinity is established by extending the solution to the radial direction to a value at which the buoyancy integral is satisfied to the fourth decimal place. The profiles calculated by this technique are identical to those obtained for a more limited range of R_T and P_T by Hamilton and George (16) using a shooting method which required approximately twice the computer time of the present method.

2.6 Results of the Calculations and Comparison with Experiment

It was shown earlier that the form of the solutions depended only on the variables P_T and R_TQ. Figure 7 shows the interdependence of the centerline velocity and temperature as functions of the parameters R_TQ and P_T. The calculations cover the range of the existing data ($9 \leq t(o) \leq 13.7$, $2.7 \leq f(o) \leq 4.7$). Also shown are the lines corresponding to Yih's closed form solutions for $P_T = 1.1$ and 2, and the aforementioned calculations of Hamilton and George (16).

The experimental values obtained by Schmidt (4), Yih (15), and George, Alpert, and Tamanini (22) are also shown. The measurements of Schmidt (4) have been suspect since these do not satisfy the momentum equation. The measurements of Yih have recently been questioned by Yih himself (15) because of problems with the velocity probe, and by George, et al. (23) who questioned whether Yih's flow development length was long enough to allow sufficient momentum buildup from a heat source to achieve an asymptotic state. In view of the fact that turbulent Prandtl numbers are generally accepted to be near unity for free turbulent shear flows, Figure 7 indicates that these suspicions about the earliest measurements are well-founded, and they will not be used further here.

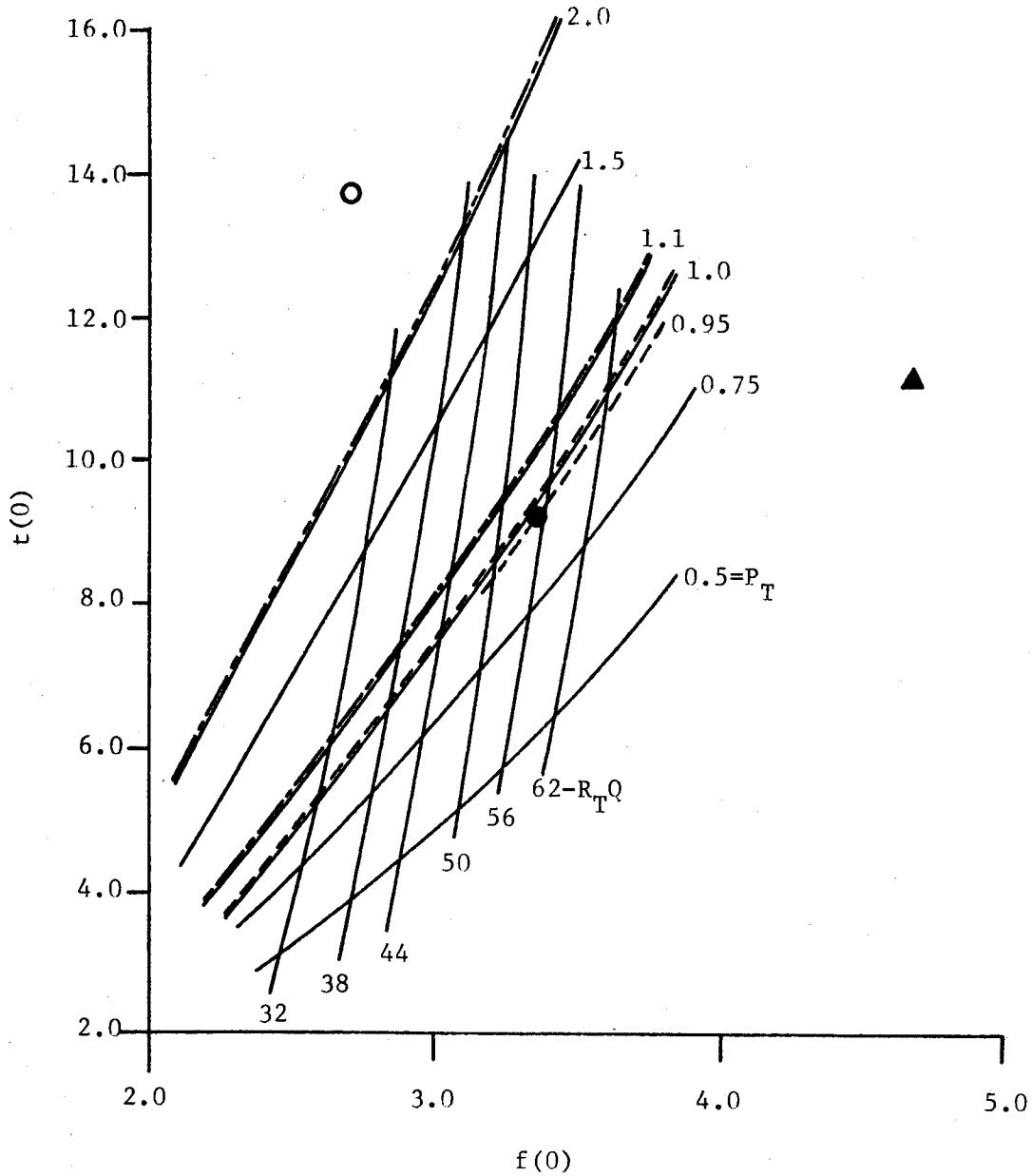

Figure 7. Parametric map of plume mean centerline temperature and velocity. o - Schmidt (4). ▲ - Rouse, et al. (6). ● - George, et al. (22). ——— Theory Yih (15). --- Theory Hamilton and George (16). —— Theory Baker, et al. (17).

Figures 8 and 9 show the calculated profiles of velocity and temperature for $P_T = 1$ and several values of R_TQ. Also shown for comparison are the data of George, et al. (23). The agreement between the measured profiles and those calculated for $R_TQ = 50$ is striking.

As might be expected from the results shown in Figure 7, Yih's solution for $P_T = 1.1$ is very close to those shown above. In fact if the width parameter is chosen to be $A = 28$, the profiles given by equations 2.4.1 and 2.4.2, if normalized by the centerline values, are indistinguishable from the $R_TQ = 50$ contours in Figures 8 and 9. In view of this, Yih's profiles should be used in place of the commonly used Gaussian profiles whenever an analytical expression is desired, since the fit to the velocity profile is superior.

Figures 10 and 11 show the calculated Reynolds stress and radial turbulent heat flux corresponding to the $R_TQ = 50$, $P_T = 1.0$ case presented above. In order to obtain these graphs it is necessary to know R_T explicitly, thereby necessitating a choice for Q. A value $Q = 0.85$ is selected which corresponds to the estimate of George, et al. (23) based on measurements of $\overline{u\theta}$. Also plotted are the Reynolds stress and radial turbulent heat flux measurements of Beuther and George (40). Agreement between the calculated and measured values is excellent near the centerline and in the core region of the plume. The fact that the calculated and measured values of the heat flux deviate at large η may be due to the non-negligible influence of the vertical turbulent heat flux on the temperature equation in this region (see discussion 2.7). The agreement between calculated and measured Reynolds stress at <u>all</u> values of η is surprising in view of the uncertainty of the measurements.

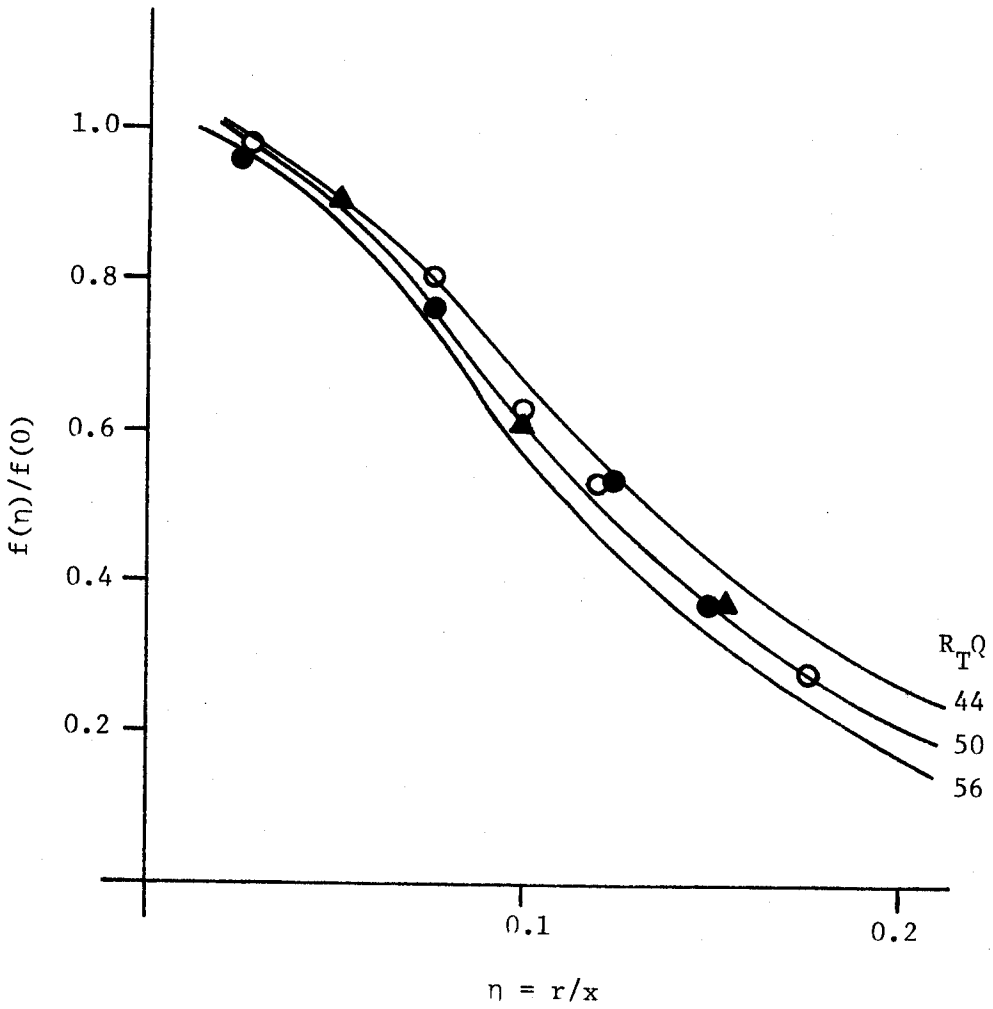

Figure 8. Comparison of plume mean velocity data with similarity theory (data George, et al. (22)).

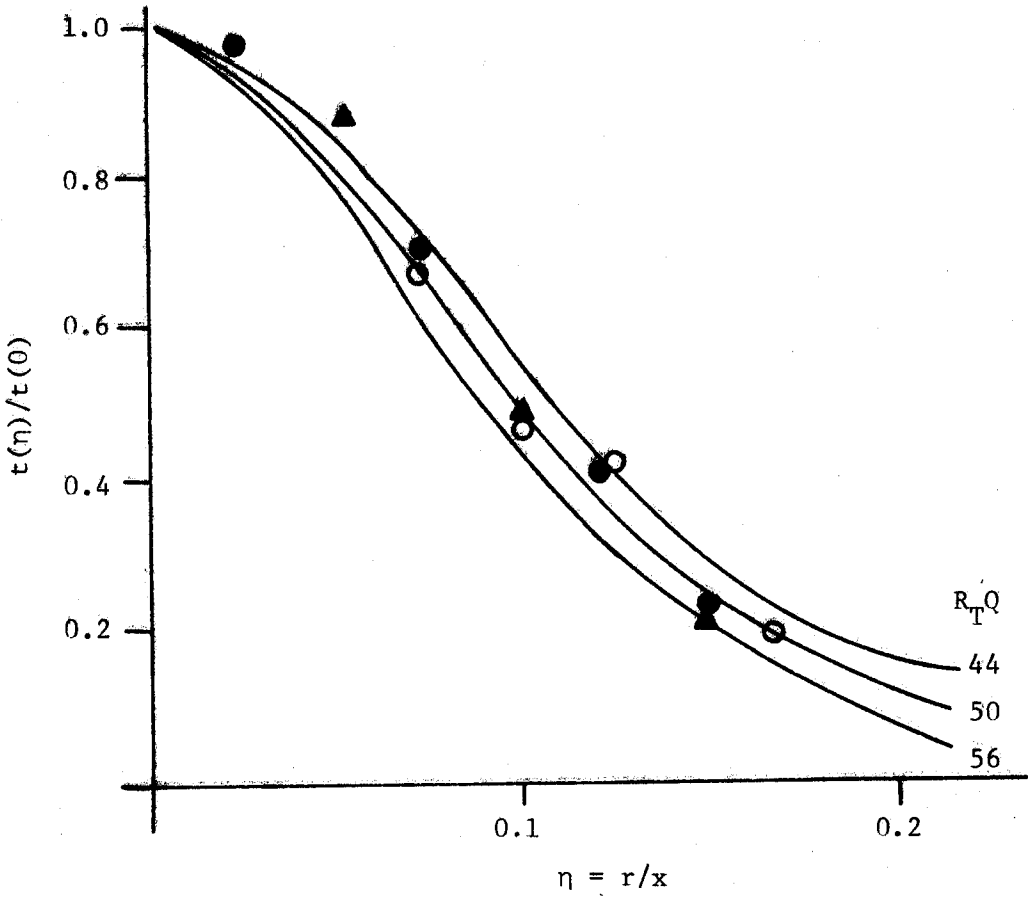

Figure 9. Comparison of plume mean velocity data with similarity theory (data George, et al. (22)).

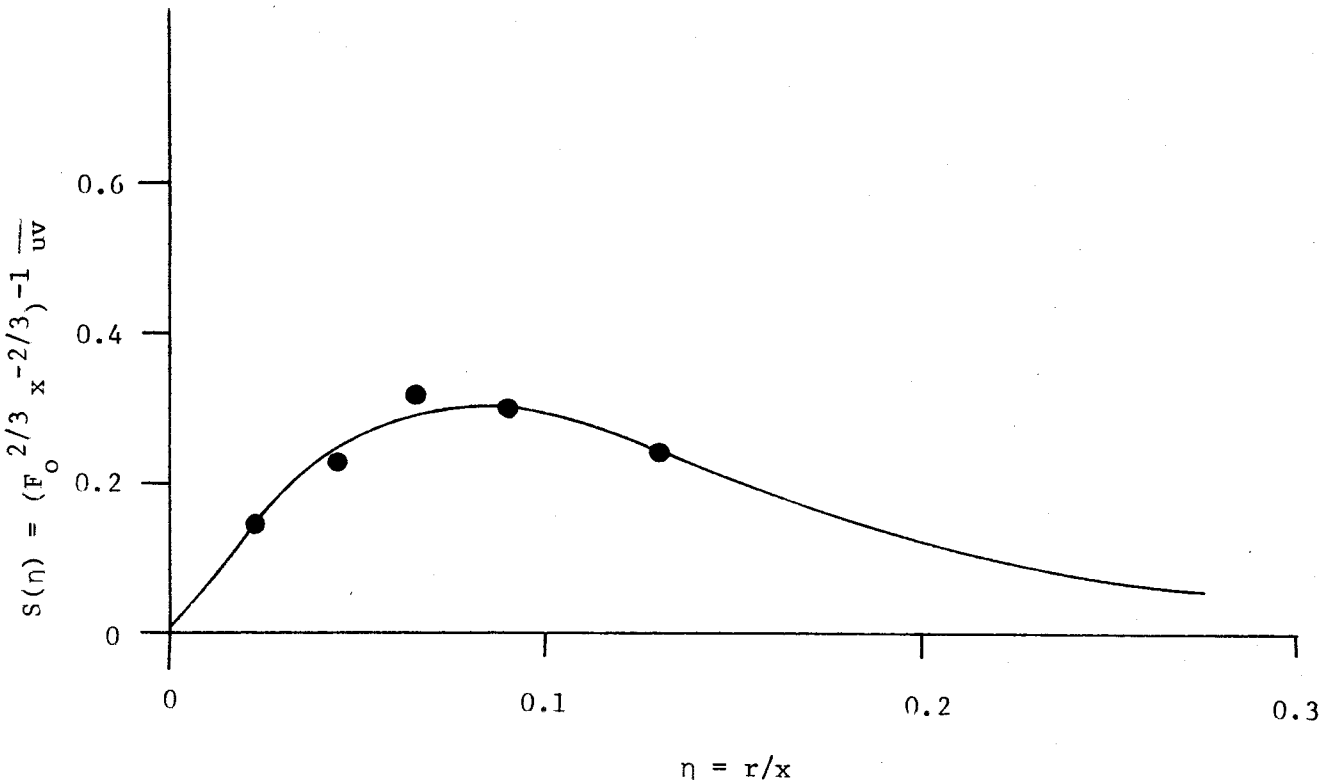

Figure 10. Comparison of plume Reynolds stress data with similarity theory (data Beuther, et al. (25)).

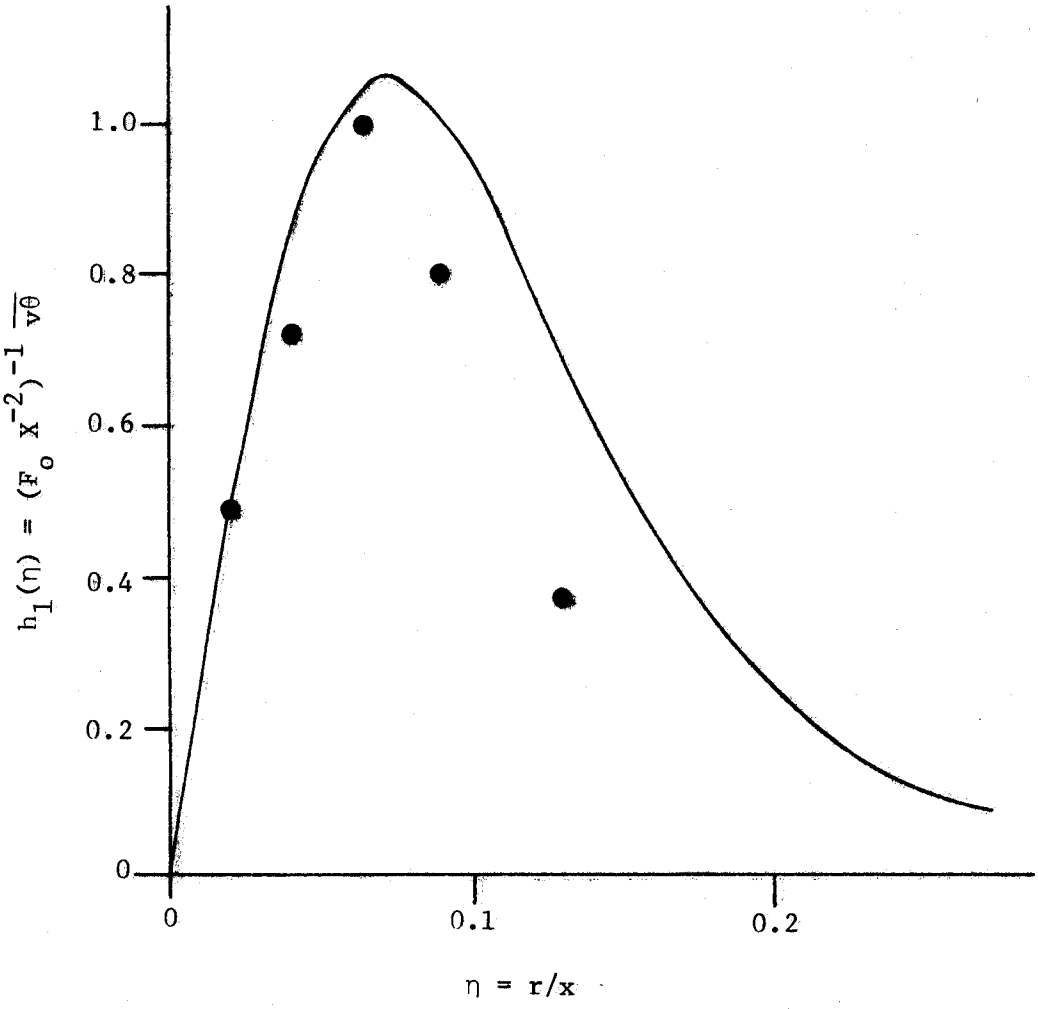

Figure 11. Comparison of plume radial turbulent heat flux data with similarity theory (data Beuther, et al. (25)).

2.7 Discussion

It is both surprising and somewhat misleading that such excellent agreement can be obtained between measured profiles and the predictions of a simple eddy viscosity model which accounts for the large turbulence contribution to the vertical heat flux in only the most elementary manner. It is interesting to speculate on the reasons for this success. This is particularly important when considering extended applications of this model to other problems dominated by bouyancy.

The vertical turbulent heat flux profiles ($\overline{u\theta}$) measured by George, et al. (23) are shown in Figure 12. It is obvious that the profile is considerably broader than the temperature or velocity profiles (normalized to the same maximum value). Over the core region of the plume it is reasonable to approximate $\overline{u\theta}$ by a simple top hat function. This constancy in the core region accounts for the fact that it has no influence over the shape of the velocity and temperature profiles except through integral parameter Q. As the intermittency at the outer edge begins to play a role in the actual profile shape, this effect would probably be seen first in the temperature equation and probably accounts for the deviations between calculated and measured values of radial heat flux.

An attempt was made to calculate directly the vertical turbulent heat flux $-\overline{u\theta}$, using the same value for the eddy diffusivity as used for the radial component. This corresponds to the commonly assumed isotropic medium model

$$-\overline{u_i\theta} = \alpha_e \frac{\partial T}{\partial x_i} \quad . \qquad 2.7.1$$

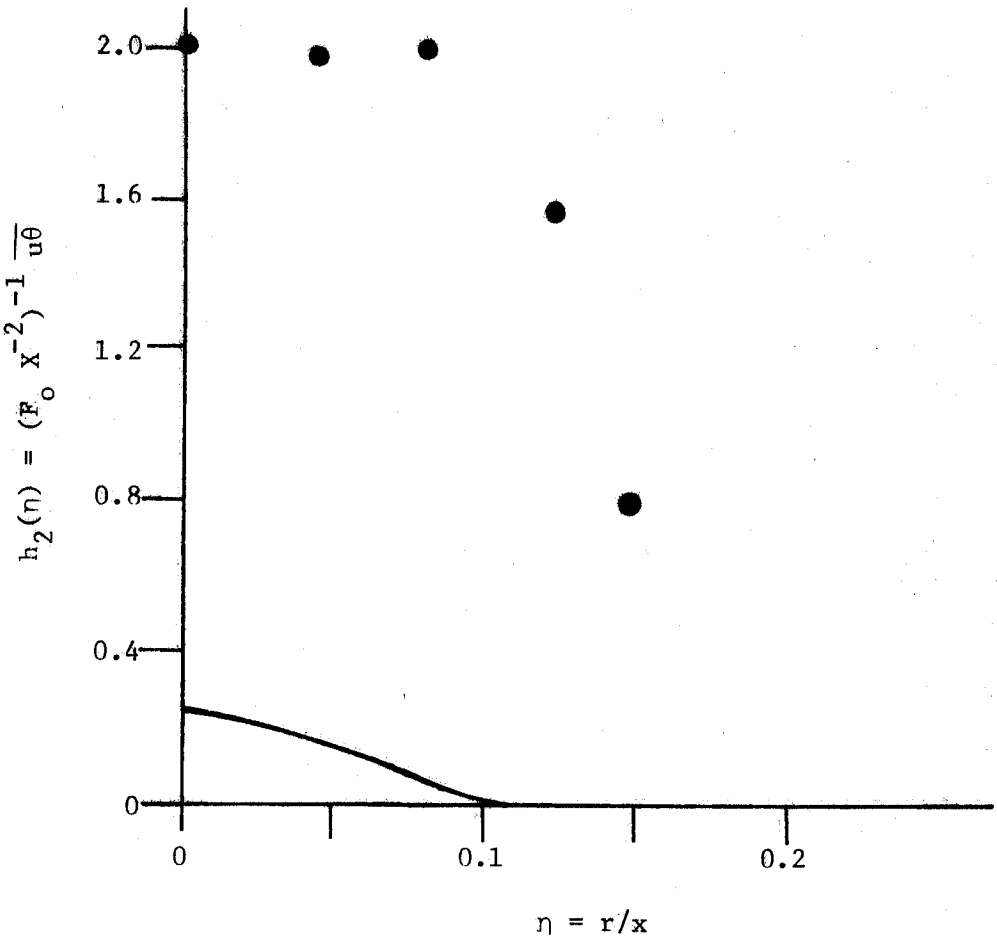

Figure 12. Comparison of plume vertical turbulent heat flux data with similarity theory (data Beuther, et al. (25)).

The result for the case $P_T = 1$, $R_T = 60$ is plotted in Figure 12. It is clear that the actual vertical heat flux is substantially underestimated.

The reasons for this are obvious when one considers the dynamical equation for $-\overline{u\theta}$. Unlike the equation for $-\overline{v\theta}$ where the dominant source terms arise only from mean gradient terms, the $-\overline{u\theta}$ equation has, in addition, a direct buoyancy source term which depends only on gravity and the temperature fluctuations. Thus it is not surprising that a "gradient transport" model fails in accounting for its behavior. One can infer from this that isotropic eddy viscosity models will probably always fail in problems involving buoyancy when the directions of the mean flow and gravity are aligned. Note that this does not exclude the possibility that additional techniques (like the Q factor introduced above) can be employed to account independently for the vertical turbulent heat flux contribution to the problem.

2.8 Summary

It has been shown that a simple eddy viscosity model can accurately predict the velocity and temperature profiles of a simple buoyant plume in a neutral environment if the contribution of turbulence to the vertical heat transport is accounted for separately. This result was anticipated from the fact that the flow could be characterized by a single time and a single length scale.

The computed centerline values proved to be useful in sorting conflicting experimental data. The best fit to the experimental data of references (23) and (4) is given by $P_T = 1.0$ and

$$\nu_e = \frac{1}{60} F_o^{1/3} x^{2/3} \quad . \qquad 2.8.1$$

This correaponds to $R_T Q = 50$ for which 85% of the vertical heat transport is carried by the mean flow.

Since the computed profiles from turbulent Prandtl numbers near unity are virtually indistinguishable from Yih's analytical solution for $P_T = 1.1$ (equations 2.4.1 and 2.4.2) it is recommended that Yih's solution be used as empirical profiles (with constants to be determined from the data) in place of the Gaussian forms. It is recommended that

$$f(\eta) = \frac{3.4}{[1+28\eta^2]^2} \qquad 2.8.2$$

$$t(\eta) = \frac{9.1}{[1+28\eta^2]^3} \qquad 2.8.3$$

be used to estimate the velocity and temperature respectively.

CHAPTER 3

THE AXISYMMETRIC JET

3.1 Introduction

For a forced turbulent jet (with no buoyancy) issuing from a point source of momentum, a single parameter characterizes the flow. That parameter is M_o, the rate at which momentum is discharged from the source. Since there is no other parameter, the flow has no intrinsic time or length scale. Consequently, the only parameters available to form a length and time scale are M_o and the distance from the source x. This situation is similar to that of a plume, and a similarity analysis can be developed.

Unlike the plume, the jet has been the subject of several investigations beginning with Prandtl; however, the analytical results which have been reported are at odds with the experimental data, particularly if the momentum integral constraint is imposed. This fact is not well known and is completely ignored in the recent review by Hinze, as well as in the original works of Wygnanski and Fiedler (21).

In this chapter, the jet similarity equations are derived, and the eddy viscosity solutions for the mean profiles are reviewed. The approach used here will be similar to that originally introduced by Zel'dovich (3), Tollmien (8), Görtler (9), and Schlichting (32). Their analysis will be extended to examine the effects of the non-negligible axial transport of mean momentum and heat by the turbulent fluctuations. The solutions are compared to the available experimental data, and an

assessment of the validity of the solution is made. The result of this assessment is that the analytical solution might be a better approximation to the jet mean velocity profile than the experimental data.

3.2 The Similarity Equation

The dynamical equations in dimensional form for the jet are identical to those of the plume except for the absence of the buoyancy terms. To the same order of approximation used earlier, they reduce to

$$U \frac{\partial U}{\partial x} + V \frac{\partial u}{\partial r} = \frac{1}{r} \frac{\partial}{\partial r} (-r\overline{uv}) \qquad 3.2.1$$

$$U \frac{\partial T}{\partial x} + V \frac{\partial T}{\partial r} = \frac{1}{r} \frac{\partial}{\partial r} (-r\overline{v\theta}) + \frac{\partial}{\partial x} (-\overline{u\theta}) \ . \qquad 3.2.2$$

The velocity equation clearly is dynamically independent of the temperature field, and the temperature (or heat) is transported as a passive scalar.

The complete jet mean momentum and energy equations can be integrated to yield the following integral constraints:[1]

$$2\pi \int_o^\infty (U^2 + \overline{u^2} - \overline{v^2} + \frac{\overline{w^2}}{2}) r dr = 1 \qquad 3.2.3$$

$$2\pi \int_o^\infty g\beta(\Delta T + \overline{v\theta}) U r dr = 1 \ . \qquad 3.2.4$$

The first of these states that momentum is conserved. The second states that energy is conserved. Energy conservation for the jet is analogous

---

[1] See Appendix C.

to buoyancy conservation for the plume. (The $g\beta$ has been retained here to facilitate comparison with later chapters even though buoyancy does not play a role in the pure jet.)

By analogy with the approach used in Chapter 2 for the plume, equations 3.2.3 and 3.2.4 can be modified to account for the turbulence contribution to the axial transport by introducing Q-factors as follows:

$$\int_o^\infty U^2 r dr = Q_1 M_o / 2\pi \qquad 3.2.3$$

$$\int_o^\infty g\beta \Delta T U r dr = Q F_o / 2\pi \quad . \qquad 3.2.4$$

As before, Q_1 or Q equal unity corresponds to the case where all transport is due to the mean flow.

The equations can be closed by an eddy viscosity model which is similar to that derived for the plume:

$$-\overline{uv} = \nu_e \frac{\partial u}{\partial r}$$

$$-\overline{v\theta} = \alpha_e \frac{\partial \Delta T}{\partial r} \quad . \qquad 3.2.5$$

Since the jet has only a single length and time scale, the model is expected to work at least as well as for the plume.

The following type of similarity solutions will be developed

$$U = U_j f(\eta), \quad \Delta T = T_j t(\eta), \quad \overline{uv} = U_j^2 S(\eta), \quad -\overline{v\theta} = U_j T_j h(\eta) \qquad 3.2.6$$

The closure approximations of equation 3.2.5 are readily seen to imply that

$$S(\eta) = \frac{1}{R_T} f'(\eta)$$

$$h(\eta) = \frac{1}{P_T R_T} t'(\eta) \qquad 3.2.7$$

where R_T and P_T are constants, the latter serving as the turbulence Prandtl number.

Substitution of these into the equations of motion, and insistence that the terms in the equation maintain the same relative balance (similarity) yields the following forms for U_j, T_j, ν_e, and α_e.

$$U_j = M_o^{1/2} X^{-1}$$

$$T_j = \frac{F_o X^{-1}}{M_o^{1/2}}$$

$$\nu_e = \frac{1}{R_T} M_o^{1/2}$$

$$\alpha_e = \frac{1}{P_T R_T} M_o^{1/2} \quad . \qquad 3.2.8$$

It follows immediately by substitution that the similarity forms of the equations are given by:

$$f^2 + \frac{f'}{\eta} \int_o^\eta f\eta d\eta + \frac{1}{R_T} f'' = 0 \qquad 3.2.9$$

$$f \cdot t + \frac{t'}{\eta} \int_o^\eta f\eta d\eta + \frac{1}{P_T R_T} t'' = 0 \qquad 3.2.10$$

$$\int_o^\infty f^2 \eta d\eta = Q_1/2\pi \qquad 3.2.11$$

$$\int_o^\infty f \cdot f\eta d\eta = Q/2\pi \ . \qquad 3.2.12$$

The only boundary condition is that the solutions vanish as $\eta \to \infty$. These equations can be solved either analytically or numerically if R_T and P_T are specified, and Q_1 and Q must also be appropriately chosen.

3.3 Effect of Turbulent Transport on Solutions

Analagous to preceding Section 2.3, R_T can be incorporated into the radial coordinate as follows:

$$\rho = \sqrt{R_T}\, \eta$$

$$f(\eta) \to f(\rho), \quad t(\eta) \to t(\rho), \quad k(\eta) \to R_T^{-1/2} k(\rho) \ . \qquad 3.3.1$$

Substitution into equations 3.2.9 through 3.2.12 yields

$$f^2(\rho) + \frac{f'(\rho)}{\rho} \int_o^\rho f(\rho)\rho d\rho + f''(\rho) = 0 \qquad 3.3.2$$

$$f(\rho)t(\rho) + \frac{t'(\rho)}{\rho} \int_o^\rho f(\rho)\rho d\rho + \frac{1}{P_T} t''(\rho) = 0 \qquad 3.3.3$$

$$\int_o^\infty f(\rho)^2 \rho d\rho = Q_1 R_T/2\pi \qquad 3.3.4$$

$$\int_0^\infty t(\rho)f(\rho)\rho d\rho = Q\ R_T/2\pi\ . \qquad 3.3.5$$

The magnitude of the velocity solution depends only on the combination R_TQ_1 and not on R_T or Q_1 separately. The "width" of the profile in the η-coordinate retains a dependence on R_T as in the case of the plume. The magnitude of the temperature solution depends on R_TQ only. Note that because the velocity enters the equations linearly there is no dependence of the magnitude of the temperature on R_TQ_1.

3.4 An Exact Solution[2]

Schlichting (32) and Hinze (20) report exact solutions to these equations with $Q = Q_1 = 1$. These solutions can be modified to include the Q-factors with the following results.

$$f(\eta) = B/(1+A\eta^2)^2 \qquad 3.4.1$$

$$t(\eta) = C/(1+A\eta^2)^{2P_T} \qquad 3.4.2$$

where A and C are constants dependent on R_T and P_T, which must be chosen to satisfy the integral constraints. The results are

$$B = f(0) = 3R_TQ_1/8\pi \qquad 3.4.3$$

$$A = 3R_T^2Q_1/64\pi \qquad 3.4.4$$

$$C = t(0) = (1+2P_T)R_TQ/8\pi\ . \qquad 3.4.5$$

---

[2] Development of Jet Exact Solutions is given in Appendix D.

3.5 Comparison with Experiment

A comparison will be made between the calculated mean velocity and temperature profile and data of Hinze and van der Hegge Zignen (13) and Wygnanski and Fiedler (21). The data of the former include profiles of both temperature and velocity. The data of Wygnanski and Fiedler are considered to be the best available data for an ambient jet. The velocity data of Hinze and van der Hegge Zignen are almost identical to that of Wygnanski and Fiedler. The data will also be used to compare the calculated and measured Reynolds stress and to determine the integrated transport due to the turbulence fluctuations. A word of caution is in order, however, since George and Beuther (40) have recently shown that there is substantial doubt that these profiles are correct beyond $\eta \simeq 0.05\text{-}0.1$.

3.5.1 The Velocity Profile

The velocity profile data normalized to unity at the axis are shown in Figure 13. The centerline value quoted by various authors is given by

$$U_{\mathfrak{L}} = B\, M_o^{1/2}/(x-x_o) \qquad 3.5.1$$

where $x_o \sim 7d$ and $B \sim 5.6$. Wygnanski and Fiedler showed that a higher value for B could be obtained if the data were not taken at sufficient distance from the source for the flow to have achieved a self-preserving state.

Figure 14 is taken from Wygnanski and Fiedler (21) and shows the profile of the rms axial velocity fluctuation as a fraction of the mean centerline velocity. Also indicated are the data of earlier investigations.

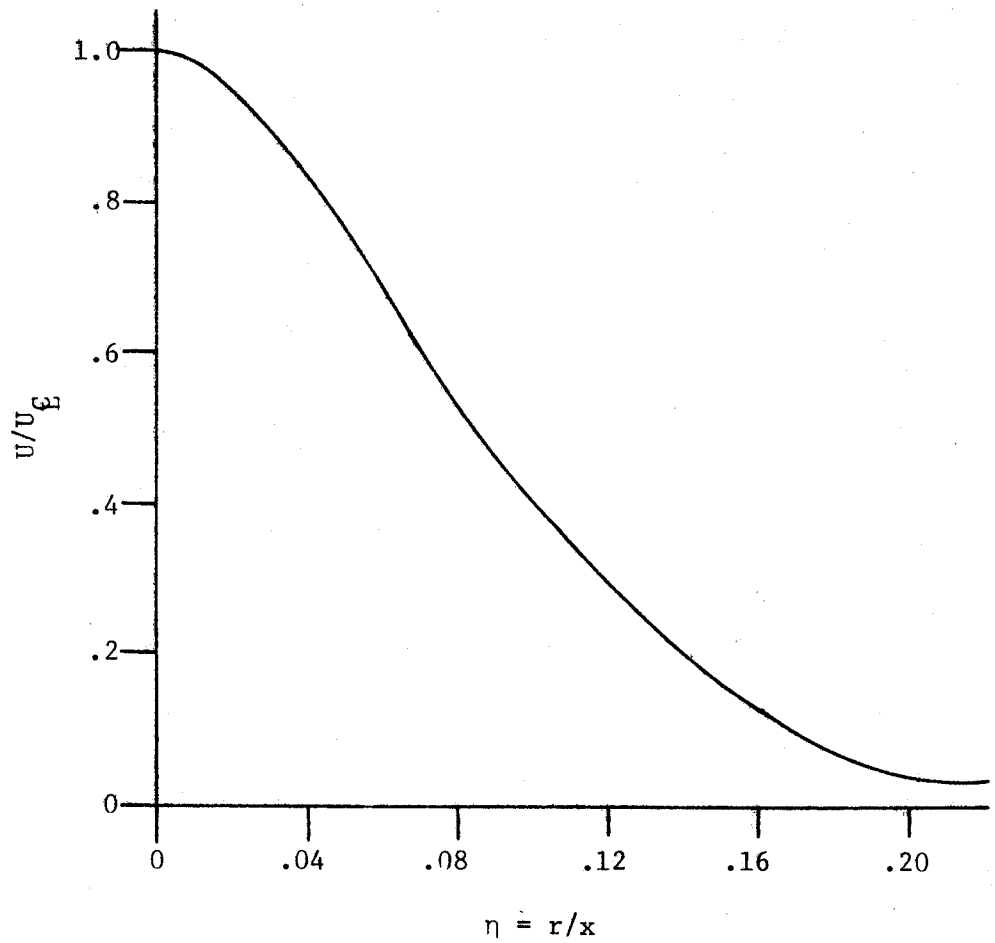

Figure 13. Measured jet mean velocity profile (Wygnanski and Fiedler (21)).

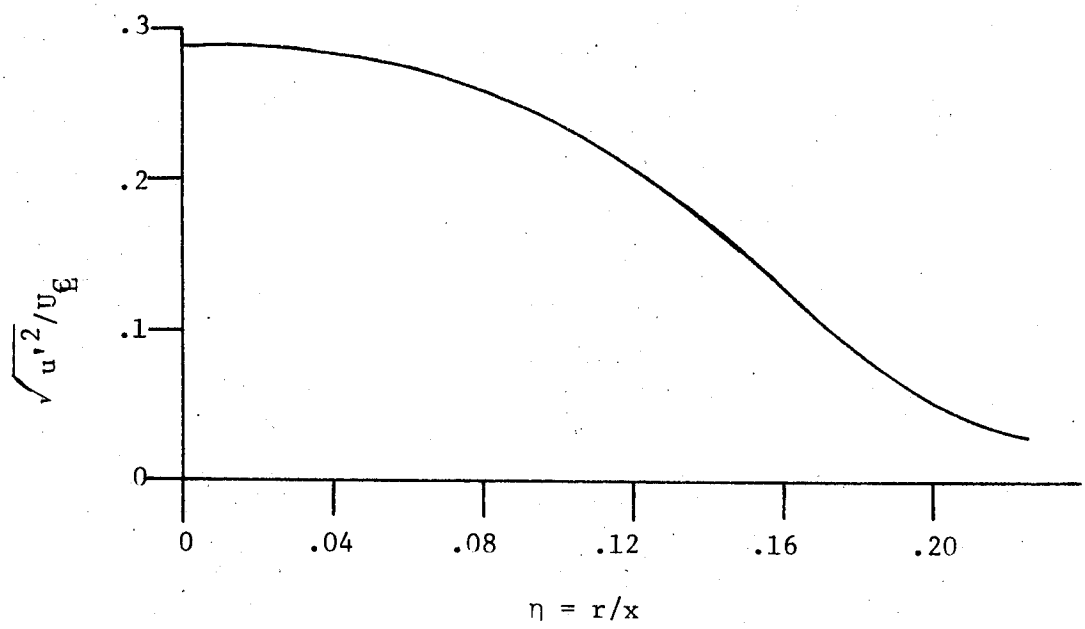

Figure 14. Measured rms axial velocity fluctuation (Wygnanski and Fiedler (21)).

The earlier data are believed to be unreliable because of the filtering of low-frequency components.

Figure 15 shows Wygnanski and Fiedler's data along with the eddy viscosity solutions generated earlier. Using the measured centerline value in Equation 3.4.3 the value of $R_T Q_1$ can be determined as

$$R_T Q_1 = 8\pi B/3 \simeq 47.2 \ . \qquad 3.5.2$$

The value of Q_1 can be computed by performing the integral

$$2\pi \int_o^\infty \overline{u^2}\, r dr = (1-Q_1) M_o \ . \qquad 3.5.3$$

If the data of Figure 14 are used in equation 3.5.3 and the integration is performed graphically, the result is $1-Q_1 \simeq 0.11$ or $Q_1 \equiv 0.89$ (i.e., 11% of the total axial momentum is carried by the turbulence).

The profile width parameter A computed from equation 3.4.4 is listed in Table 2 for a range of values of Q_1. The need for these values will soon be obvious. The corresponding value of R_T is also computed using $R_T Q_1 = 47.2$.

Inspection of the velocity profiles plotted in Figure 15 for various values of Q_1 reveals that only the value of $Q_1 \equiv 0.5$ approximates the profile. This implies that 50% of the momentum is carried by fluctuating quantities. The mean velocity data of Wygnanski and Fiedler have been integrated. These data do not satisfy momentum and the results are given in Figure 16. Shown in this figure are the parameters $f^2(\eta) \cdot \eta/B^2$, the intermittency γ, and the value of $\int_o^\eta f^2(\eta) \cdot \eta d\eta$. The data account for approximately 52% of the momentum and from Figure 16 it can be seen that the integral is close to a horizontal asymptote at $\eta = 0.20$.

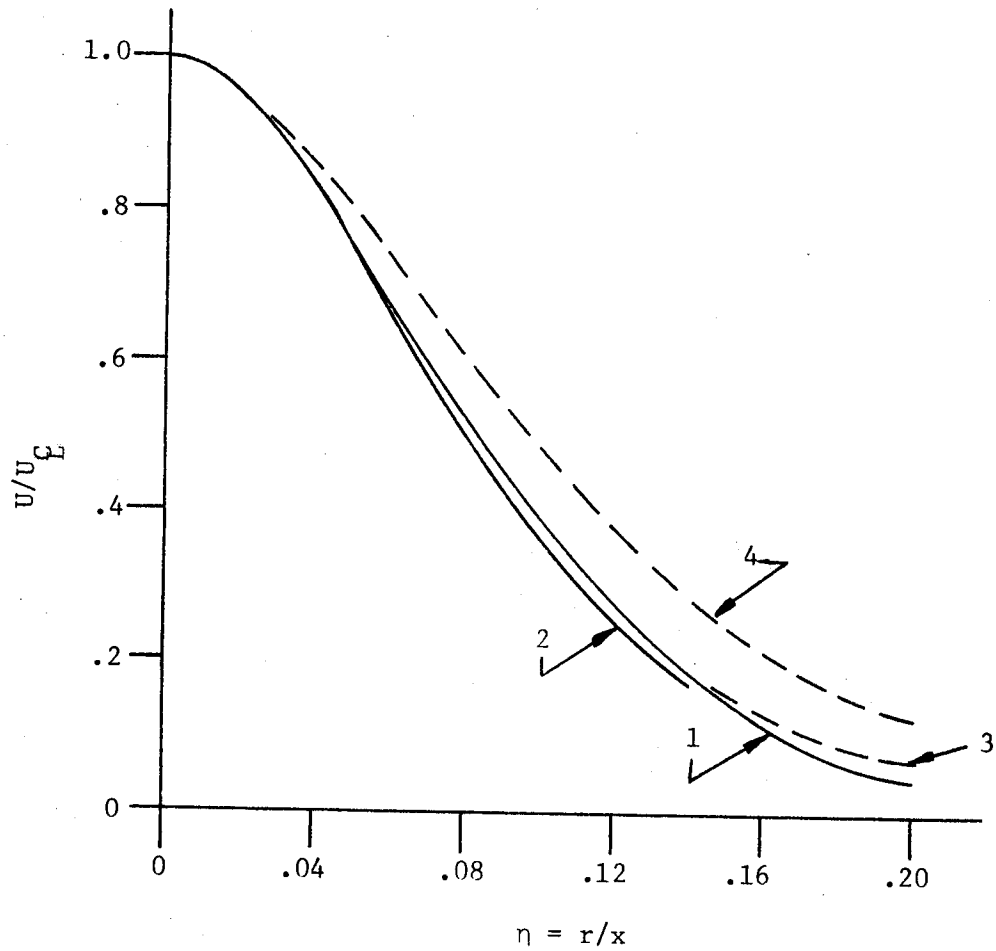

Figure 15. Comparison of measured jet mean velocity profiles with eddy viscosity model. 1 - Wygnanski and Fiedler (21). 2 - Hinze and van der Hegge Zignen (13). 3 - Equation 3.4.1, $Q_1 = 0.5$. 4 - Equation 3.4.1, $Q_1 = 0.85$.

Table 2. Calculated values of jet velocity profile width parameter.

$R_T Q_1 = 47.2$							
Q_1	1.0	0.9	0.85	0.8	0.7	0.6	0.5
R_T	47.2	52	55.5	59	67.4	78.7	94.4
A	33.2	36.9	39.1	41.6	47.5	55.4	66.5

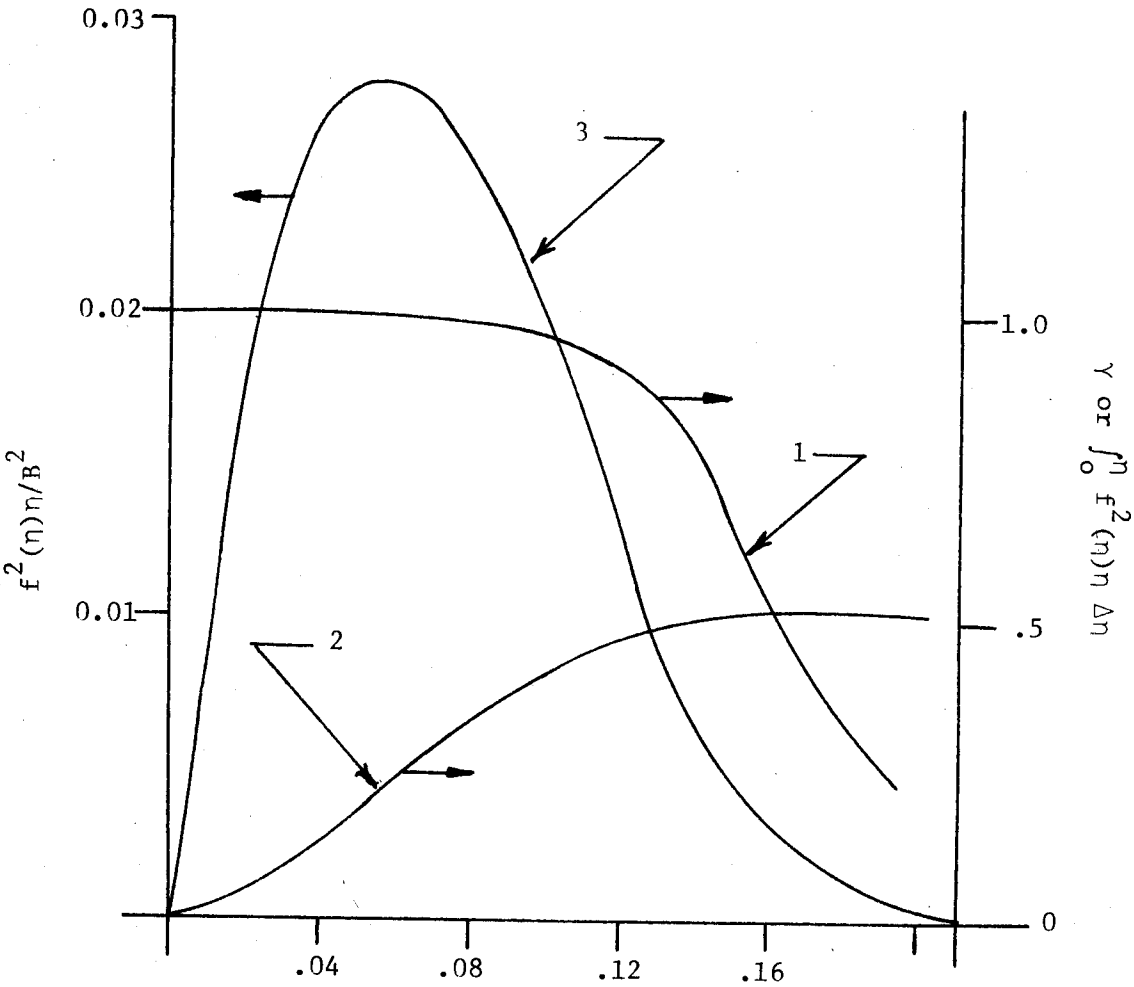

Figure 16. Momentum balance for jet mean velocity profile measured by Wygnanski and Fiedler (21). 1 - Intermittency γ. 2 - $\int_o^\eta f^2(\eta)\,\eta d\eta$. 3 - $f^2(\eta)\eta$.

An alternate approach to the data is to fit the profile first and work backwards to determine the centerline velocity from an assumed value of Q_1 (or the measured value). The profile (normalized to unity at $\eta = 0$) given by $A = 66.5$ provides an excellent fit out to $\eta \simeq 0.15$ (or most of the data). The corresponding centerline values are listed in Table 3 for various values of Q_1.

It is clear that either the solution is inadequate to describe the data, or that the data are seriously in error. It appears that the problem lies primarily in the data. This is easily shown to be true by substituting the measured mean profile into equation 3.2.3 and integrating graphically. The result is

$$2\pi \int_o^\infty U^2 r dr \approx 0.46\ M_o \ . \qquad 3.5.4$$

If the $0.11\ M_o$ obtained by integrating the profile of the mean square fluctuating velocity is added, this accounts for only 57% of the momentum flux provided at the source. This problem does not appear to have been addressed by previous investigators.

The missing momentum cannot be attributed to a neglected part of the integral at large values of η or to intermittency. Intermittency of the turbulence near the outer edge is believed to reduce the velocity there and increase the rate of roll-off. Thus an asymptotic estimate of the tails of the profile based on an eddy viscosity should provide an overestimate of the neglected part of the integral. Even this overestimate proves negligible.

There is considerable reason to believe that the measured profiles by all investigators may be seriously in error. Figure 17 shows a graph of the turbulence intensity versus η. Unlike most experimental graphs in

Table 3. Calculated values of jet centerline velocity.

A = 66.5							
Q_1	1.0	0.9	0.85	0.8	0.7	0.6	0.5
R_T	67	74	79	83	95	111	134
B	8.0	7.6	7.3	7.1	6.7	6.2	5.6

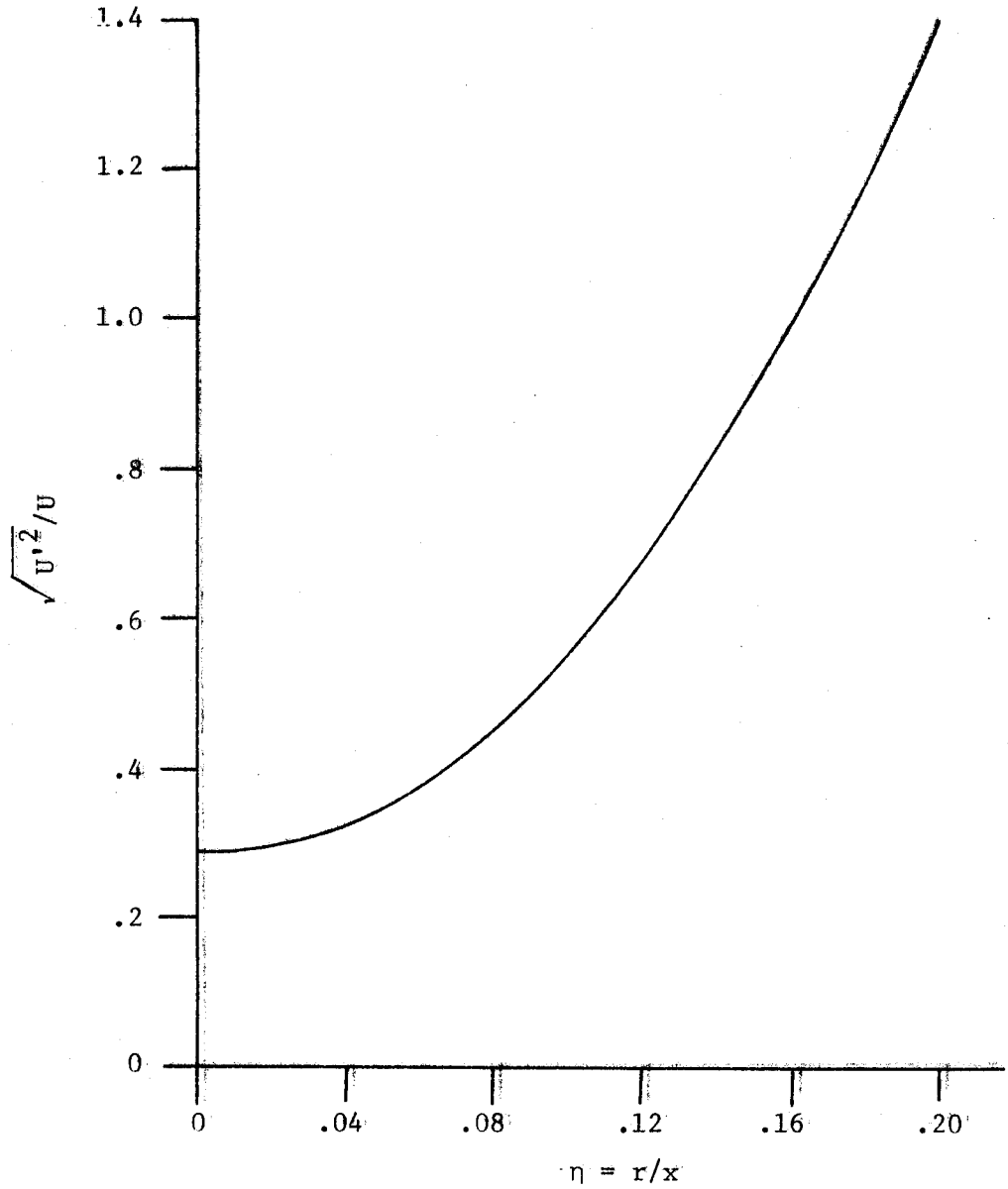

Figure 17. Measured rms axial velocity fluctuations normalized to local mean velocity for jet from data of Wygnanski and Fiedler (21).

which the fluctuating data have been normalized by the centerline mean velocity, here the local mean has been used for normalization. The turbulence intensity is nearly 30% at the centerline and increases rapidly as radius is increased. At $\eta = 0.15$, the turbulence intensity seen by the probe is nearly 100%. It is well-known that both hot-wire and pitot-tubes simply cannot provide reliable results at turbulence intensities approaching these values. In fact, the centerline values are near the limit for standard linearized hot-wire anemometry techniques.

In summary, the only reliable velocity profile data are the centerline values where the turbulence intensity is the lowest. Accordingly a value $B = 5.6$ is used to obtain $R_T Q_1 \simeq 47$. For lack of a better choice, Q_1 is selected to be approximately 0.85 (which is probably a reasonable guess based on the data). The velocity profile corresponding to this selection of Q_1 and $R_T Q_1$ is:

$$f(\eta) = [1+39\eta^2]^{-2} \quad . \qquad 3.5.5$$

In the final stages of this investigation, a paper by Abbiss, et al. (45) was found which presents measurements in a jet by standard hot-wire techniques, a photon correlation technique and a pulsed-wire technique. The standard hot-wire measurements and the photon correlation results are in very close agreement with the results of other works cited earlier. While the pulsed-wire profiles are considerably broader, the turbulence intensity measurements were the same for all three techniques. It was the conclusion of these authors that the hot-wire and photon correlation measurements were correct. A careful integration of the momentum flux indicates precisely the opposite to be the case. The

pulsed-wire profile is in virtually perfect agreement with the profile predicted above and integrates to 85-90% of the momentum, the remainder being accounted for by the turbulent transport.

Figure 18 shows the Reynolds stress data of Wygnanski and Fiedler and that computed from the analytical solution for $R_T = 55.5$ which corresponds to $R_T Q_1 = 47.2$ and $Q_1 = .85$. The analytical solution predicts the linear region of the Reynolds stress near the origin. This confirms the relative accuracy of the measurements in this region since in axisymmetric flows this slope is determined by the mean centerline velocity. According to George and Beuther (40) the Reynolds stress measurements outside the core region are probably in error by 20 to 30% near the peak because of the hot-wire drop out problem mentioned previously. Thus the predicted Reynolds stress is consistent with a careful analysis of the measurements. It should be noted that the velocity and Reynolds stress profiles measured by Wygnanski and Fiedler satisfy the differential momentum equation 3.2.1, even though the integrated momentum is in error by approximately 50%. This could be the result of a consistent error in all the measurements, but regardless of the cause further experimental studies are required to resolve these questions.

3.5.2 The Temperature Profile

The mean temperature profile due to van der Hegge Zignen (13) is shown in Figure 19. These data are cited in Hinze (20) and shown to agree with the results of other authors. The concentration profiles of Becker, et al. (43) are in excellent agreement with those of reference (13) which are also shown. The centerline temperature is reported as

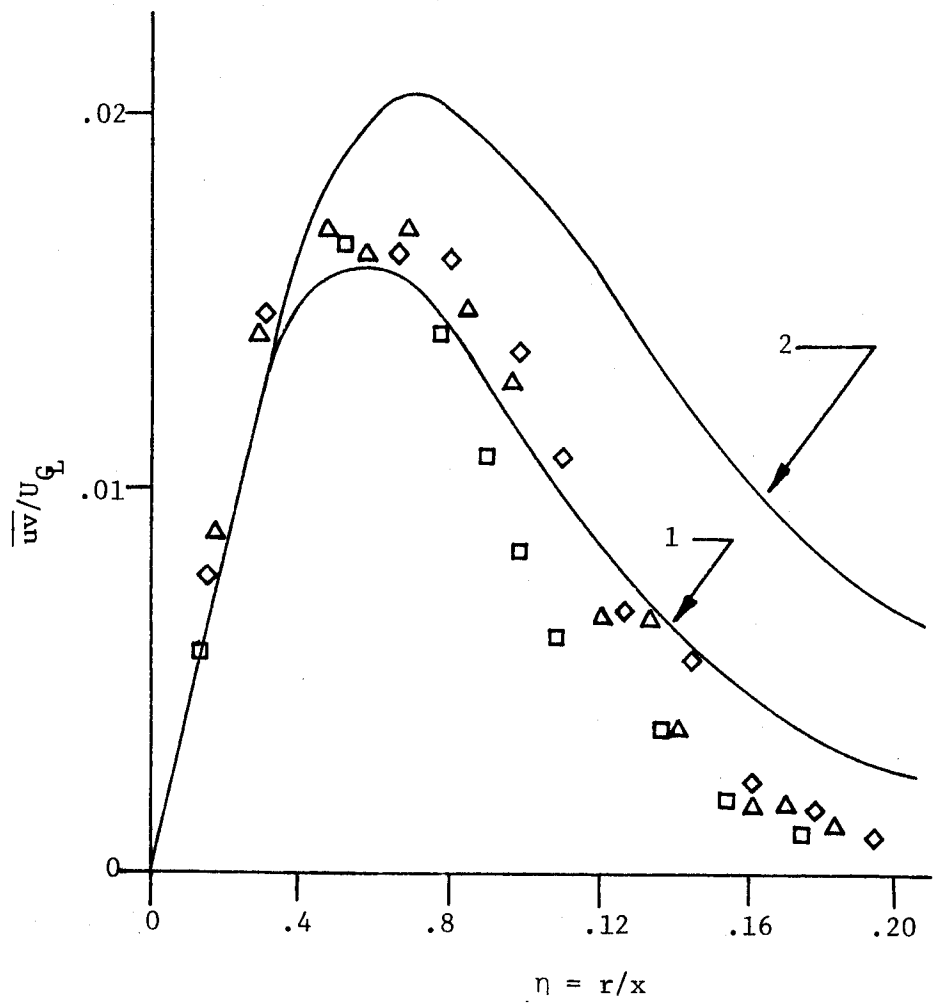

Figure 18. Comparison of measured and calculated jet Reynolds stress data (Wygnanski and Fiedler (21)). 1 - Calculated using mean velocity profile to fit data. 2 - Calculated using mean velocity profile to satisfy momentum integral constraint.

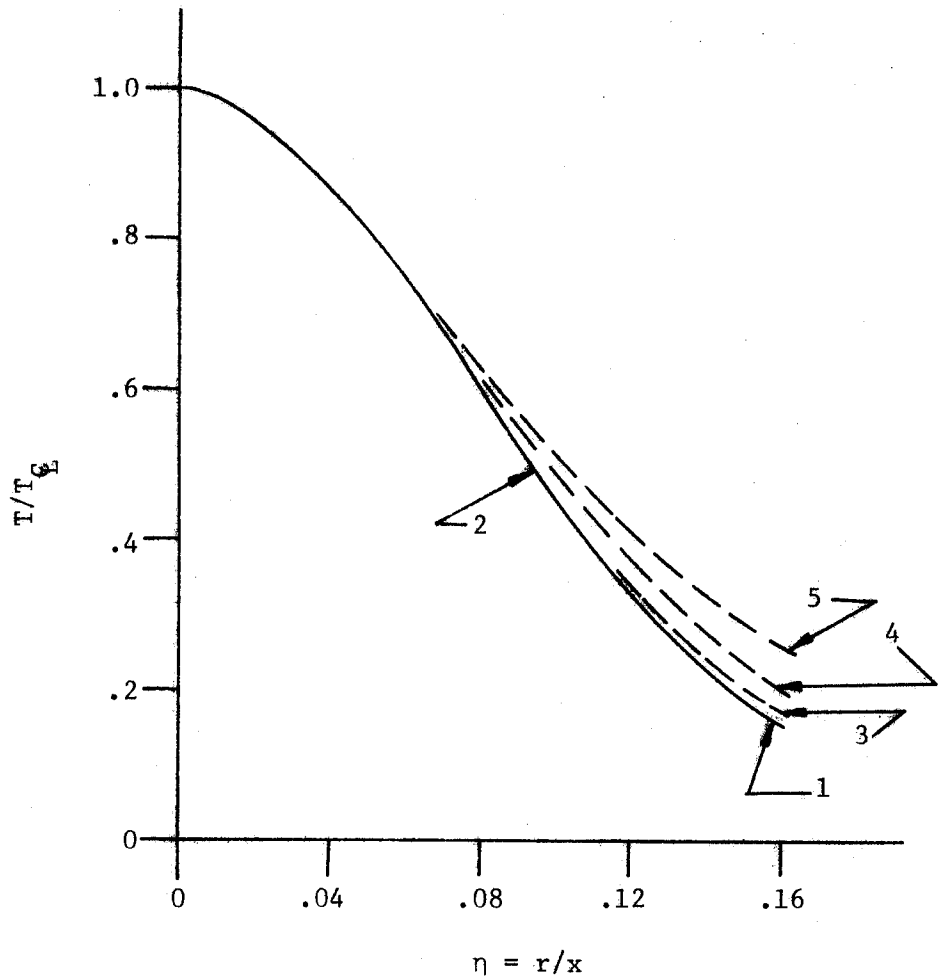

Figure 19. Comparison of measured jet mean temperature profiles and eddy viscosity model. 1 - Data fit Hinze and van der Hegge Zignen (13). 2 - Data fit Becker, et al. (43). 3 - Equation 3.4.2, $P_T = 1.18$. 4 - Equation 3.4.2, $P_T = 1.05$. 5 - Equation 3.4.2, $P_T = 1.0$.

$$g\beta\Delta T_{\ell} = 5.95\ F_o/\sqrt{M_o}\ x \quad . \qquad 3.5.6$$

Using this in equation 3.4.5 along with the previously determined value of $R_T = 55.5$ the turbulent Prandtl number is calculated as a function of Q (Table 4).

These profiles are plotted in Figure 19 with P_T as a parameter. The $P_T = 1.2$ case is seen to provide an excellent fit to the measured profile; however, the axial transport of heat by the turbulence is expected to be less than in the plume since the velocity and temperature are not as strongly correlated (i.e., $\frac{\overline{ut}}{u't} \simeq 0.2 - 0.3$ for jet versus 0.6 - 0.7 for the plume). This appears to indicate that a turbulent Prandtl number closer to unity might be desirable.

In summary, the calculated temperature profiles show good agreement with the measured profiles. Since temperature measurements involve linear instruments and are not subject to the types of problems encountered for the velocity, these profiles should be reliable. That the theory disagrees with the measured velocity but gives a reasonable prediction of the temperature profile provides additional evidence for the validity of the conclusions that the measured mean velocity profiles are in error. The following equation will be used to describe the jet mean temperature profile:

$$t_j = 6.0/(1+39\eta^2)^2 \quad . \qquad 3.5.7$$

Table 4. Calculated values of jet turbulent Prandtl numbers.

$R_T = 55.5$				
Q	1.0	0.9	0.85	0.8
P_T	0.85	1.0	1.08	1.18

CHAPTER 4

THE BUOYANT JET

4.1 Introduction

The buoyant jet is defined in Chapter 1 as a flow driven by both momentum and buoyancy addition at the source. In this chapter a set of dimensionless equations are derived which describe the mean velocity and temperature (buoyancy) profiles for a buoyant jet as it evolves from a jet to a plume. For a turbulent buoyant jet the only parameters which can govern the evolution of the flow are either those occurring in the equations of motion or those imposed at the source of the flow. The only parameter in the equations of motion is $g\beta$ and, at the source, the rate at which momentum and buoyancy are added:[1]

$$M_o = 2\pi \int_o^\infty U^2 r dr \qquad 4.1.1$$

$$F_o = 2\pi \int_o^\infty g\beta\Delta T U r dr \ . \qquad 4.1.2$$

The dimensions of the above parameters are $M_o = [\ell^4/\tau^2]$ and $F_o = [\ell^4/\tau^3]$. At any given cross-section the radial distribution of the quantities which describe the mean flow must be considered a function of the distance from the source and the three parameters $g\beta$, F_o, and M_o.

---

[1] For simplicity in presentation, the Q-factors are not included in the following chapters but will be included in the solution. Note that they do not enter the perturbation solution above order zero.

From this basic set of parameters only two independent dimensionless ratios can be formed. A convenient choice for these ratios is:

$$\eta = r/x \qquad 4.1.3$$

$$\xi = x/L \qquad 4.1.4$$

where L is defined by:

$$L = M_o^{3/4}/F_o^{1/2} \ . \qquad 4.1.5$$

The coordinate η is that used in the jet and plume analyses in which case no length scale was imposed on the flow, and the natural length scale is the distance from the source, x.

The coordinate ξ is new and is a consequence of the new characteristic length L, which is imposed on the flow by the simultaneous addition of momentum and buoyancy at the source. The length, L, is used to nondimensionalize the distance from the source, x, since it is known that a buoyant jet will evolve into a plume, and L is the only parameter depending on buoyancy. The parameter ξ reflects the evolution of a jet into a plume since $L \to \infty$ as $F_o \to 0$, and $\xi \to 0$ in which case the jet source is approached. As the buoyancy increases, so does ξ and plume behavior is approached. Thus, the dimensionless coordinate ξ reflects the effect of buoyancy on the flow in a manner consistent with the physical evolution of the flow.

Morton (1), List and Imberger (33), and Kotsovinos and List (28) recognized the importance of a coordinate proportional to $\xi = x/L$ in presenting the results of their experimental data and theoretical calculations. The recognition of L, the "forced length scale" as a

natural length scale arising from the physics of the problem does not appear to have been made before now. Moreover, the scaling laws arising from this recognition are new.

The equations derived and presented here show explicitly how the parameter ξ "controls" the buoyancy term in the mean flow equations thereby modifying the solutions. The details of the derivation are included as Appendix E.

4.2 The Dynamical Equations for the Buoyant Jet[2]

Consider a fully developed, axisymmetric hot turbulent jet discharging vertically into a constant temperature (neutral) environment of infinite extent as in Figure 20. The mean equations for momentum, temperature and mass conservation can readily be reduced to

$$U \frac{\partial U}{\partial x} + V \frac{\partial u}{\partial r} = \frac{1}{r} \frac{\partial}{\partial r} (-r\overline{uv}) + g\beta\Delta T \qquad 4.2.1$$

$$U \frac{\partial \Delta T}{\partial x} + V \frac{\partial \Delta T}{\partial r} = \frac{1}{r} \frac{\partial}{\partial r} (-r\overline{v\theta}) \qquad 4.2.2$$

$$\frac{\partial U}{\partial x} + \frac{1}{r} \frac{\partial (rV)}{\partial r} = 0 \ . \qquad 4.2.3$$

In these equations the Boussinesq approximations are employed, and the molecular diffusion of momentum and heat is assumed negligible

---

[2] Throughout the analysis the buoyant jet is assumed to be a point source of momentum and buoyancy. In practice, the source also has finite mass discharge. This can be combined with the momentum discharge rate to obtain another length scale which manifests itself in the virtual origin needed to collapse the data in jet coordinates.

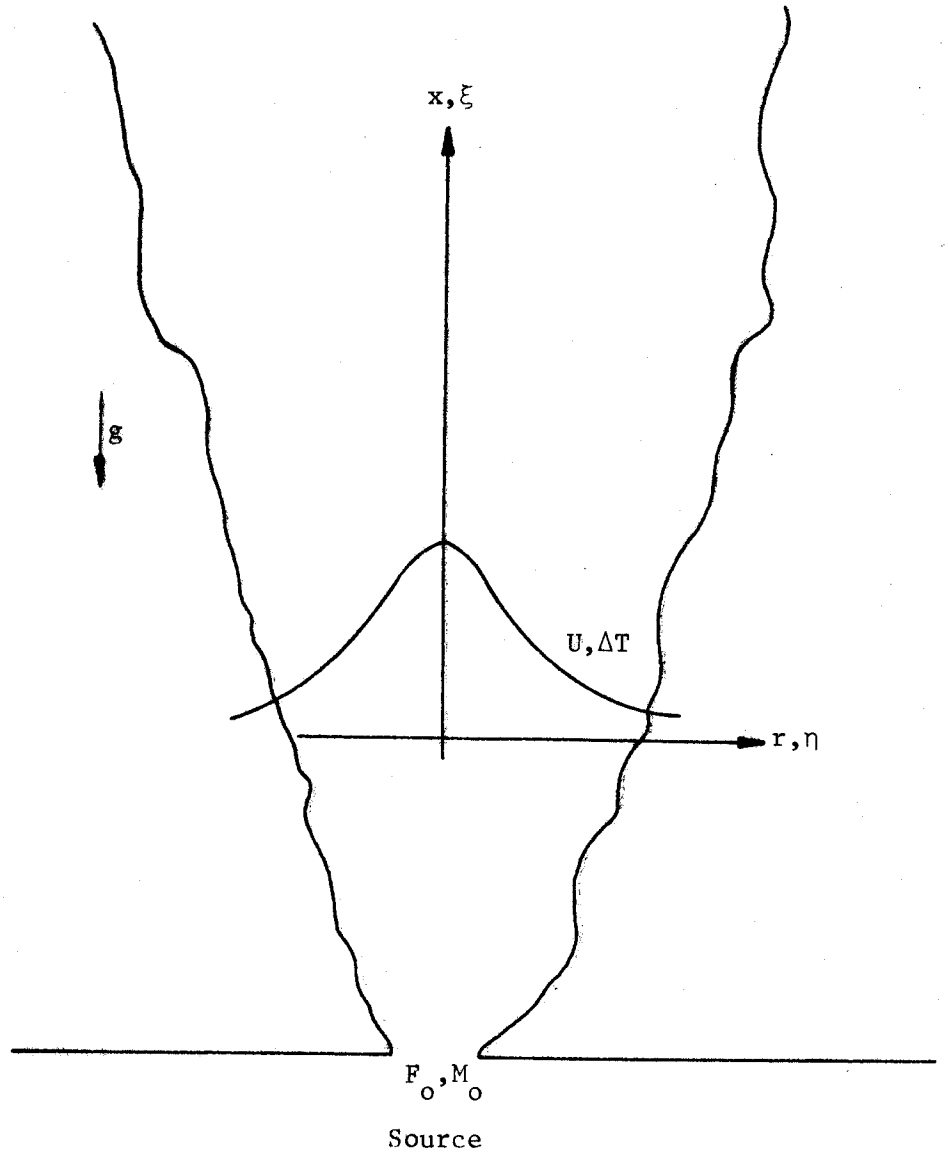

Figure 20. Schematic of buoyant jet and coordinates.

relative to the transport of these quantities by the turbulence. Moreover, the streamwise gradient of the turbulent normal stress difference $(\bar{u}^2-\bar{v}^2)$ has been neglected in the momentum equation as has the streamwise gradient of the streamwise turbulent heat flux $\overline{u\theta}$. The neglect of both has been seen to be acceptable for both jet and plume (Chapters 2 and 3), at least as far as the shape of the profiles is concerned.

Both the momentum and temperature equations can be integrated across the flow to yield the integral equations used by previous investigators. These are

$$\text{Momentum:}\quad \frac{d}{dx}\int_o^\infty U^2 r\,dr = \int_o^\infty g\beta\Delta T\, r\,dr \qquad 4.2.4$$

$$\text{Temperature: (Buoyancy)}\quad \int_o^\infty g\beta\Delta T U r\,dr = \frac{F_o}{2\pi}. \qquad 4.2.5$$

The initial condition for the momentum integral equation is,

$$\int_o^\infty U^2 r\,dr = \frac{M_o}{2\pi} \qquad 4.2.6$$

which is the rate at which momentum is discharged at the source.

4.3 The Transformed Equations

A hot jet is expected to behave initially as a forced jet, and the buoyancy is expected to affect the flow gradually. A model to represent the velocity and temperature profiles for this flow must reduce to the equations for a forced jet presented in Chapter 2 as either: 1) the buoyancy is reduced; or 2) the momentum and buoyancy source is approached.

The appropriate transformations which accomplish these goals are

$$\eta = r/x$$

$$\xi = x/L$$

$$U = U_j(x)\, f_j(\eta,\xi)$$

$$V = U_j(x)\, k_j(\eta,\xi)$$

$$\overline{uv} = R_j(x)\, S_j(\eta,\xi)$$

$$g\beta\Delta T = T_j(x)\, t_j(\eta,\xi)$$

$$g\beta\overline{v\theta} = H_j(x)\, h_j(\eta,\xi)\,. \qquad 4.2.7$$

The subscript j denotes the previously derived (Chapter 2) similarity forms for the jet given by:

$$U_j = M_o^{1/2}\, x^{-1}$$

$$R_j = M_o\, x^{-2}$$

$$T_j = F_{00} M^{-1/2}\, x^{-1}$$

$$H_j = F_o\, x^{-2}\,. \qquad 4.2.8$$

It should be recalled that for the jet, the solution to the momentum equation depends on only x and M_o. Moreover, the presence of F_o in T_j does not feed back (in the jet) into the momentum equation since temperature is a passive scalar. Thus, in the representation presented above, the buoyancy manifests its presence only through the new dependence on ξ and the coupling of the temperature and velocity equations through the buoyancy term.

Substituting equations 4.2.7 and 4.2.8 into the dynamical equations 4.2.1 and 4.2.2, differentiating and collecting terms, and using the continuity equation 4.2.3 to eliminate the radial velocity yields

$$f_j^2 + \frac{f_j'}{\eta}\int_o^\eta f_j \eta d\eta - \frac{(\eta s_j)'}{\eta} = -\xi^2 t_j + \xi\left[f_j \frac{\partial f_j}{\partial \xi} - \frac{f_j'}{\eta}\int_o^\eta \frac{\partial f_j'}{\partial \xi}\eta d\eta\right]$$

4.2.9

$$t_j f_j + \frac{t_j'}{\eta}\int_o^\eta f_j \eta d\eta - \frac{(\eta h_j)'}{\eta} = \xi\left[f_j \frac{\partial t_j}{\partial \xi} - \frac{t_j'}{\eta}\int_o^\eta \frac{\partial f_j}{\partial \eta}\eta d\eta\right] .$$

4.2.10

The terms on the left hand side are independent of ξ and are readily identified as the only terms required to represent the forced jet (equation 3.2.9 - 3.2.10 in Chapter 3). The terms on the right hand side are seen to vanish identically in the limit as $\xi \to 0$. In particular the buoyancy term in the momentum equation $\xi^2 t_j$ vanishes in this limit.

Equations 4.2.9 and 4.2.10 are seen to exhibit precisely the characteristics which are sought. The pure jet equations are recovered as $\xi \to 0$ and thus the jet solutions are recognized as limiting solutions for vanishing buoyancy. (Note that prior to this there was no formal assurance that the jet solutions were approached smoothly.) It is clear from the equations that the buoyancy terms are controlled by ξ and begin to modify the profiles as the flow moves away from the source or as the rate at which buoyancy (or heat) is added increases.

The transformed integral equations can similarly be shown to be given by

$$\frac{d}{d\xi}\int_o^\infty f_j^2 \eta d\eta = \xi \int_o^\infty t_j \eta d\eta \qquad 4.2.11$$

$$\int_o^\infty f_j t_j \eta d\eta = \frac{1}{2\pi}. \qquad 4.2.12$$

It is clear from the first of these equations that in the limit as $\xi \to 0$, the initial momentum is conserved as it should be for a jet. The second equation expresses the now familiar conservation of energy (or buoyancy).

4.4 Scaling Laws for the Buoyant Jet

The system of equations and integral constraints together with the prescribed initial conditions and boundary conditions contains all the information present in the original set (equations 4.2.1 and 4.2.3). These equations could be solved directly if closure approximations were made; however, there is little to suggest at this point which modifications to the previously used closure approximations might account for the modifying influence of the buoyancy correctly. More can be gained at this point by seeking limiting solutions for small and large values of ξ for which perturbation and asymptotic expansion techniques provide both insight into the nature of the problem and guidance in closing the equations.

A perturbation solution for small values of ξ is developed in Chapter 5, and both analytical and numerical solutions are presented., In Chapter 6, the plume solutions developed in Chapter 2 are shown to be asymptotic solutions to equations 4.2.9 and 4.2.10 for large values

Before developing these solutions, however, it is important to recognize the fact that since equations 4.2.9 and 4.2.10 result from the solution forms given in equations 4.2.7 and 4.2.8, these latter equations can be used as scaling relations to collapse data for all forced plumes or buoyant jets.

As pointed out earlier, the data in the mixed regime of buoyant jets is limited to measurements of centerline temperature (or buoyancy). If the scaling proposed is correct, all of these data should collapse if plotted as

$$\frac{g\beta\Delta T_{\ell}}{T_j} \text{ versus } \xi$$

where T_S is the jet-like similarity variable given hy equation 4.2.8, i.e.,

$$T_j = F_o M_o^{-1/2} x^{-1}.$$

Figure 21, adapted from data given by Kotsovinos (34), summarizes most of the available data on buoyant jets. The data are seen to collapse around a single curve to within the experimental error. This curve is the function $f_j(\eta,\xi)$ for $\eta = 0$. The jet asymptote ($\xi \to 0$) is seen to he horizontal as it should be since the temperature is normalized by jet-like parameters. The plume asymptote ($\xi \to \infty$) is seen to roll off as $\xi^{-2/3}$. This is what is to be expected from the analysis of Chapter 6.

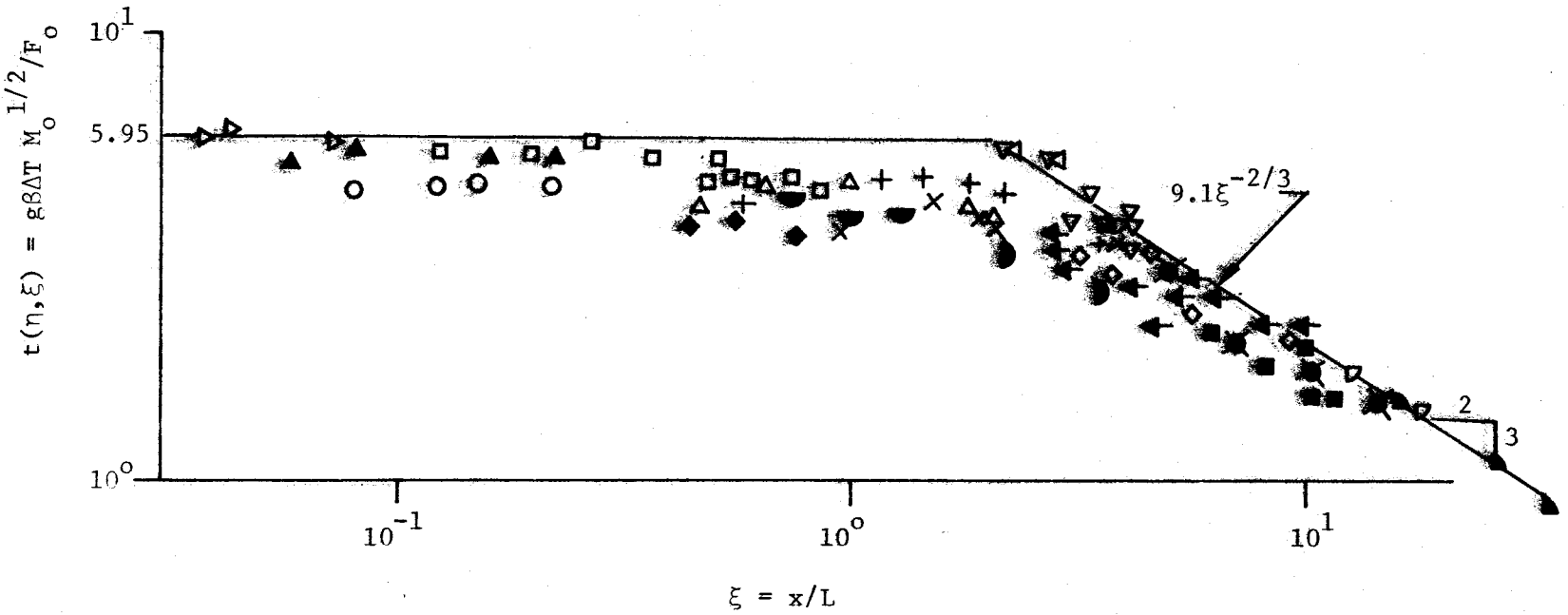

Froude No.	Investigator
10 3.5-7	
1.3-3	Abraham (27)
1.4	George, et al. (23)
251	Hinze (13)
1.7	Rouse (6)
1.0	Ahmad (44)

Froude No.		Investigator
297	121	
70	48	Kotsovinos, et al. (28)
4.2	1.3	
66	17	
8	4	Ryskiewich, et al. (29)
2.1		

Figure 21. Buoyant jet centerline temperature data.

CHAPTER 5

PERTURBATION EXPANSION EQUATIONS AND SOLUTIONS FOR THE NEAR-JET

5.1 The Perturbation Equations[1]

In Chapter 4 it was shown that as ξ approaches zero, the buoyant jet equations reduce to those for the pure jet in Chapter 2. This gives reason to hope that it might be possible to obtain solutions for the near-jet region (small ξ) by expanding about the jet solution. To this end solutions of the following form will be tried:

$$f_j(\eta,\xi) = f_j(\eta) + \xi f_{j1}(\eta) + \xi^2 f_{j2}(\eta) + \cdots$$

$$t_j(\eta,\xi) = t_j(\eta) + \xi t_{j1}(\eta) + \xi^2 t_{j2}(\eta) + \cdots \qquad 5.1.1$$

Before substituting these into the equations of motion the closure problem for the Reynolds stress and turbulent heat flux must be addressed. For the pure jet it is assumed

$$-\overline{uv} = \nu_e \frac{\partial u}{\partial r}$$

$$-\overline{v\theta} = \alpha_e \frac{\partial T}{\partial r} \qquad 5.1.2$$

where

$$\nu_e \equiv U_j x \cdot \frac{1}{R_T}, \qquad \alpha_e = U_j x \frac{1}{R_T P_T} . \qquad 5.1.3$$

---

[1] Development given in Appendix F.

The similarity versions of equations 5.1.2 are

$$S_j'(\eta) = \frac{1}{R_T} f_j'(\eta)$$

$$h_j'(\eta) = \frac{1}{P_T R_T} \quad . \qquad 5.1.4$$

It would be tempting to try a closure scheme which preserves this basic form with R_T a constant. (This could be justified from the fact that R_T for the plume is nearly the same as that for the jet.) Such a closure approximation would be

$$S_j(\eta,\xi) = \frac{1}{R_T} f_j'(\eta,\xi)$$

$$h_j(\eta,\xi) = \frac{1}{P_T R_T} t_j'(\eta,\xi) \qquad 5.1.5$$

and

$$h_j(\eta,\xi) = \frac{1}{P_T R_T} t_j'(\eta,\xi) \quad . \qquad 5.1.6$$

It follows immediately that the Reynolds stress and turbulent heat flux expansions would assume the form

$$S_j(\eta,\xi) = S_{j1}(\eta) + \xi S_{j1}(\eta) + \xi^2 S_{j2}(\eta) + \cdots \qquad 5.1.7$$

and

$$h_j(\eta,\xi) = h_{j1}(\eta) + \xi h_{j1}(\eta) + \xi^2 h_{j2}(\eta) + \cdots \qquad 5.1.8$$

where S_j and h_j are the jet Reynolds stress and turbulent heat flux profiles, respectively.

Although this scheme is attractive, a more general closure approximation can be suggested which allows the eddy viscosity to be directly modified by the increasing effect of buoyancy as the distance from the source increases. It can be argued that this makes sense since the dynamical equations for the turbulence fluctuations indicate clearly that buoyancy can directly affect the turbulence and its transport. Expanding about $\xi \simeq 0$, such a closure mode takes the form:

$$\nu_e = \frac{1}{R_T} (1 + \nu_1 \xi + \nu_2 \xi^2 + \cdots) \qquad 5.1.9$$

and

$$\alpha_e = \frac{1}{P_T R_T} (1 + \alpha_1 \xi + \alpha_2 \xi^2 + \cdots) \qquad 5.1.10$$

where P_T and R_T are taken as the jet values. Note also that choosing different coefficients for the ν_n and α_n allows the turbulent Prandtl number to vary with ξ. Equations 5.1.5 - 5.1.6 can be recovered by setting the ν_n and α_n equal to zero.

Substituting equations 5.1.1 into equations 4.2.9 - 4.2.10, using the closure approximation suggested by equations 5.1.9 - 5.1.10, and equating like powers of ξ yields, to second order, the following set of equations:[2]

Order 1:

$$f_j^2 + \frac{f_j'}{\eta} \int_o^\eta f_j \eta d\eta + \frac{1}{R_T} \frac{(\eta f_j')'}{\eta} = 0$$

$$f_j t_j + \frac{t_j'}{\eta} \int_o^\eta f_j \eta d\eta + \frac{1}{P_T R_T} \frac{(\eta t_j')'}{\eta} = 0$$

---

[2]The equations are developed in Appendix D.

$$\int_o^\eta f_j{}^2 \eta d\eta = \frac{1}{2\pi}$$

$$\int_o^\infty t_j f_j \eta d\eta = \frac{1}{2\pi} \qquad 5.1.11$$

Order ξ:

$$f_j f_{j1} + \frac{f_{j1}{}'}{\eta} \int_o^\eta f_j \eta d\eta + \frac{2f_j{}'}{\eta} \int_o^\infty f_{j1} \eta d\eta$$

$$+ \frac{1}{R_T} \frac{(\eta f_{j1}{}')'}{\eta} = - \frac{\nu_1}{R_T} \frac{(\eta f_j{}')}{\eta}$$

$$f_{j1} t_{j1} + \frac{t_{j1}{}'}{\eta} \int_o^\eta f_j \eta d\eta + \frac{2t_j{}'}{\eta} \int_o^\eta f_{j1} \eta d\eta$$

$$+ \frac{1}{P_T R_T} \frac{(\eta t_{j1}{}')'}{\eta} = - \frac{\alpha_1}{P_T R_T} \frac{(\eta t_j{}')'}{\eta}$$

$$\int_o^\infty f_j f_{j1} \eta d\eta = 0$$

$$\int_o^\infty (f_j t_{j1} + f_{j1} t_j) \eta d\eta = 0 \qquad 5.1.12$$

Order ξ^2:

$$\frac{3f_j{}'}{\eta} \int_o^\eta f_{j2} \eta d\eta + \frac{f_{j2}{}'}{\eta} \int_o^\eta f_j \eta d\eta + \frac{1}{R_T} \frac{(\eta f_{j2}{}')'}{\eta}$$

$$= -t_j - \frac{2f_{j1}{}'}{\eta} \int_o^\eta f_{j1} \eta d\eta - \frac{\nu_1}{R_T} \frac{(\eta f_{j1}{}')'}{\eta} - \frac{\nu_2}{R_T} \frac{(\eta f_j{}')'}{\eta}$$

$$-f_j t_{j2} + f_{j2} t_j + \frac{3t_j'}{\eta} \int_o^\eta f_{j2}\eta d\eta + \frac{t_{j2}'}{\eta} \int_o^\eta f_j \eta d\eta + \frac{1}{P_T R_T} \frac{(\eta t_{j2}')'}{\eta}$$

$$= -\frac{2t_{j1}'}{\eta} \int_o^\eta f_{j1}\eta d\eta - \frac{\alpha_1}{P_T R_T} \frac{(\eta t_{j1}')'}{\eta} - \frac{\alpha_2}{P_T R_T} \frac{(\eta t_j')'}{\eta}$$

$$2\int_o^\infty (2f_j f_{j2} + f_{j1}^2)\eta d\eta = \int_o^\infty t_j \eta d\eta$$

$$\int_o^\infty (f_j t_{j2} + f_{j2} t_j + f_{j1} t_{j1})\eta d\eta = 0 \ . \qquad 5.1.13$$

It is interesting to note that the buoyancy does not begin to modify the momentum equation until the ξ^2 equation. This could have been anticipated from equation 4.2.9 where ξ^2 multiplies the buoyancy term. The appropriate boundary condition is that all solutions vanish as $\eta \to \infty$.

These equations can be solved directly if the unknown coefficients R_T, P_T, $\nu_1, \ldots$, and $\alpha_1, \ldots$ are specified. If the equations are carried to fourth order, this requires that 10 coefficients be specified which is hopeless considering the buoyant jet data that are available. An analytical solution is developed for which ν_1, $\nu_3, \ldots$, α_1, $\alpha_3, \ldots$ are equal to zero.

The neglect of the odd coefficients in the eddy viscosity and diffusivity expansion has an interesting consequence which implies that the solutions to the equations for odd powers of ξ are identically zero. This follows from the fact that the perturbation equations for order higher than unity are linear. The equations of odd order in ξ are homogeneous, and both the equations and the integral constraints are

satisfied by trivial solutions. The linearity insures uniqueness. The equations corresponding to even powers of ξ have a buoyancy forcing term which depends on the solution of two orders less. Therefore, these are not homogeneous and must be solved.

In summary, in the following sections an analytical solution will be developed in which the even coefficients $\nu_2, \nu_4, \ldots$, and $\alpha_2, \alpha_4, \ldots$ are non zero. Attempts to derive other types of analytical solutions were unsuccessful and the results of numerical computations are presented.

5.2 Analytical Solutions for the Perturbation Equations[3]

A close inspection of the eddy viscosity solution for the jet given by Schlichting (32), and the eddy viscosity solution for the plume given by Yih (15), provided a strong motivation to seek an analytical solution for the buoyant jet. The eddy viscosity solutions for the jet and plume gave the following relations for the mean profiles

$$f_j(\eta) = 2A_jB_j\lambda_j(1+A_j\eta^2)^{-2}$$

$$t_j(\eta) = C_j\lambda_j^2(1+A_j\eta^2)^{-2}$$

$$f_p(\eta) = 2A_pB_p\lambda_p(1+A_p\eta_p^2)^{-2}$$

$$t_p(\eta) = C_p\lambda_p^2(1+A_p\eta^2)^{-4} \qquad 5.2.1$$

---

[3] Development given in Appendix G.

where the plume solution is that obtained by Yih for a Prandtl number of 2.0. The jet solution is applicable for all Prandtl numbers. For a Prandtl number of 2.0 the jet and plume velocity profiles have the same dependence on η, $(1+A\eta^2)^{-2}$ and $(1+A\eta^2)^{-4}$ respectively. However, there is no reason to believe that the A's are the same in both cases although the values are close enough to make this idea appealing. The best fit for the jet data is obtained at a turbulent Reynolds number ($R_T=1/\lambda$) of 56, and of 60 in the plume case (with Q factor ignored). Again these values are the same to within experimental error.

Based on the analytical solutions it was determined that the form of the plume and jet solutions for $P_T=2$ does not identically satisfy the buoyant jet equations for all ξ as had been hoped. It was found to be possible, however, to derive an analytical solution to the perturbation equations for the case where α_1, α_3,... and ν_1, ν_3,... are zero and the even values simply related to R_T.

For this case the dimensionless momentum and temperature equations 4.2.10 - 4.2.11 are rewritten as

$$\lambda f'' + [\lambda + \int_o^\eta f\eta d\eta]\frac{f'}{\eta} + f^2 + \xi[\frac{f'}{\eta}\int_o^\eta \frac{\partial f}{\partial \xi}\eta d\eta - f\frac{\partial f}{\partial \xi}] + \xi^2 t = 0 \qquad 5.2.2$$

$$\frac{\lambda}{\sigma}t'' + [\frac{\lambda}{\sigma} + \int_o^\eta f\eta d\eta]\frac{t'}{\eta} + ft + \xi[\frac{t'}{\eta}\int_o^\eta \frac{\partial f}{\partial \xi}\eta d\eta - f\frac{\partial t}{\partial \xi}] = 0 \qquad 5.2.3$$

where

$$\lambda = 1/R_T$$

$$\sigma = P_T$$

$$f = f(\eta,\xi)$$

$$t = t(\eta,\xi)$$

$$f'' = \frac{\partial^2 f(\eta,\xi)}{\partial \eta 2}$$

$$t'' = \frac{\partial^2 t(\eta,\xi)}{\partial \eta 2} \quad . \qquad 5.2.4$$

A solution of the following form is assumed

$$f(\eta,\xi) = \phi(\eta)\ F(\xi)$$

$$t(\eta,\xi) = \phi^2(\eta)\ G(\xi) \qquad 5.2.5$$

where

$$\phi(\eta) = (1+A\eta^2)^{-2}$$

$$F(\xi) = B_o + \xi^2 B_2 + \xi^4 B_4 + \cdots$$

$$G(\xi) = C_o + \xi^2 C_2 + \xi^4 C_4 + \cdots$$

$$\lambda(\xi) = \lambda_o + \lambda_2 \xi^2 + \lambda_4 \xi^4 + \cdots$$

$$\lambda_o = 1/R_T$$

$$\lambda_2 = \nu_2/R_T$$

$$\lambda_4 = \nu_4/R_T \quad . \qquad 5.2.6$$

Substitution of ϕ, F, and G into the previous momentum and temperature relations yields

$$\lambda F\phi'' + [\lambda F + F^2 \int_o^\eta \phi\eta d\eta] \frac{\phi'}{\eta} + F^2\phi^2$$

$$+ \xi F'F[\frac{\phi'}{\eta} \int_o^\eta \phi\eta d\eta = \phi^2] + \xi^2 G\phi^2 = 0 \qquad 5.2.7$$

$$\frac{\lambda}{\sigma} G\phi^{2}'' + [\frac{\lambda}{\sigma} G + FG \int_o^\eta \phi\eta d\eta] \frac{\phi^{2}'}{\eta} + FG\phi^3$$

$$\xi[F'G \frac{\phi^{2}'}{\eta} \int_o^\eta \phi\eta d\eta - FG'\phi^3] = 0 \qquad 5.2.8$$

where

$$\phi'' = \frac{\partial^2\phi}{\partial\eta^2} \qquad \phi' = \frac{\partial\phi}{\partial\eta}$$

$$\phi^{2}'' = \frac{\partial^2(\phi^2)}{\partial\eta^2} \qquad \phi^{2}' = \frac{\partial(\phi^2)}{\partial\eta}$$

$$F' = \frac{\partial F}{\partial\xi} \qquad G' = \frac{\partial G}{\partial\xi} \quad . \qquad 5.2.9$$

The integral constraints 4.2.12 - 4.2.13 assume the form

$$\frac{d}{d\xi} [F^2 \int_o^\infty \phi^2\eta d\eta] = \xi G \int_o^\infty \phi^2\eta d\eta \qquad 5.2.10$$

$$2\pi F \cdot G \int_o^\infty \phi^2\eta d\eta = 1.0 \quad . \qquad 5.2.11$$

Substitution of the assumed forms for $F(\xi)$ and $G(\xi)$ into the integral constraints provide the following relationships for the coefficients of ξ:

$$B_o^2 = 3A/\pi \qquad C_o = \frac{5A}{\pi B_o}$$

$$B_2 = C_o/4B_o \qquad C_2 = \frac{B_2 C_o}{B_o}$$

$$B_4 = \left(\frac{C_4}{4} - B_2^2\right)\frac{1}{2B_o} \qquad C_4 = \frac{B_2 C_2 + B_4 C_o}{B_o} . \qquad 5.2.12$$

If the functional relations for ϕ, F, and G are substituted into equations 5.2.7 - 5.2.8, two equations are obtained which contain zeroth, second, and fourth order terms in ξ. Requiring that the sum of all terms to the same order in ξ equal zero results in six equations which can be solved. These equations have been solved with the following result:

$$A = \frac{3}{64\pi\lambda_o^2} \qquad C_o = \frac{5}{8\pi\lambda}$$

$$B_o = \frac{3}{8\pi\lambda} \qquad C_2 = -\frac{25}{36}$$

$$B_2 = \frac{5}{12} \qquad C_4 = \frac{125\pi\lambda}{3^4}$$

$$B_4 = -\frac{25\pi\lambda}{2.3^3} \qquad C_6 = -\frac{10.25^2 \cdot \pi^2 \cdot \lambda^2}{3^7}$$

$$B_6 = +\frac{125\pi^2\lambda^2}{3^6} \qquad 5.2.13$$

The coefficients are substituted into the functional relations 5.2.5 - 5.2.6 to obtain the final form of the solutions to sixth order as

$$f(\eta,\xi) = (1+A\eta^2)^{-2}\left(\frac{3}{8\pi\lambda} + \xi^2\frac{5}{12} - \xi^4\frac{25\pi\lambda}{2.3^3} + \xi^6\frac{125\pi^2\lambda^2}{3^6}\right)$$

$$t(\eta,\xi) = (1+A\eta^2)^{-4}\left(\frac{5}{8\pi\lambda} - \xi^2\frac{25}{36} + \xi^4\frac{125\pi\lambda}{3^4} - \xi^6\frac{10\cdot 25^2\pi^2\lambda^2}{3^7}\right) . \qquad 5.2.14$$

No attempt was made to extend the solution beyond sixth order, and the sixth order terms are evaluated from the integral constraint only. Recall that these solutions are valid only for a Prandtl number of 2.0.

5.3 Solutions for the Perturbation and Analytical Equations

The perturbation equations presented in Section 5.1 require that a total of 10 coefficients be specified if the solution is carried to fourth order in ξ. In Section 5.2 it was shown that an analytical solution exists for the odd coefficient ν_1, ν_3,..., and α_1, α_3,... equal zero. The analytical solution is applicable for $P_T = 2.0$; the case for arbitrary P_T must be solved numerically. Unfortunately, a solution requires that six coefficients be specified if the calculations are to be carried to sixth order in ξ since, unlike the analytical solution, the coefficients are not determined by the solution. The experimental data simply do not justify the choice of this many constants. Consequently, the numerical solution for the perturbation equations is restricted to the original eddy viscosity closure model given by equations 5.1.2 and 5.1.3. In this case all coefficients ν_1, ν_2,..., and α_1, α_2,... are set equal to zero,

which results in a set of equations which are manageable to sixth order in ξ. As an example equations 5.1.11 - 5.1.13 reduce to

$$f_j^2 + \frac{f_j'}{\eta}\int_o^\eta f_j \eta d\eta + \frac{1}{R_T}\frac{(\eta f_j')'}{\eta} = 0$$

$$f_j t_j + \frac{t_j'}{\eta}\int_o^\eta f_j \eta d\eta + \frac{1}{P_T R_T}\frac{(\eta t_j')'}{\eta} = 0$$

$$\int_o^\infty f_j^2 \eta d\eta = \frac{1}{2\pi}$$

$$\int_o^\infty t_j f_{1j} \eta d\eta = \frac{1}{2\pi} \qquad 5.3.1$$

$$\frac{3f_j'}{\eta}\int_o^\eta f_{j2}\eta d\eta + \frac{f_{j2}'}{\eta}\int_o^\eta f_j \eta d\eta + \frac{1}{R_T}\frac{(\eta f_{j2}')'}{\eta} = -t_j$$

$$- f_j t_{j2} + f_{j2} t_j + \frac{3t_j'}{\eta}\int_o^\eta f_{j2}\eta d\eta + \frac{t_{j2}'}{\eta}\int_o^\eta f_j \eta d\eta$$

$$+ \frac{1}{P_T R_T}\frac{(\eta t_{j2}')'}{\eta} = 0$$

$$4\int_o^\infty f_j f_{j2}\eta d\eta = \int_o^\infty t_j \eta d\eta$$

$$\int_o^\infty (f_j \cdot t_{j2} + f_{j2} t_j)\eta d\eta = 0 \quad .$$

The solutions to these equations to sixth order in ξ are obtained using the scheme presented in Section 2.5. The procedure is simplified

since the temperature equations are homogeneous and can be solved without iteration.

5.4 Results of the Perturbation Solutions

The centerline temperature and velocity have been calculated from the numerical and analytical solutions as a function of ξ and are shown in Figures 22 and 23. Figure 22 also shows a line which represents the temperature data presented in Figure 21. Figure 23 shows only the velocity asymptotes for large and small ξ.

Both analytical and numerical solutions show the expected trends to higher values of ξ (for a small perturbation expansion) than anticipated. The validity at high values of ξ can be explained by the form of the exact solution in equations 5.2.14 which suggests that the appropriate expansion parameter is $\xi/\sqrt{R_T}$, rather than ξ. Since $\xi = 1$ corresponds to $\xi/\sqrt{R_T} \simeq 0.13$, the stability of the expansion to high values of ξ is not surprising.

There are differences in the two solutions which are shown in Figures 22 and 23. These differences apparently result from the difference in the turbulent Prandtl number ($P_T = 1$ for the numerical solution and $P_T = 2$ for the analytical solution) and the ξ-dependent eddy viscosity used in the analytical solution. The differences in the solutions are most evident in Figure 22 where the increased lateral diffusion for the analytical solution causes the centerline temperature to drop more rapidly.

Figures 24 and 25 show the temperature and velocity profiles computed from the analytical solution for $\xi = 0$, 1.0, and 1.5. The temperature profile has narrowed slightly with increasing ξ, while the velocity profile has broadened. Both these trends are in accord with the expected jet and plume limits.

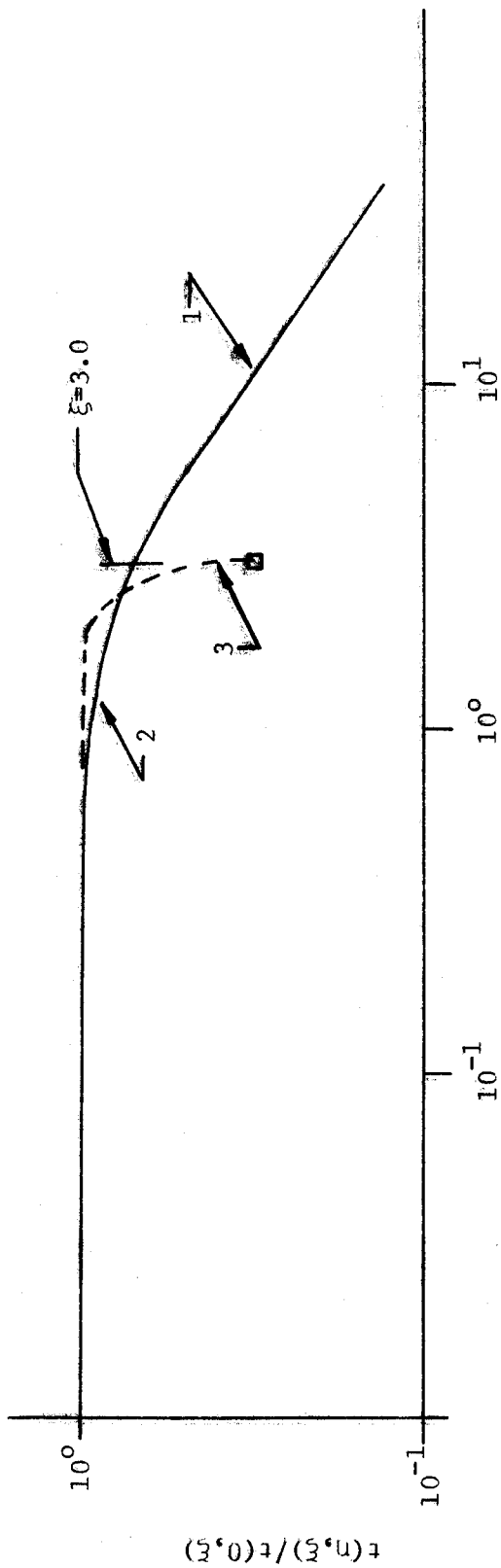

Figure 22. Comparison of buoyant jet mean centerline temperature with calculated analytical and perturbation solutions. 1 - Fit to data Figure 21. 2 - Analytical solution, $P_T = 2.0$, $R_T = 55$ valid for $\xi \leq 3.0$. 3 - Perturbation solution $P_T = 1.0$, $R_T = 55$.

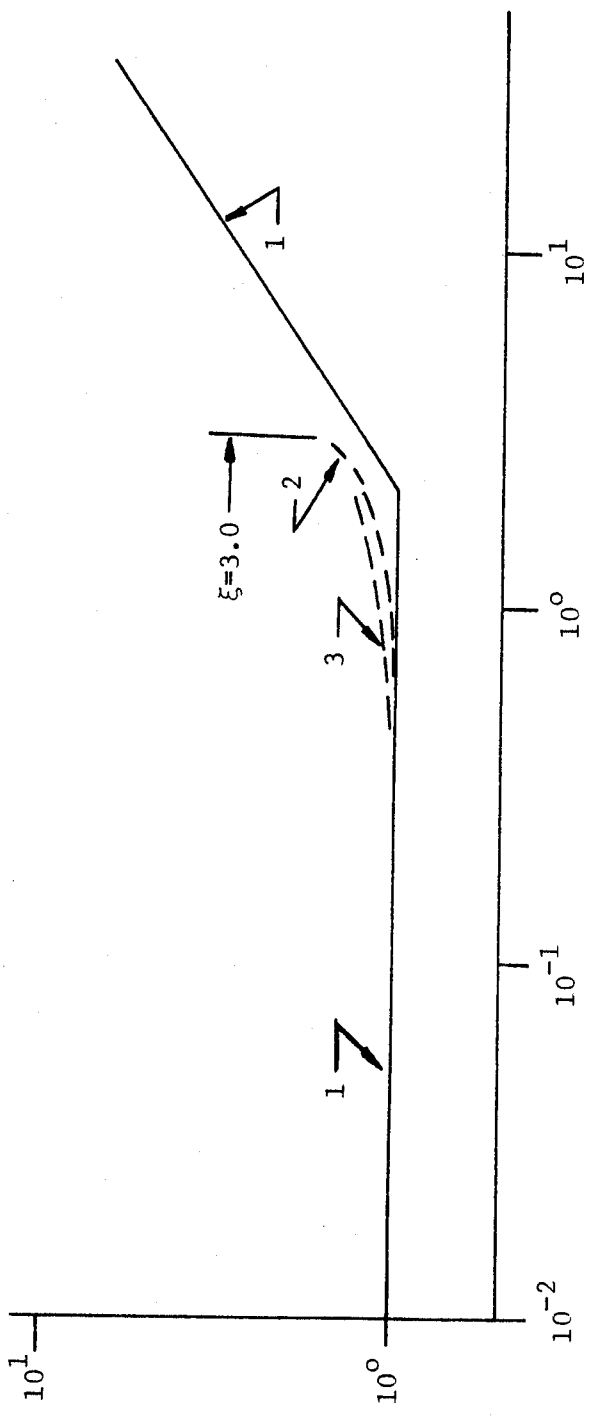

Figure 23. Buoyant jet mean centerline velocity calculated from analytical and perturbation solutions. 1 - Asymptotes. 2 - Analytical solution, P_T = 2.0, R_T = 55. 3 - Perturbation solution, P_T = 1.0, R_T = 55.

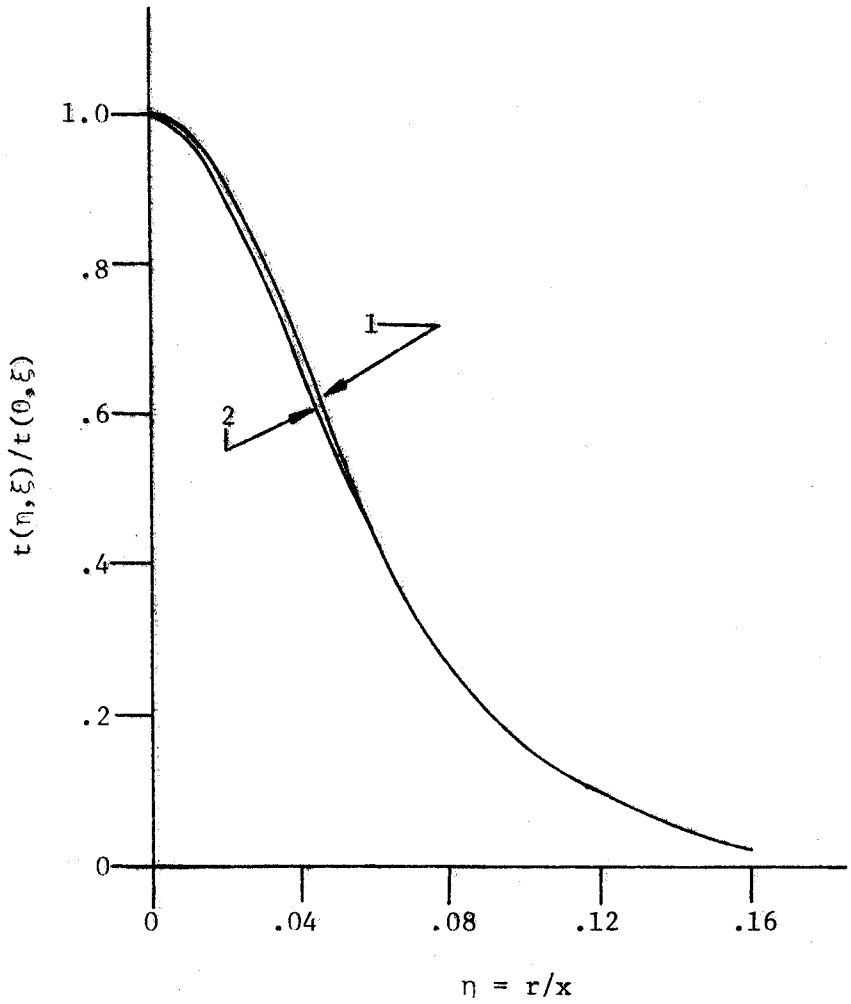

Figure 24. Buoyant jet mean temperature profiles computed from analytical solution, R_T = 55, P_T = 2.0. 1 - ξ = 0. 2 - ξ = 1.0, 1.5.

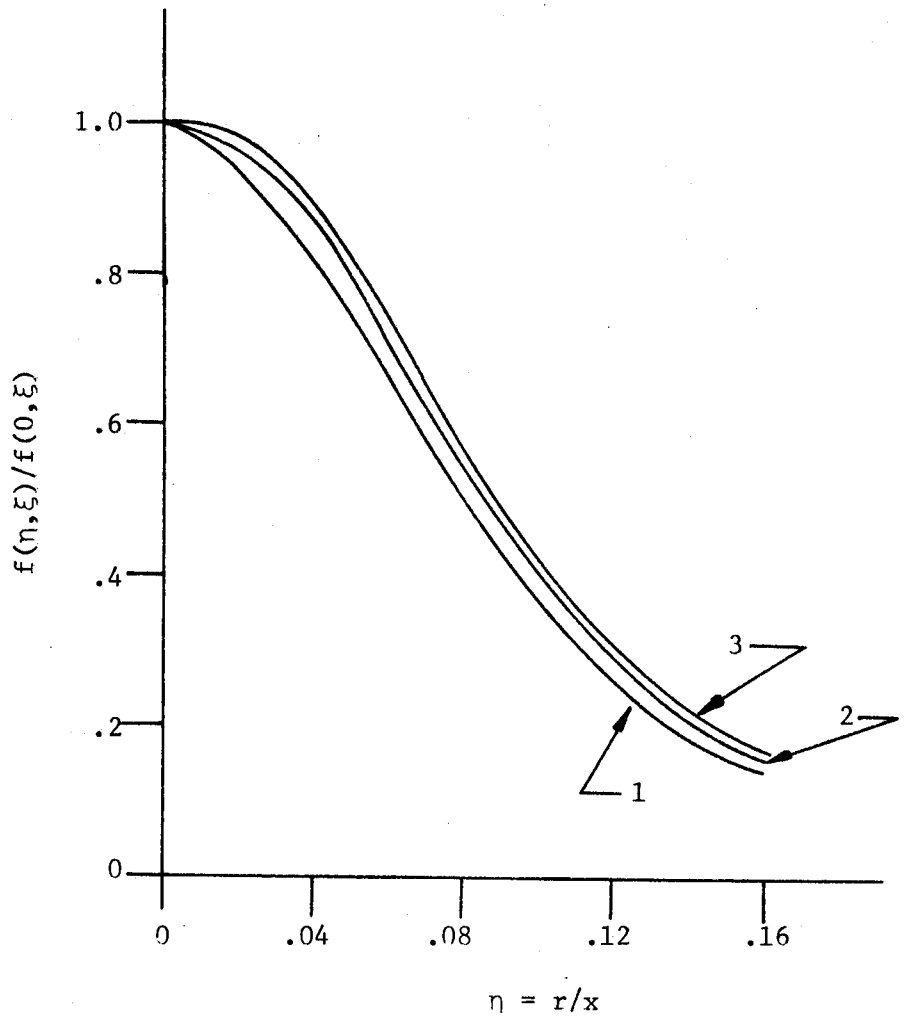

Figure 25. Buoyant jet mean velocity profiles computed from analytical solution, R_T = 55, P_T = 2.0. 1 - ξ = 0. 2 - ξ = 1.0. 3 - ξ = 1.5.

Figures 26 and 27 present the temperature and velocity profiles calculated from the numerical solutions. While the velocity profile is modified slightly in a direction opposite to that of the analytical solution, the differences are within the integration errors, and the velocity profile may be assumed unchanged. The temperature profile, on the other hand, shows a marked width decrease. While some narrowing is expected, the amount indicated is larger than expected.

In summary, the perturbation analyses show trends that might be expected if the jet and plume data are considered; an increase in velocity with slight broadening of the profile; and a decrease in temperature with a narrowing of the profile. Also, the ξ-dependence of the eddy viscosity on physical grounds is important, even in the initial stages of the buoyant jet's development.

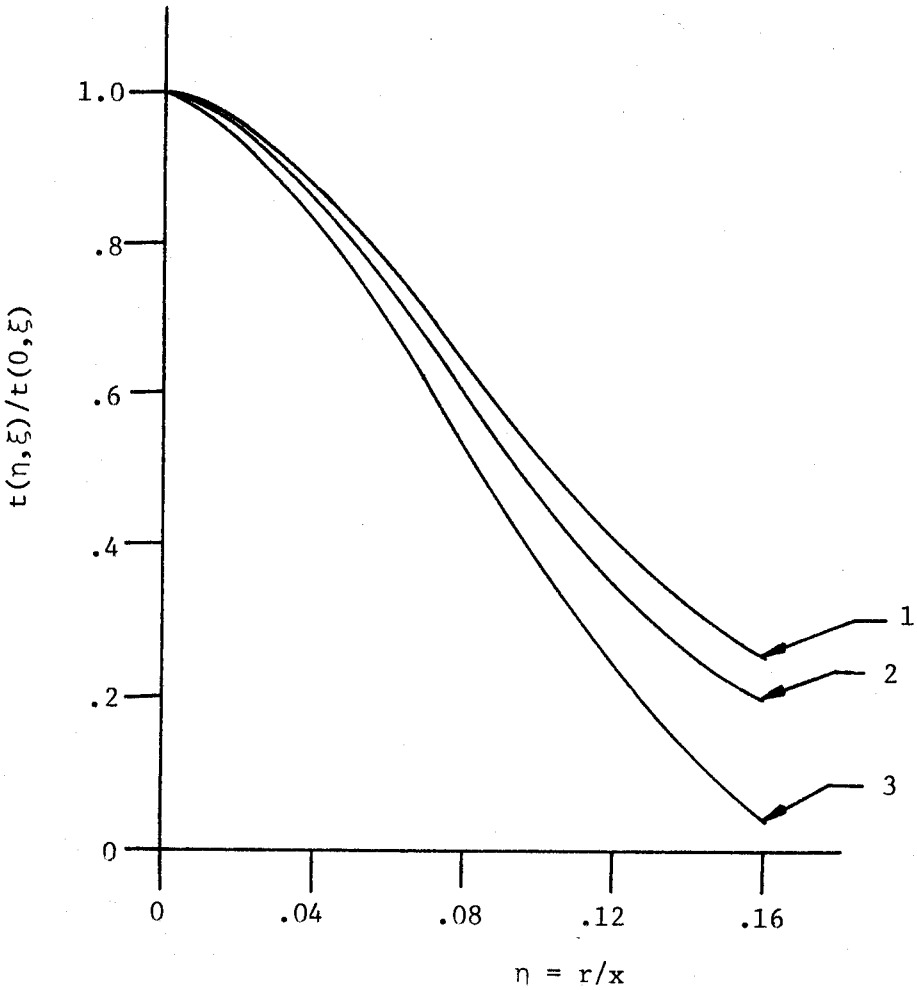

Figure 26. Buoyant jet mean temperature profiles from numerical solution of perturbation equations, R_T = 55, P_T = 1.0, Q = 0.9. 1 - ξ = 0. 2 - ξ = 1.0. 3 - ξ = 1.5.

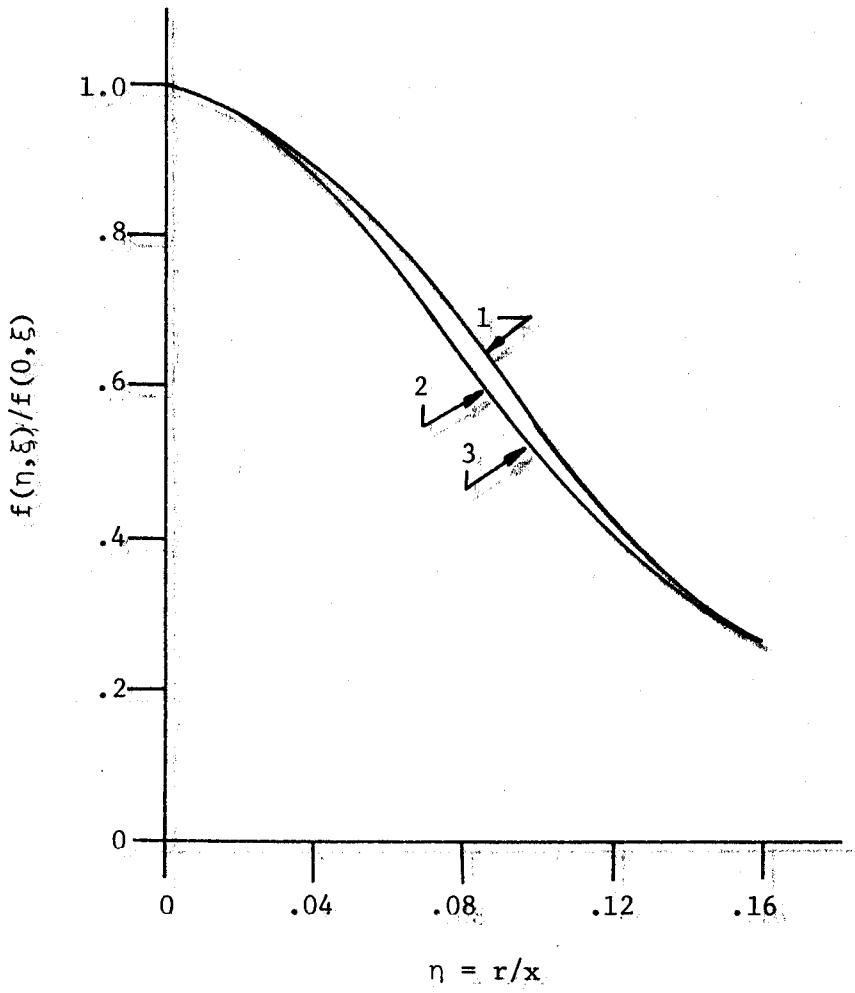

Figure 27. Buoyant jet mean velocity profiles from numerical solution of perturbation equations, $R_T = 55$, $P_T = 1.0$, $Q_1 = 0.85$. 1 - $\xi = 0$. 2 - $\xi = 1.0$. 3 - $\xi = 1.5$.

CHAPTER 6

ASYMPTOTIC EQUATIONS AND SOLUTIONS FOR THE NEAR-PLUME

6.1 The Dynamical Equations $\xi \to \infty$

The equations 4.2.9 and 4.2.10 derived in Chapter 4 continue to describe the flow, even though ξ appears explicitly on the right hand side. (This must be so since these equations were derived directly from the momentum and temperature equations.) These equations, however, are not easily analyzed at large values of ξ; it is not obvious from these equations whether or not the plume equations derived in Chapter 3 are in fact the asymptotic equations of a buoyant jet. A transformation will be developed which can be applied to the equations of motion and results in equations which are easily manageable at large ξ and which make clear the role of the plume equations and solutions derived earlier.

Transformed variables which become plume-like as the buoyancy is increased and/or the distance from the source is increased can be developed using a new dimensionless coordinate

$$\varepsilon = L/x = \xi^{-1} \quad . \qquad 6.1.1$$

It is clear that both the limits desired are achieved in the limit as $\varepsilon \to o$ $(\xi \to \infty)$.

Since it is desired that the equations of motion reduce to the plume equations as $\varepsilon \to o$, equations 4.2.1 through 4.1.3 are transformed using plume-like variables:

$$\eta = r/x \qquad g\beta\Delta T = T_p t(\eta,\xi)$$

$$\varepsilon = L/x \qquad -\overline{uv} = R_p S(\eta,\xi)$$

$$U = U_p f(\eta,\xi) \qquad -\overline{v\theta} = H_p h(\eta,\xi)$$

$$V = U_p k(\eta,\xi) \qquad 6.1.2$$

where

$$U_p = F_o^{1/3}\, x^{-1/3}$$

$$T_p = F_o^{2/3}\, x^{-5/3}$$

$$R_p = F_o^{2/3}\, x^{-2/3}$$

$$H_p = F_o\, x^{-2} \quad . \qquad 6.1.3$$

It is appropriate to recall that the plume solutions derived in Chapter 2 do not involve the M_o momentum discharge at the source (assumed zero). This fact is reflected in the above transformation since M_o enters only through ε which approaches zero with M_o.

After substitutions and elimination of v using continuity, the momentum and temperature equations become

$$\frac{1}{3} f^2 + \frac{5}{3}\frac{f'}{\eta}\int_o^\eta f\eta d\eta + \frac{(\eta S')'}{\eta} + t = \varepsilon\left(\frac{f'}{\eta}\int_o^\eta \frac{\partial f}{\partial \varepsilon}\,\eta d\eta - f\,\frac{\partial f}{\partial \varepsilon}\right)$$

6.1.4

$$\frac{5}{3} ft + \frac{5}{3} \frac{t'}{\eta} \int_o^\eta f\eta d\eta + \frac{(\eta h')'}{\eta} = \varepsilon \left(\frac{t'}{\eta} \int_o^\eta \frac{\partial f}{\partial \varepsilon} \eta d\eta - f \frac{\partial t}{\partial \varepsilon} \right) .$$

6.1.5

The left-hand sides of these equations are seen to be identical to those equations derived in Chapter 2 for the pure buoyant plume. The right hand side consists solely of terms which vanish identically in the limit as $\varepsilon \to o$ or $\xi \to \infty$. Thus the plume solutions derived earlier do, in fact, represent asymptotic solutions to the buoyant jet. Moreover, these solutions are approached smoothly as the limit is approached.

The integral equations 4.2.11 0 4.2.12 can be similarly transformed to yield

$$\frac{4}{3} \int_o^\infty f^2 \eta d\eta - \int_o^\infty t\eta d\eta = 2\varepsilon \int_o^\infty f \frac{\partial f}{\partial \varepsilon} \eta d\eta \qquad 6.1.4$$

$$\int_o^\infty ft\eta d\eta = \frac{1}{2\pi} . \qquad 6.1.5$$

The second of these integral equations is the familiar statement that energy (or buoyancy) is conserved. The first integral equation shows that the difference between the total momentum flux at any cross-section and that produced by buoyancy vanishes as $\varepsilon \to o$ or as $\xi \to \infty$. In other words the initial momentum is dominated by that momentum continuously produced by buoyancy, and plume-like flow is approached.

6.2 The Plume Solution as an Asymptotic Solution

In Chapter 2, an eddy viscosity model was used to calculate solutions to the turbulent buoyant plume. In the preceding section it was shown that these solutions represent an asymptotic solution to the buoyant

jet equations. Here it is shown how this asymptotic solution can be expressed in the jet-like coordinates of Chapter 4.

Following the representation of Chapters 4 and 5 (equations 4.2.7 - 4.2.8) it is noted that

$$U = U_j f_j(\eta,\xi)$$

$$\Delta T = T_j t_j(\eta,\xi) \qquad 6.2.1$$

and that

$$\lim_{\xi\to\infty} U = U_p f_p(\eta) \qquad 6.2.2$$

$$\lim_{\xi\to\infty} \Delta T = T_p t_p(\eta) \qquad 6.2.3$$

where f_p and t_p are the plume profiles.

It follows immediately that

$$\lim_{\xi\to\infty} f_j(\eta,\xi) = \frac{U_p}{U_j} f_p(\eta) \qquad 6.2.4$$

$$\lim_{\xi\to\infty} t_j(\eta,\xi) = \frac{T_p}{T_j} t_p(\eta) \; . \qquad 6.2.5$$

From the defining equation for U_j, T_j, U_p, T_p, and L (equations 4.2.8, 6.1.3 - 4.1.5, respectively) it is easy to show that

$$\frac{U_p}{U_j} = \frac{F_o^{1/3}\, x^{-1/3}}{M_o^{1/2}\, x^{-1}} = \left(\frac{x}{L}\right)^{2/3} = \xi^{2/3} \qquad 6.2.6$$

and

$$\frac{T_p}{T_j} = \frac{F_o^{2/3} x^{-5/3}}{F_o M_o^{-1/2} x^{-1}} = \left(\frac{x}{L}\right)^{-2/3} = \xi^{-2/3} \quad . \qquad 6.2.7$$

Thus the asymptotic solutions to the buoyant jet equations (equations 4.2.9 - 4.2.10) are given by

$$\lim_{\xi \to \infty} f_j(\eta,\xi) = \xi^{2/3} f_p(\eta) \qquad 6.2.8$$

and

$$\lim_{\xi \to \infty} t_j(\eta,\xi) = \xi^{-2/3} t_p(\eta) \qquad 6.2.9$$

where f_p and t_p are the plume solutions of Chapter 2.

6.3 Perturbation Equations for the Near-Plume[1]

In Chapter 5, an expansion of the buoyant jet equations about the jet solution yielded equations which describe the near-jet. It is clear from the preceding sections that similar techniques can be applied to the near-plume by expanding around the plume solution. Expanded solutions to equations 6.1.4 - 6.1.5 of the following form will be developed

$$f_p(\eta,\xi) = f_{2p}(\eta) + \varepsilon f_{p1}(\eta) + \varepsilon^2 f_{p2}(\eta) + \cdots$$

$$t_p(\eta,\xi) = t_{2p}(\eta) + \varepsilon t_{p1}(\eta) + \varepsilon^2 t_{p2}(\eta) + \cdots \qquad 6.3.1$$

where the plume solutions f_p and t_p are known from Chapter 2.

Before developing these solutions the closure problem is addressed. By analogy with the development of Chapter 5

---

[1] Development technique same as Appendix F.

$$-\overline{uv} = \nu_e \frac{\partial u}{\partial r}$$

$$-\overline{v\theta} = \alpha_e \frac{\partial T}{\partial r} \quad . \qquad 6.3.2$$

Since there is no a priori reason that ν_t, α_t are not dependent on ε, these terms are expected in powers of ε to obtain

$$\nu_e = \frac{U_p X}{R_T} (1 + \nu_1 \varepsilon + \nu_2 \varepsilon^2 + \cdots)$$

$$\alpha_e = \frac{\nu_e}{P_T} = \frac{U_p X}{P_T R_T} (1 + \alpha_1 \varepsilon + \alpha_2 \varepsilon^2 + \cdots) \qquad 6.3.3$$

where ν_1, ν_2 and α_1, α_2 are unknown coefficients, as are R_T and P_T, which we have previously encountered. Allowing ν_n and α_n to be different allows the turbulent Prandtl number to vary with ε.

Substituting equations 6.3.2 - 6.3.3 into equations 6.1.4 - 6.1.7 and grouping terms of similar order in ε yields the following sets of equations to second order in ε:

Order 1:

$$\frac{1}{3} f_p^2 + \frac{5}{3} \frac{f_p'}{\eta} \int_o^\eta f_p \eta d\eta + \frac{1}{R_T} \frac{(\eta f_p')'}{\eta} + t_p = 0$$

$$\frac{5}{3} f_p t_p + \frac{5}{3} \frac{t_p'}{\eta} \int_o^\eta f_p \eta d\eta + \frac{1}{P_T R_T} \frac{(\eta t_p')'}{\eta} = 0$$

$$\frac{4}{3} \int_o^\infty f_p^2 \eta d\eta = \int_o^\infty t_p \eta d\eta$$

$$\int_o^\infty f_p t_p \eta d\eta = \frac{1}{2\pi} \qquad 6.3.4$$

Order ε:

$$\frac{5}{3} f_p f_{p1} + \frac{5}{3} \frac{f_p'}{\eta} \int_o^\eta f_{p1} \eta d\eta + \frac{5}{3} \frac{f_{p1}'}{\eta} \int_o^\eta f_p \eta d\eta$$

$$+ \frac{1}{R_T} \frac{(\eta f_{p1}')'}{\eta} + t_{p1} = \frac{\nu_1}{R_T} \frac{(\eta f_p')'}{\eta} \qquad 6.3.5$$

$$\frac{8}{3} f_p t_{p1} + \frac{5}{3} f_{p1} t_p + \frac{5}{3} \frac{t_p'}{\eta} \int_o^\eta f_{p1} \eta d\eta + \frac{5}{3} \frac{t_{p1}'}{\eta} \int_o^\eta f_p \eta d\eta$$

$$+ \frac{1}{P_T R_T} \frac{(\eta t_{p1}')'}{\eta} = \frac{\alpha_1}{P_T R_T} \frac{(\eta t_p')'}{\eta}$$

$$\frac{2}{3} \int_o^\infty f_p f_{p1} \eta d\eta = \int_o^\infty t_{p1} \eta d\eta$$

$$\int_o^\infty (f_p t_{p1} + f_{p1} t_p) \eta d\eta = 0 \qquad 6.3.5$$

Order ε^2:

$$\frac{2}{3} f_p f_{p2} - \frac{1}{3} \frac{f_p'}{\eta} \int_o^\eta f_{p2} \eta d\eta + \frac{5}{3} \frac{f_{p2}'}{\eta} \int_o^\eta f_p \eta d\eta + t_{p2}$$

$$+ \frac{1}{R_T} \frac{(\eta f_{p2}')'}{\eta} = - f_{p1}' - \frac{2}{3} \frac{f_{p1}'}{\eta} \int_o^\eta f_{p1} \eta d\eta + \frac{\nu_1}{R_T} \frac{(\eta f_{p1}')'}{\eta}$$

$$+ \frac{\nu_2}{R_T} \frac{(\eta f_p')'}{\eta}$$

$$\frac{11}{3} f_p t_{p2} + \frac{5}{3} f_{p2} t_p + \frac{11}{3} \frac{t_p'}{\eta} \int_o^\eta f_{p2} \eta d\eta + \frac{t_{p2}'}{\eta} \int_o^\eta f_p \eta d\eta$$

$$+\frac{1}{P_T R_T}\frac{(\eta t_{p2}')'}{\eta} = -f_{p1}t_{p1} + \frac{t_{p1}'}{\eta}\int_o^\eta f_{p1}\eta d\eta + \frac{\alpha_1}{P_T R_T}\frac{(\eta t_{p1}')'}{\eta}$$

$$+\frac{\alpha_2}{P_T R_T}\frac{(\eta t_p')'}{\eta}$$

$$\frac{4}{3}\int_o^\infty (f_p t_{p2} + \frac{3}{2} f_{p1}^2)\eta d\eta = \int_o^\infty t_{p2}\eta d\eta$$

$$\int_o^\infty (f_p t_{p2} + f_{p2}t_p + f_{p1}t_{p1})\eta d\eta = 0 \quad . \qquad 6.3.6$$

Equations 6.3.4, the order zero equations, are, of course, the plume equations treated in Chapter 3 which have already been shown to be the asymptotic forms of the buoyant jet equations. Equations 6.3.5 and 6.3.6 are seen to be sets of coupled linear differential equations with homogeneous integral constraints.

In the analysis of the near-jet, the values of ν_1, ν_3,... and α_1, α_3,..., were arbitrarily assigned the value zero. This was done since the data was felt to be inadequate to determine them and since the equations remained coupled to ξ through the temperature field. The data for the near-plume are even more inadequate than for the near-jet, and the same assumption must be made here.

These assumptions result in an eddy viscosity which is made up of two limiting forms

$$\nu_e = \begin{cases} \frac{1}{R_T} U_j x & \text{small } \xi \\ \frac{1}{R_T} U_p x & \text{large } \xi \end{cases}$$

or in dimensionless jet-like variables

$$\nu(\xi) = \begin{cases} \dfrac{1}{R_T} & \text{small } \xi \\ \xi^{2/3} \cdot 1/R_T & \text{large } \xi \end{cases}$$

While these assumptions work well for the near-jet, it has interesting consequences for the near-plume. Examination of the order ε equations with $\alpha_1 = \nu_1 = o$ indicates these equations are linear, homogeneous equations in f_{p1} and t_{p1}. Moreover, $f_{p1} = o$, $t_{p1} = 0$ is a solution satisfying the boundary conditions. Since the equations are linear, this solution is unique.

The conclusion above is similar to that arrived at for the near-jet equations. However, unlike the near-jet, a similar inspection of the ε^2 and higher order equations reveals that all are solved by trivial solutions. Hence by neglecting the additional perturbation of the eddy viscosity and diffusivity, the possibility of a perturbation solution involving powers of ε has been negated. Dr. Philip Morris, a member of this thesis committee, has indicated that it may be possible to develop alternate expansions if the boundary conditions of the higher order functions are investigated more closely. Explanations for this failure may be either, that the correct asymptotic expansion is not dependent only on powers of ε, or that the higher order expansion terms depend on outer expansions which modify the boundary conditions at infinity.

Since the data remain inadequate to determine additional coefficients beyond P_T and R_T, there appears to be little point in continuing this type of analysis. Thus the results are limited to the asymptotic

or in dimensionless jet-like variables

$$\nu(\xi) = \begin{cases} \dfrac{1}{R_T} & \text{small } \xi \\ \xi^{2/3} \cdot 1/R_T & \text{large } \xi \end{cases}$$

While these assumptions work well for the near-jet, it has interesting consequences for the near-plume. Examination of the order ε equations with $\alpha_1 = \nu_1 = o$ indicates these equations are linear, homogeneous equations in f_{p1} and t_{p1}. Moreover, $f_{p1} = o$, $t_{p1} = 0$ is a solution satisfying the boundary conditions. Since the equations are linear, this solution is unique.

The conclusion above is similar to that arrived at for the near-jet equations. However, unlike the near-jet, a similar inspection of the ε^2 and higher order equations reveals that all are solved by trivial solutions. Hence by neglecting the additional perturbation of the eddy viscosity and diffusivity, the possibility of a perturbation solution involving powers of ε has been negated. Dr. Philip Morris, a member of this thesis committee, has indicated that it may be possible to develop alternate expansions if the boundary conditions of the higher order functions are investigated more closely. Explanations for this failure may be either, that the correct asymptotic expansion is not dependent only on powers of ε, or that the higher order expansion terms depend on outer expansions which modify the boundary conditions at infinity.

Since the data remain inadequate to determine additional coefficients beyond P_T and R_T, there appears to be little point in continuing this type of analysis. Thus the results are limited to the asymptotic

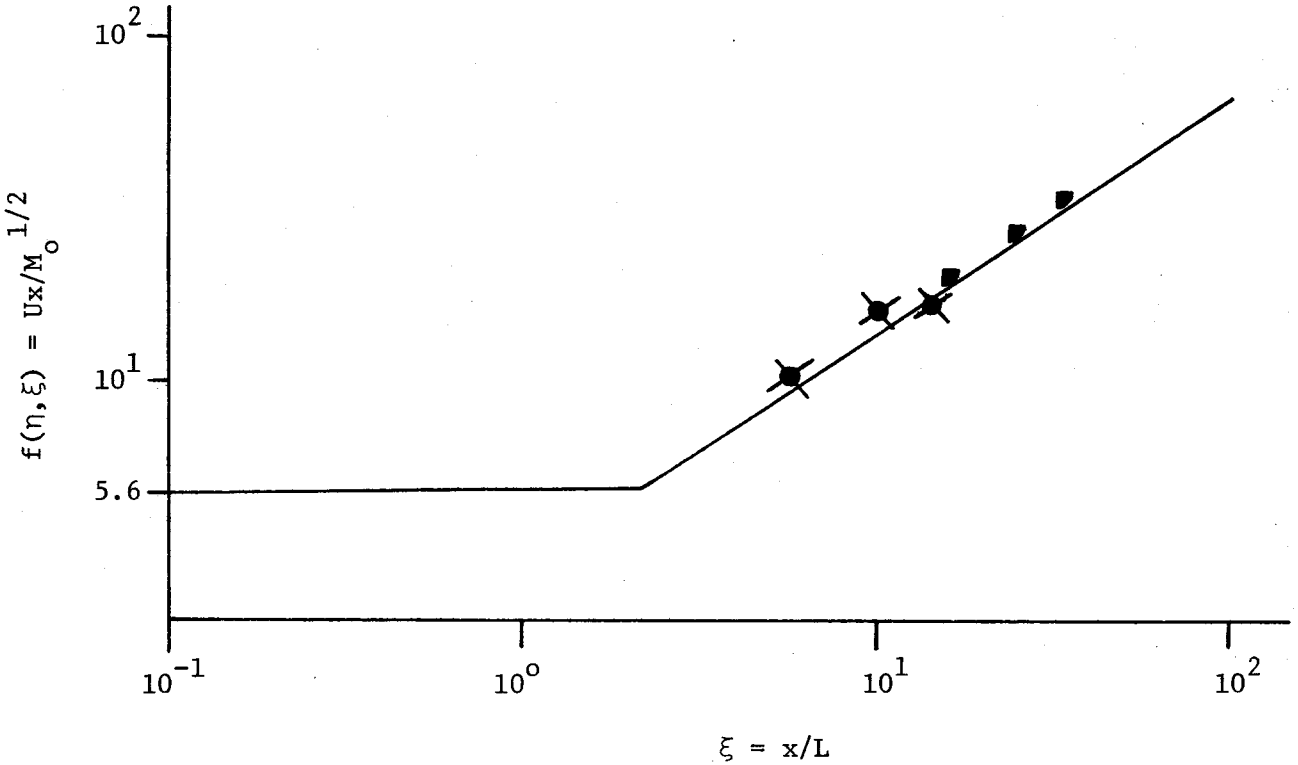

Figure 28. Buoyant jet mean centerline velocity asymptotes and data. ✕ - George, et al. (23). ● - Ahmad (44).

to the residual momentum effects. The cold jet results give the small-ξ asymptote $\overline{U}\, x/M_o^{1/2} \simeq 5.6$.

In summary, there is abundant evidence that the plume represents the asymptotic state of the buoyant jet, and that the approach to that state is completely dependent on the values of ξ. Moreover, the introduction of the length scale L and its use in graphing data has proven to be invaluable in evaluating the state of plume-like data.

CHAPTER 7

A COMPOSITE CLOSURE MODEL AND SOLUTION FOR THE BUOYANT JET

7.1 Asymptotic Considerations

In the preceding chapters the dynamical equations for the buoyant jet have been examined in the limits of the near-jet ($\xi \to o$) and the plume ($\xi \to \infty$). The appropriate eddy viscosity for the jet was shown from dimensional and physical considerations to be

$$\nu_T = \frac{1}{R_T} [M_o^{1/2} x^{-1}] \cdot x \ . \qquad 7.1.1$$

Similar considerations for the plume led to an eddy viscosity formulation for the plume as

$$\nu_T = \frac{1}{R_T} [F_o^{1/3} x^{-1/3}] \cdot x \qquad 7.1.2$$

or

$$\nu_T = \frac{1}{R_T} [M_o^{1/2} x^{-1}] \xi^{2/3} \qquad 7.1.3$$

using $\xi \equiv x/L$ and L defined by

$$L = M_o^{3/4}/F_o^{1/2} \ . \qquad 7.1.4$$

In dimensionless jet-like coordinates these results are summarized by the following:

$$\frac{\nu_T}{M_o^{1/2}} = \begin{cases} \dfrac{1}{R_T} & \text{as} \quad \xi \to \infty \\ \dfrac{\xi^{2/3}}{R_T} & \text{as} \quad \xi \to \infty \end{cases} . \qquad 7.1.5$$

While the data, strictly interpreted, indicate that R_T is not constant (56 for the jet, 60 for the plume), it certainly is consistent within experimental error (particularly in view of the results of Chapter 3) to assume R_T to be constant throughout the flow.

An immediately obvious choice for a composite ν_T which has the correct asymptotic behavior is:

$$\frac{\nu_T}{M_o^{1/2}} = \frac{1}{R_T}\left(1 + \xi^{2/3}\right) . \qquad 7.1.6$$

Inspection of the centerline velocity and temperature plots of Figures 20 and 21 reveals two things: First, the centerline values vary little from their jet values until $\xi > 1$; Second, the constant eddy viscosity perturbation solution of Section 5.3 differs little from the measurements over this same range. Thus it would seem that although equation 7.1.6 has the right asymptotic behavior, it developes too rapidly as ξ increases. This suspicion has been confirmed by numerical calculation using equation 7.1.6.

What is needed then is a function which permits the $\xi^{2/3}$ term in the eddy viscosity to dominate for $\xi > 1$ while minimizing its effect for $\xi < 1$. Since the considerations of Chapters 4 and 5 have indicated that ξ^2 is the appropriate expansion parameter for the near-jet, the control function should preserve this dependence.

An empirical formulation which controls the $\xi^{2/3}$ term in an appropriate manner is:

$$\nu(\xi) = \frac{\nu_T}{M_o^{1/2}} = \frac{1}{R_T} \left(1 + \xi^{2/3}(1-\exp(-\alpha\xi^{4/3}))\right) . \qquad 7.1.7$$

It is easy to show by expanding the exponential for small values of ξ that the desired near-jet dependence on ξ is obtained; i.e.,

$$\frac{\nu_T}{M_o^{1/2}} \simeq \frac{1}{R_T} \left[1 + \alpha\xi^2 + \frac{1}{2}\alpha^2\xi^4 + \cdots\right] . \qquad 7.1.8$$

This is recognized as the form of the eddy viscosity obtained from the exact solution of Section 5.2. The success of that solution and the direct correspondence of the terms in the expansion indicates that the appropriate choice for α in equation 7.1.7 might be the value of ν_2 from equation 5.1.9; that is,

$$\alpha = \nu_2 = \frac{10\pi}{3}\frac{1}{R_T} . \qquad 7.1.9$$

Using $R_T = 55.5$, results in $\alpha \simeq 0.19$.

The closure model given by equation 7.1.8 and 7.1.9 is thus seen to result naturally from the perturbation and asymptotic solution and thus provides a natural "bridge" for the mixed region of the buoyant jet where neither the plume nor jet solution technique is applicable.

In the following section a numerical integration of equations 4.2.9 and 4.2.10 is described in which the equations are closed by

$$S(\eta,\xi) = \nu(\xi)\frac{\partial}{\partial\eta} f(\eta,\xi) \qquad 7.1.10$$

$$h(\eta,\xi) = \frac{1}{P_T}\nu(\xi)\frac{\partial}{\partial\eta} t(\eta,\xi) \qquad 7.1.11$$

where $\nu(\xi)$ is determined by equation 7.1.7. P_T equal to unity has been established as being a satisfactory choice at both jet and plume limits and therefore will be used here. A value of $\alpha \simeq 0.2$ was used in the computation and was found to provide satisfactory results.

7.2 The Numerical Integration

The governing partial differential equations 4.2.9 and 4.2.10 are parabolic, being initial valued in the ξ-direction and boundary valued in the η-direction. This characterization suggests that a marching scheme be used in ξ-direction starting with the jet profiles, solving a boundary value problem at each value of ξ for the profiles of f and t. A simple implicit method, using first-order accurate backward-difference formuli for $\partial f/\partial\xi$ and $\partial t/\partial\xi$, was employed to resolve the ξ-dependence. This method is unconditionally stable (see Roache (45)) for the linear convection-diffusion equation and, hence, superior in stability characteristics to the equivalent explicit procedure using a forward difference in the ξ-direction.

Equations 4.2.9 and 4.2.10 are written

$$\frac{\nu}{R_T}\frac{\partial^2 f}{\partial\eta^2} + \left(\frac{\nu}{R_T} + F\right)\frac{1}{\eta}\frac{\partial f}{\partial\eta} + f^2 + \xi^2 t$$

$$= \xi\left[f\,\frac{f-f(\xi-\Delta\xi,\eta)}{\Delta\xi} - \frac{\partial f}{\partial\eta}\,\frac{F-F(\xi-\Delta\xi,\eta)}{\Delta\xi}\right] \qquad 7.2.1$$

$$\frac{\nu}{R_T P_T}\frac{\partial^2 t}{\partial\eta^2} + \left(\frac{\nu}{R_T P_T} + F\right)\frac{1}{\eta}\frac{\partial t}{\partial\eta} + ft$$

$$= \xi\left[f\,\frac{t-t(\xi-\Delta\xi,\eta)}{\Delta\xi} - \frac{\partial t}{\partial\eta}\,\frac{F-F(\xi-\Delta\xi,\eta)}{\Delta\xi}\right] . \qquad 7.2.2$$

For given upstream profiles $f(\xi-\Delta\xi,\eta)$ and $t(\xi-\Delta\xi,\eta)$, determined via solution at the previous station or from the jet solution at the initial station, equations 7.2.1 and 7.2.2 are in effect ordinary differential equations to be solved for f and t as functions of η. Since 7.2.1 and 7.2.2 are coupled and nonlinear, an iterative method is used to solve them. Each step in the iterative procedure involves solving a linearized set of equations obtained by considering the coefficients in equations 7.2.1 and 7.2.2 to be known.

$$\frac{\nu}{R_T}\frac{\partial^2 f}{\partial\eta^2} + \left(\frac{\nu}{R_T} + \tilde{F}\right)\frac{1}{\eta}\frac{\partial f}{\partial\eta} + \tilde{f}\, f + \xi^2\,\tilde{t}$$

$$= \xi\left[\tilde{f}\,\frac{f-f(\xi-\Delta\xi,\eta)}{\Delta\xi} - \frac{\partial f}{\partial\eta}\,\frac{\tilde{F}-F(\xi-\Delta\xi,\eta)}{\Delta\xi}\right] \qquad 7.2.3$$

$$\frac{\nu}{R_T P_T}\frac{\partial^2 t}{\partial\eta^2} + \left(\frac{\nu}{R_T P_T} + \tilde{F}\right)\frac{1}{\eta}\frac{\partial t}{\partial\eta} + \tilde{f}t$$

$$= \xi\left[\tilde{t}\,\frac{t-t(\xi-\Delta\xi,\eta)}{\Delta\xi} - \frac{\partial t}{\partial\eta}\,\frac{\tilde{F}-F(\xi-\Delta\xi,\eta)}{\Delta\xi}\right] \qquad 7.2.4$$

where the tilde denotes the function determined from the previous iteration or the function extrapolated from the previous two upstream stations in the case of the first iteration. Rearranging these equations:

$$\frac{\nu}{R_T}\frac{\partial^2 f}{\partial\eta^2} + \left[\frac{\nu}{R_T} + \tilde{F} + \frac{\tilde{F}-F(\xi-\Delta\xi,\eta)}{\Delta\xi}\right]\frac{\partial f}{\partial\eta} + \left(1 - \frac{\xi}{\Delta\xi}\right)\tilde{f}\, f$$

$$= -\frac{\xi}{\Delta\xi}\,\tilde{f}\, f(\xi-\Delta\xi,\eta) - \xi^2\tilde{t} \qquad 7.2.5$$

$$\frac{\nu}{R_T P_T}\frac{\partial^2 t}{\partial \eta^2} + \left(\frac{\nu}{P_T R_T} + \tilde{F} + \frac{\tilde{F} - F(\xi-\Delta\xi,\eta)}{\Delta\xi}\right)\frac{\partial t}{\partial \eta} + \left(1 - \frac{\xi}{\Delta\xi}\right)\tilde{f}\, t$$

$$= -\frac{\xi}{\Delta\xi}\tilde{f}\, t(\xi-\Delta\xi,\eta) \quad . \qquad 7.2.6$$

Both of these equations are of the form

$$PY'' + QY' + RY = S \quad . \qquad 7.2.7$$

As discussed in Section 2.5 the finite differencing of such an equation leads to a set of linear algebraic equations whose coefficient matrix is tridiagonal. The solution to the algebraic equations is accomplished by an elimination procedure.

The solution for the f and t profiles at a given ξ-station consists of first extrapolating from two previous stations to determine initial guesses of f and t which are set equal to $\tilde{f}$ and $\tilde{t}$. $\tilde{F}$ is determined by integrating $\eta\tilde{f}$. Equations 7.2.5 and 7.2.6, in the form of algebraic equations, are solved for new values of the profiles f and t. These profiles are then set equal to $\tilde{f}$ and $\tilde{t}$ and the procedure is repeated until convergence is achieved, i.e.,

$$(f-\tilde{f})/\tilde{f} \leq \varepsilon \qquad\qquad (t-\tilde{t})/\tilde{t} \leq \varepsilon$$

for every η. The quantity ε is a prescribed tolerance taken to be 10^{-5} in the calculations.

7.3 The Results of the Composite Model

The calculated values of centerline velocity and temperature are plotted in the now familiar jet coordinates in Figures 29 and 30. The eddy viscosity used is given by equation 7.1.7 with $R_T = 55.5$, $\alpha = 0.2$

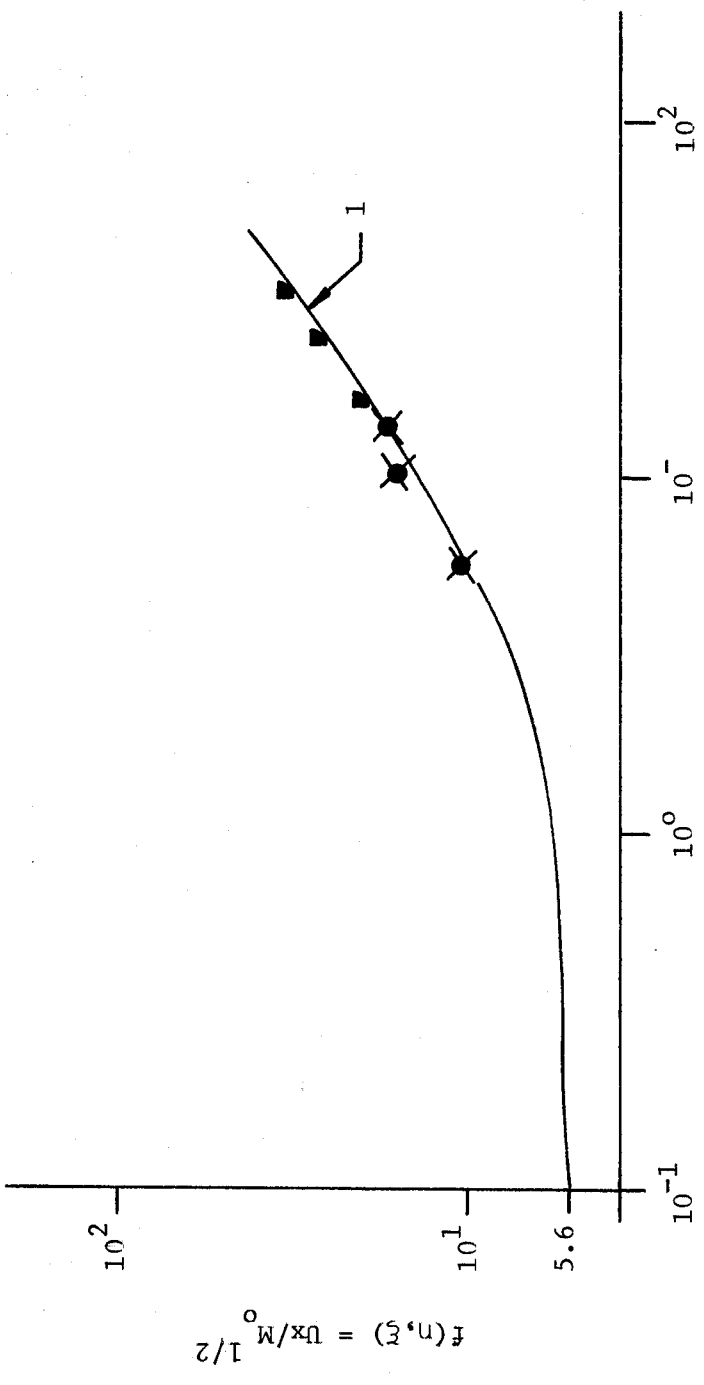

Figure 29. Comparison of calculated buoyant jet mean centerline velocity with data. 1 - Equations 7.2.1 and 7.2.2. ✕ - George, et al. (23). ◗ - Ahmad (44).

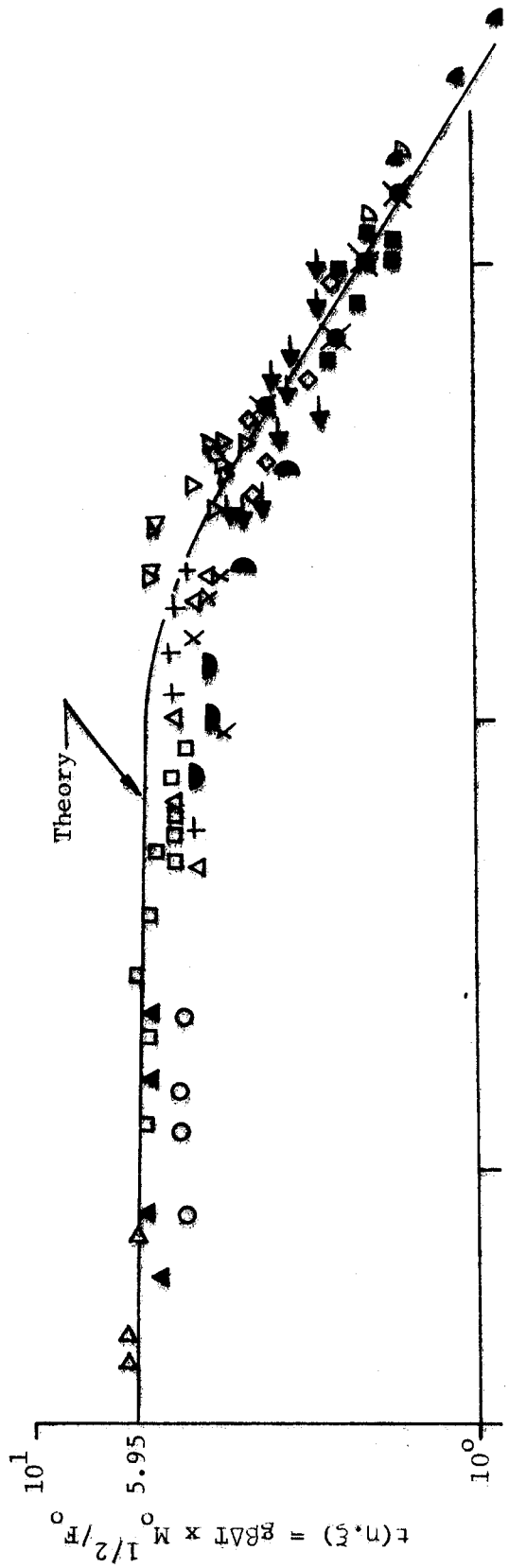

Figure 30. Comparison of calculated buoyant jet centerline temperature. Theory - equations 7.2.1 and 7.2.2. Data - Figure 19.

and $P_T = 1.0$. The results are seen to be in excellent agreement with the experimental results, even at large values of ξ. The fact that such a simple model can begin at the jet and so accurately predict the plume results with only one additional parameter α is indeed surprising.

The calculated profiles of temperature and velocity, normalized to unity, are shown in Figures 31 and 32 for ξ = o, 2.5, 5, and 10. The value ξ = o is, of course, the jet; ξ = 10 is in the fully developed plume region while ξ = 2.5 and 5.0 are in the mixed region. Also shown in Figure 31 are the plume data of George, et al. (23) and the jet data of Becker, et al. (43). The recommended velocity profiles from Chapters 2 and 3 are included in Figure 32.

Immediately apparent is the fact that the shape of the temperature profile is nearly independent of ξ. Thus to within experimental error, the shape of the temperature profile appears to be constant and independent of buoyancy.

The calculated velocity profiles do show a definite increase in width with increasing ξ. While the predicted increase is greater than that suggested by the data, the errors present in the measurements and the integration errors in the calculations make a quantitative evaluation difficult. It is believed that a substantial improvement in velocity measuring techniques is needed before a more sophisticated analysis is warranted.

In summary, the proposed composite eddy viscosity model appears to be remarkably successful, both in predicting the profile shapes and the centerline values. Moreover, the solutions indicate that the profile shapes are only weakly dependent on bouyancy, a fact which would have been very difficult to determine from the scattered experimental data

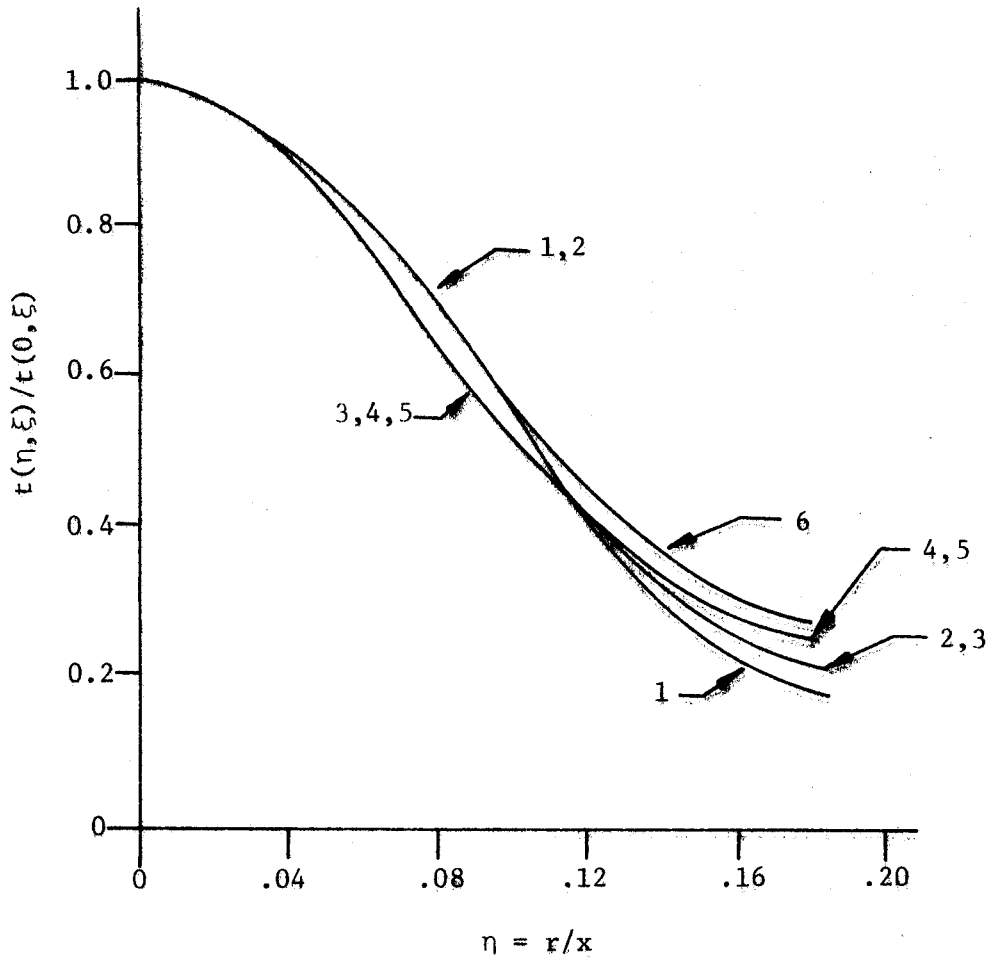

Figure 31. Comparison of buoyant jet mean temperature profile and theory. 1 - Measured George, et al. (23). 2 - Measured Becker, et al. (41). 3 - Theory $\xi = 0$. 4 - Theory $\xi = 2.5$. 5 - Theory $\xi = 5.0$. 6 - Theory $\xi = 10.0$.

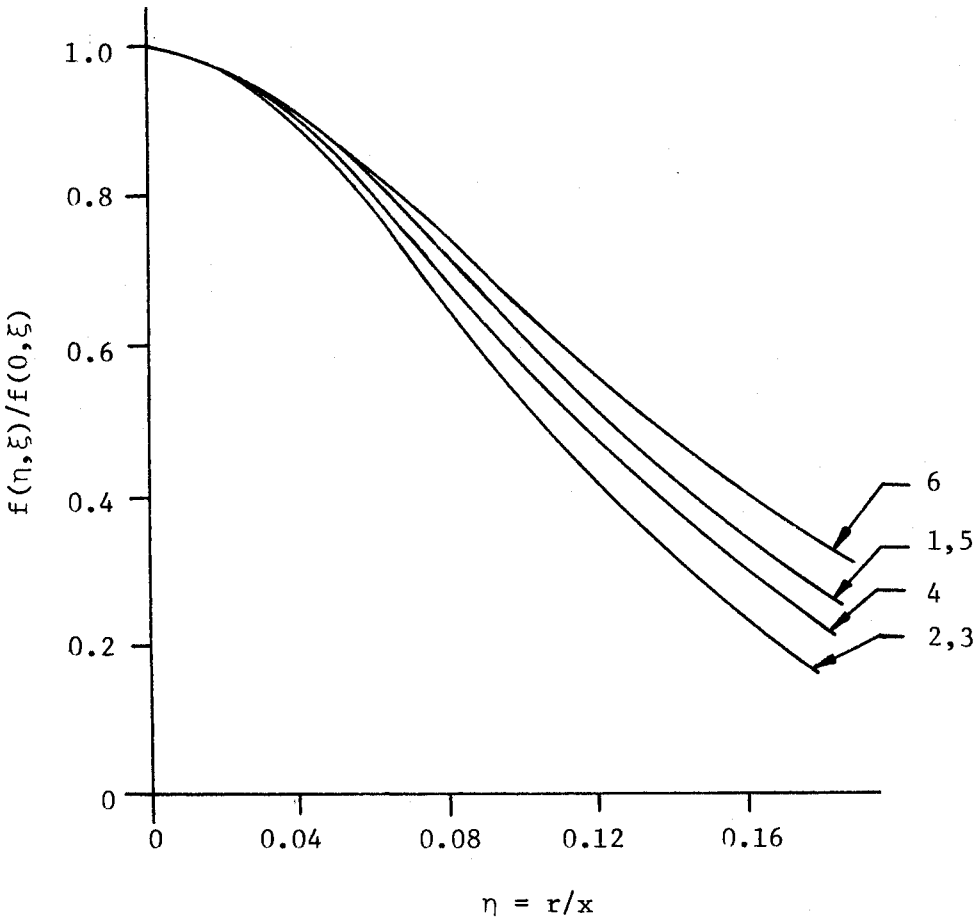

Figure 32. Comparison of buoyant jet mean velocity profiles. 1 - Plume equation 2.8.2. 2 - Jet equation 3.5.5. 3 - Theory $\xi = 0$. 4 - Theory, $\xi = 2.5$. 5 - Theory, $\xi = 5.0$. 6 - Theory, $\xi = 10$.

alone. It should be noted that the solution retains the effects of the choices of $Q_1 = 0.85$ and $Q = 0.9$ which were used to determine the starting profiles.

CHAPTER 8

ENTRAINMENT

8.1 Dependence of Mass Entrainment on Bouyancy

Entrainment is of interest in jet and plume flows because of the dilution introduced by this process and the integral models used by other authors. The mass per unit length entrained by the flow, ρE, is given by

$$E = \lim_{r\to\infty} (2\pi r V) = \frac{d}{dx} (2\pi \int_o^\infty Urdr) \qquad 8.1.1$$

which is the rate of change in the mass flux in the axial direction. In the ξ-coordinate system the normalized entrainment is given by

$$\frac{E}{2\pi M_o^{1/2}} = \frac{d}{d\xi} (\xi \int_o^\infty f(\eta,\xi)\eta d\eta) \ . \qquad 8.1.2$$

For the case of a buoyant jet the entrainment coefficient is bounded by the jet and plume values. These can be estimated using the profiles given by equations 2.8.2 and 3.5.5. Using equation 3.5.5, the proposed jet mean velocity profile, yields

$$\frac{E_j}{2\pi M_o^{1/2}} = \frac{f_j(o)}{2A_1} = 0.07 \qquad 8.1.3$$

and using equation 2.8.2, the proposed plume mean velocity profile, yields

$$\frac{E_p}{2\pi M_o^{1/2}} = \frac{5}{3} \frac{f_p(o)}{2A_p} \xi^{2/3} = 0.10\xi^{2/3} \ . \qquad 8.1.4$$

Although these values are functionally correct, the magnitude is probably too large because the function $\eta f(\eta)$ extends over a large range in η outside the core region where, because of the intermittency, the proposed profiles might not be valid. This is shown in Figure 33, which depicts the intermittency γ from Wygnanski and Fiedler (21), $\eta f(\eta)$ and $\eta f^2(\eta)$ as a function of η as calculated from equation 3.5.5. Note that the integrand of the entrainment function extends outside the range of γ whereas the major part of the momentum flux is contained within the range of γ. Since intermittency could have a major influence on the eddy viscosity, and hence the velocity profile outside the range for which $\gamma \sim 1$, it can be expected to have an important influence on the entrainment coefficient.

In summary, it appears that intermittency may be required in the model to accurately calculate the mass flux integral and the entrainment.

8.2 Evaluation of Entrainment Hypotheses

In spite of the reservations of the previous section, an evaluation of existing entrainment hypotheses can be made. Of particular interest because of its widespread use is the entrainment hypothesis of Morton, et al. (2). Also examined is the more recent suggestion of List and Imberger (33).

Morton, et al. (2) define an entrainment function from the equivalent top hat profiles as follows:

$$b^2 W = 2 \int_o^\infty Urdr \qquad 8.2.1$$

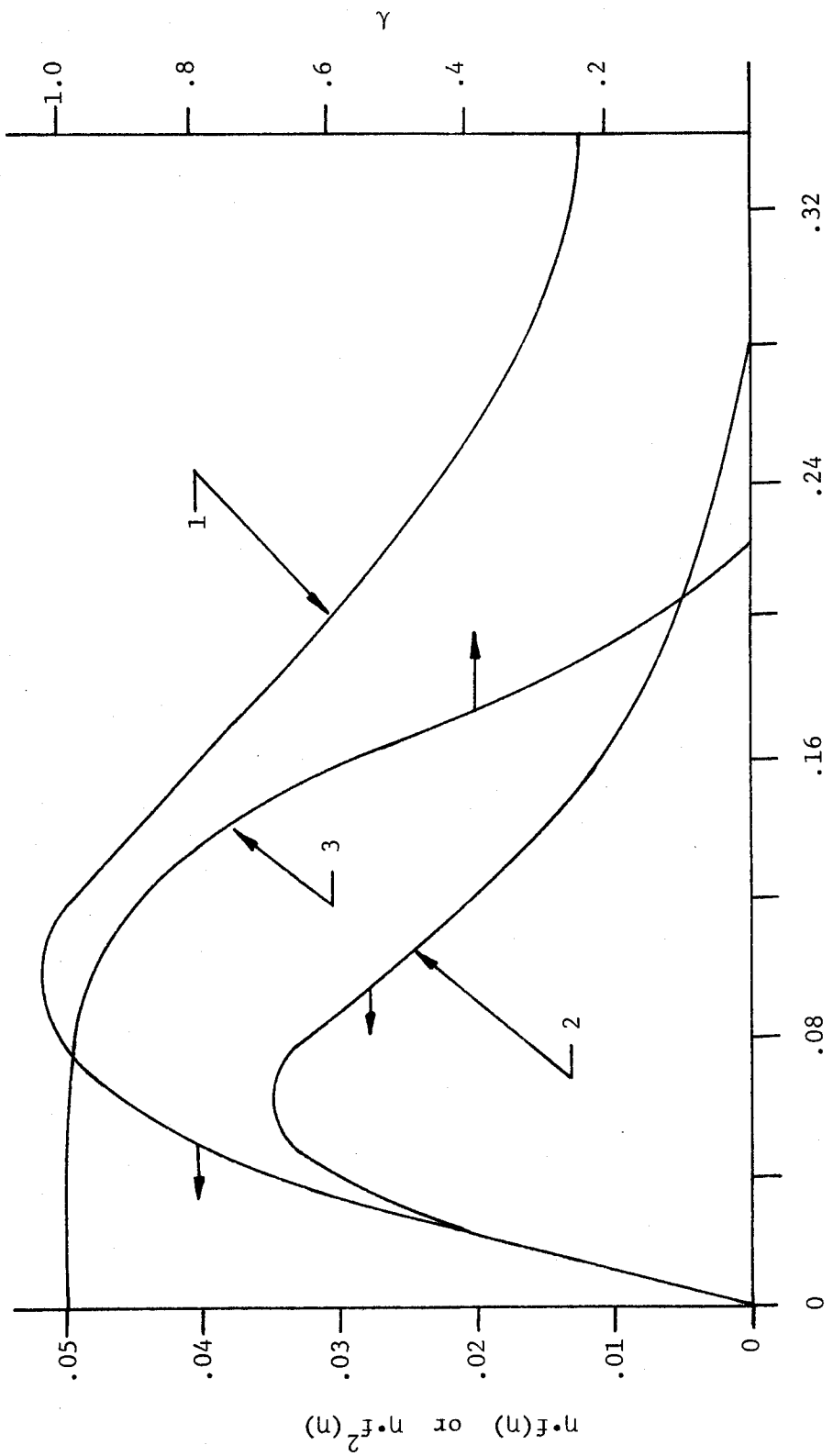

Figure 33. Comparison of mass flux parameter, momentum flux parameter, and intermittency. 1 - $\eta f(\eta)$. 2 - $\eta f^2(\eta)$. 3 - γ.

$$b^2W^2 = 2\int_o^\infty U^2 r dr \qquad 8.2.2$$

$$E' = \frac{d}{dx}\left(2\int_o^\infty Ur dr\right) \qquad 8.2.3$$

where b is the radius of the top hat velocity W. It is assumed that the entrainment coefficient α is given by

$$\alpha = \frac{E'}{2bW} = \text{constant} \; . \qquad 8.2.4$$

Applying this hypothesis to the jet and plume velocity profiles 2.8.2 and 3.5.5 gives the data shown in Table 5.

These results give $\alpha_j = 0.14$ and $\alpha_p = 0.27$. Morton (1) assumed that an $\alpha = 0.12$ would satisfy both a jet and plume flow. It appears that Morton's assumption is incorrect. Ricou and Spalding (46) found $\alpha_j = 0.08$ by direct measurements, and George, et al. (23) found $\alpha_p = 0.15$ by direct integration of Gaussian curve fitted to plume velocity data. Although data and theory are not in agreement, from the magnitude of the difference it seems unlikely that the entrainment coefficient is constant.

List and Imberger (33) suggest that α is dependent on ξ which is consistent with the approach of this study. Based on the asymptotic behavior of the velocity function it is easy to postulate a model from the theory presented in this study as:

$$\frac{E}{2\pi M_o^{1/2}} = \frac{f_j(o)}{2A_1}\left[1 + \frac{5}{3}\frac{f_o(o)A_j}{f_j(0)A_o}\xi^{2/3}\right] \; . \qquad 8.2.5$$

A more correct model which incorporates the proper behavior of the velocity for small ξ is given by:

Table 5. Calculated values of entrainment parameters.

	Jet	Plume
b	$\sqrt{3/A_j}$	$\sqrt{3/A_p}$
W	$f(0)_j/3$	$f(0)_p/3$
E	$f(0)_j/A_j$	$5f_p(0)/3A_p$
α	$\sqrt{3/2}\ \sqrt{A_j}$	$5\cdot\sqrt{3/2}\cdot 3\cdot\sqrt{A_p}$

$$\frac{E}{2\pi M_o^{1/2}} = \frac{f_j(o)}{2A_j}\left[1 + \frac{5}{3}\frac{f_o(o)A_j}{f_j(o)A_o}\xi^{2/3}\left(1 - \exp[-\alpha\xi^{4/3}]\right)\right] \qquad 8.2.6$$

which is similar to the composite eddy viscosity model of Chapter 7.

Equations 8.5.6 and 8.5.7, the asymptotes from the suggested profiles, and the entrainment calculated from the composite eddy viscosity model of Chapter 7 are shown in Figure 34 along with the data of George, et al. (23), Ricou and Spalding (46) and the assumed value of Morton (1). As previously noted, the theoretical values are higher than the data. While equation 8.5.6 is unacceptable, equation 8.5.7 is in excellent agreement with the calculated results and should be given careful consideration for incorporation into entrainment calculations.

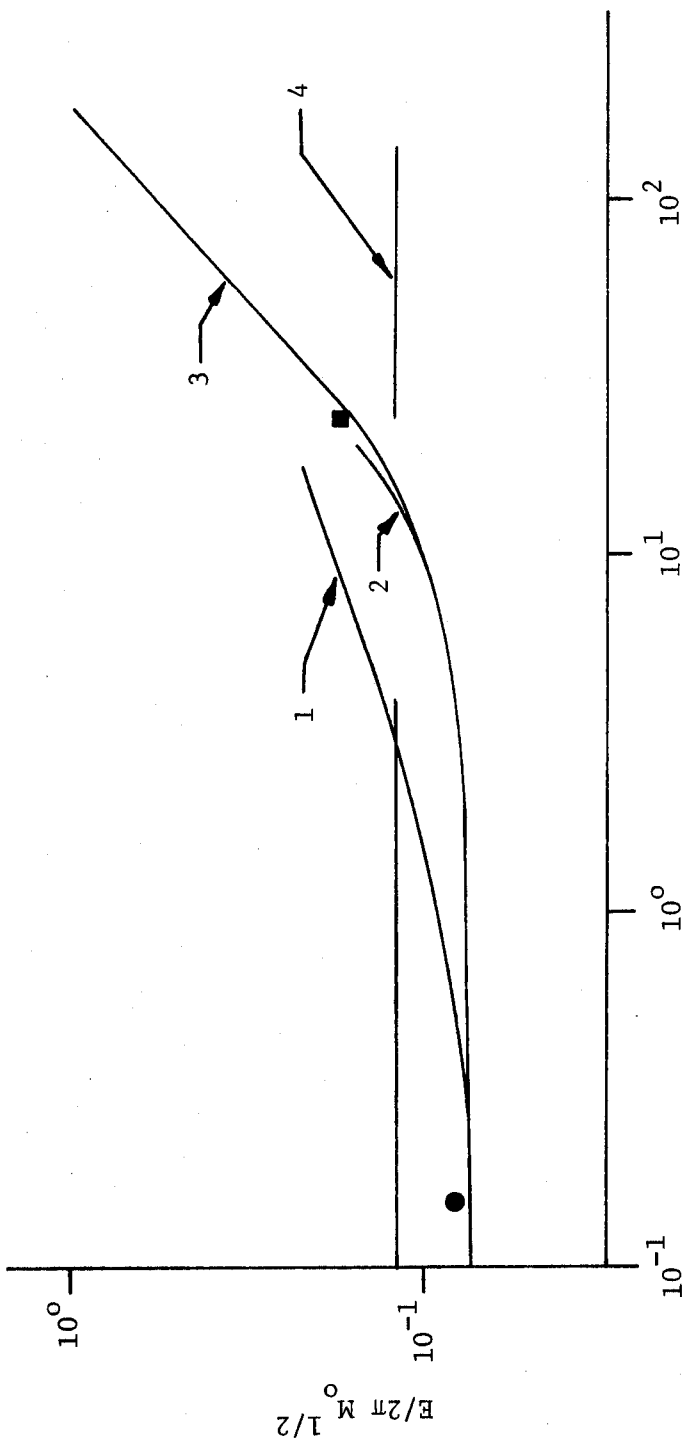

Figure 34. Comparison of buoyant jet entrainment functions. ● - Ricou and Spalding (46). ■ - George, et al. (23). 1 - Equation 8.5.6. 2 - Equation 8.5.7. 3 - Equation 4.2.9 and 4.2.10. 4 - Morton (1).

CHAPTER 9

SUMMARY AND CONCLUSIONS

9.1 Eddy Viscosity Models

The application of the eddy viscosity model to a jet, plume, and buoyant jet have been explored in detail. It has been shown that accounting for the axial transport of momentum and heat is crucial to the modeling of the jet and plume flow. Although the eddy viscosity model cannot address this problem directly, it was shown that both axial momentum and heat flux could be adjusted using the integral constraints imposed on the flow. These constraints assumed the form

$$2\pi \int_o^\infty f^2(\eta)\eta d\eta = Q_1 R_T \qquad 9.1.1$$

$$2\pi \int_o^\infty t(\eta)f(\eta)\eta d\eta = QR_T \quad . \qquad 9.1.2$$

Since neither the jet nor plume velocity data are well defined at this time, it is questionable if calculations using intermittency or higher order models are justified.

9.2 Application of Eddy Viscosity Model to Jet and Plume Data

It has been shown that existing jet velocity data do not satisfy the momentum constraint for this flow field. The mean velocity profiles integrate to yield a momentum deficit of approximately 50 to 60 percent. There are indications that the temperature data may be more reliable based on the results of Hinze and van der Hegge Zignen (13) and Becker,

et al. (43). Using these temperature data, the velocity centerline data, and reasonable choices for Q and Q_1, the following mean profiles are recommended for the jet

$$f_j(\eta) = 5.6/(1+39\eta^2)^2 \qquad 9.2.1$$

$$t_j(\eta) = 6.0/(1+39\eta^2)^2 \qquad 9.2.2$$

If the discrepancies in the jet data are resolved, some of the problems encountered in predicting this flow with models based on universal constants may be eliminated.

The plume data show more consistency than the jet since the energy and momentum balance for these data are reasonable. Using the measured Q of 0.85, the recommended mean profiles for these data are

$$f_p(\eta) = 3.4/(1+28\eta^2)^2 \qquad 9.2.3$$

$$t_p(\eta) = 9.1/(1+28\eta^2)^2 \quad . \qquad 9.2.4$$

9.3 Computations of the Buoyant Jet

Using the results of the perturbation and asymptotic analyses, a composite eddy viscosity model for the buoyant jet equations was hypothesized which would satisfy both the jet and plume asymptotes.

The chosen form was:

$$\frac{\nu_T}{M_o^{1/2}} = \frac{1}{R_T}\left[1 + \xi^{2/3}(1 - \exp[-\alpha\xi^{4/3}])\right] . \qquad 9.3.1$$

The buoyant jet equations were solved using $P_T = 1.0$, $R_T = 55$, and $\alpha = 0.2$ in equation 8.3.1. The calculated centerline values provided

good fits to the available data, and the profiles provided a reasonable match to the plume profiles for large values of ξ. The calculations showed that the mean profiles have only a weak dependence on ξ. Even this week ξ dependence, however, can be important in evaluating the mass, momentum, and buoyancy integrals.

9.4 A Framework for Experiment and Analysis

Disregarding the particulars of the equations and solutions, this dissertation has built upon the foundations laid by Morton, Yih, List, and others to establish a framework within which further studies of the buoyant jet can be carried out. Criteria can be set forth to establish the relative importance of buoyancy on the flow at a particular location. For example, flows at $\xi < 1$ will clearly be dominated by the momentum at the source and will be jet-like, while flows for $\xi > 10$ will be dominated by buoyancy and will be plume-like. These considerations should prove invaluable to designers of the next generation of experiments.

The importance of using all the available tools in carrying out a turbulence experiment has been reestablished. Since all turbulence measurements of interest press the limits of both equipment and understanding, no single measurement can stand on its own. It must be subjected to every possible validation from independent measurements to the constraints of the equations of motion.

Finally, this dissertation and the problems encountered make it clear that the turbulence theoretician cannot be content with simply trying to predict experimental results, but must also provide a careful critique of these results if he is to influence directly the course of subsequent work.

REFERENCES

1. Morton, B. R., Forced Plumes, J. Fluid Mech. 2, 151-163, 1959.

2. Morton, B. R., Taylor, G. I., and Turner, D. S., Turbulent Gravitational Convection from Maintained and Instantaneous Sources, Proc. R. Soc. 234A, 1-23, 1956.

3. Zel'dovich, Ya. B., Limiting Laws for Turbulent Flows in Free Convection, Zh. Eksp. Teoret. Fiz. 7(12), 1463, 1937.

4. Schmidt, W. Z., Turbulent Propagation of a Stream of Heated Air, Z. Angew. Math. Mech. 21, 265-351, 1941.

5. Taylor, G. I., Dynamics of a Mass of Hot Gas Rising in Air, U. S. Atomic Energy Commission, MDDC, 919, LADC 276, 1945.

6. Rouse, H., Yih, C. S., and Humphreys, H. W., Gravitational Convection from a Boundary Source, Tellus 4, 201, 1952.

7. Batchelor, G. K., Heat Convection and Buoyancy Effects in Fluids, Q. Jl. R. Met. Soc. 80, 339-358, 1954.

8. Tollmien, W., Berechnung Turbulenter Auxbreitunsvorgange, ZAMM 6, 468-478, 1926.

9. Görtler, H., Berechnung von Aufgaben der Freien Turbulenz auf Grund eines neuen Naherungsansatzes, ZAMM 22, 244-254, 1942.

10. Zimm, W., Uber die Strommungsvorgange in Frein Luftstrah, BDI-Forschungsheft, 234, 1921.

11. Ruden, P., Turbulente Aushbeitungim Freistrahl Naturwissenschaften 21, 375-378, 1933.

12. Reichardt, H., Gesetzma Bikeiten der freien Turbulenz, VDI-Forschungsheft 4.4, 1942.

13. Hinze, D. O. and van der Hegge Zignen, B. G., Transfer of Heat and Matter in the Turbulent Mixing Zone of an Axially Symmetrical Jet, Applied Scientific Research, Vol. A1, 435-461, 1949.

14. Corrsin, S. and Uberoi, M. S., Further Experiments of the Flow and Heat Transfer in a Heated Turbulent Jet, NACA Report No. 998, 1950.

15. Yih, C. S., Turbulent Buoyant Plumes, The Physics of Fluids, 20, 8, 1234-1237, 1977.

16. Hamilton, C. M. and George, W. K., Eddy Viscosity Calculations for Turbulent Buoyant Plumes, Bull. Am. Phys. Soc., Series II, Vol. 21, No. 10, 1225, 1976.

17. Baker, C. B., Taulbee, D. B., and George, W. K., Eddy Viscosity Calculations of Turbulent Buoyant Plumes, Joint ASME/AICHE. 18th National Heat Transfer Conference, San Diego, California, 1979.

18. Chen, C. J. and Rodi, W., A Mathematical Model for Stratified Turbulent Flows and its Application to Buoyant Jets, IV Congress, International Association for Hydraulic Research, San Paulo, 1975.

19. Tamanini, F., Algebraic Stress Modeling in a Buoyancy Controlled Turbulent Shear Flow, Symposium on Turbulent Shear Flows, The Pennsylvania State University, 1977.

20. Hinze, J. O., Turbulence, McGraw-Hill Book Co., 2nd edition, 1975.

21. Wygnanski, I. and Fiedler, H. E., Some Measurements in Self-Preserving Jets, J. Fluid Mech., Vol. 38, Pt. 3, 577-612, 1969.

22. George, W. K., Alpert, R. L., and Tamanini, F., Turbulence Measurements in an Axisymmetric Buoyant Plume, Factory Mutual Research, Tech. Rep. No., FMRC Serial No. 22359-2, 1976.

23. George, W. K., Jr., Alpert, R. L., and Tamanini, F., Turbulence Measurements in an Axisymmetric Buoyant Plume, Int. J. Heat Mass Trans. V. 20, 1145-1154, 1977.

24. Nakagome, H. and Hirata, M., The Structure of Turbulent Diffusion in an Axi-Symmetrical Thermal Plume, 9th International Conference for Heat and Mass Transfer International Seminar, Spalding, D., ed., Vol. I, 361-372, Hemisphere Publishing Corp., Dubrovnik, Yugoslavia, 1976.

25. Beuther, P. D., Capp, S. P., and George, W. K., Jr., Momentum and Temperature Balance Measurements in an Axisymmetric Turbulent Plume, Joint ASME/AICHE 18th National Heat Transfer Conference, San Diego, California, 1979.

26. Beuther, P. D., Experimental Investigation of the Turbulent Buoyant Axisymmetric Plume, Ph.D. Dissertation, SUNY at Buffalo, June 1980.

27. Abraham, G., Jet Diffusion in Stagnant Ambient Fluid, Delft Hydraulics Laboratory, No. 29, Delft, The Netherlands, 1963.

28. Kotsovinos, N. E. and List, E. J., Turbulent Buoyant Jets, 9th International Conference for Heat and Mass Transfer International Seminar, Spalding, D., ed., Vol. I, 349-359, Hemisphere Publishing Corp., Dubrovnik, Yugoslavia, 1976.

29. Ryskiewich, B. S. and Hafetz, L., An Experimental Study of the Surface Effect on a Buoyant Jet, General Dynamics, Electric Boat Division, Report, No. U440-74-103, Groton, Connecticut, 1975.

30. Pryputniewicz, R. J., An Experimental Study of the Free Surface Effects on a Submerged Vertical Buoyant Jet, M.S. Thesis, University of Connecticut, 1974.

31. Buchave, P., George, W. K., Jr., and Lumley, J. L., The Measurement of Turbulence with the Laser-Doppler Anemometer, Annual Review of Fluid Mechanics, Vol. 11, 443-503, 1979.

32. Schlichting, H., Boundary-Layer Theory, 2nd Ed., McGraw-Hill Book Company, 1955.

33. List, E. J. and Imberger, J., Turbulent Entrainment in Buoyant Jets and Plumes, Proc. ASCE, J. Hyd. Div., 99, 1416-1474, 1973.

34. Kotsovinos, N. E., Dilution in a Vertical Round Buoyant Jet, Proc. ASCE, J. Hyd. Div., 104, 795-798, 1978.

35. Madni, I. K. and Pletcher, R. H., Predictions of Turbulent Forced Plumes Issuing Vertically into Stratified or Uniform Ambients, Trans. ASME, J. Heat Transfer, 99-104, 1977.

36. Baker, C. B., Taulbee, D. E., and George, W. K., An Analysis of the Turbulent Buoyant Jet, Bull. Am. Phys. Soc., Series II, Vol. 24, No. 8, 1979.

37. Boussinesq, J., Essai sur la théorie des eaux Courantes, Mém. Prés. par div. savants à l'Acad. des Sci. Paris, 23, No. 7, 1-680, 1872.

38. Tennekes, H. and Lumley, J. L., A First Course in Turbulence, MIT Press, 1972.

39. Townsend, A. A., Turbulent Shear Flow, Cambridge University Press, Cambridge, 1956.

40. Beuther, P. D. and George, W. K., Measurements of the Turbulent Energy Budget in an Axisymmetric Plume, Bull. Am. Phys. Soc., Series II, 23, 8, 1014, 1978.

41. Abbiss, J. B. and Wright, M. P., Measurements on an Axi-Symmetric Jet Using a Photon Correlator, The Accuracy of Flow Measurements by Laser Doppler Methods, Proceedings LDA-Symposium, Copenhagen, 319-335, 1975.

42. George, W. K., Jr. and Beuther, P. D., Interpretation of Turbulent Measurements in High Intensity Shear Flow, Bull. Am. Phys. Soc. Series II, Vol. 24, No. 8, 1979.

43. Becker, H. A., Hottel, H. C., and Williams, G. C., The Nozzle-Fluid Concentration Field of the Round Turbulent, Free Jet, J.F.M., Vol. 30, 285-303, 1967.

44. Ahmad, M., Further Studies on the Turbulent Axisymmetric Buoyant Plume, M.S. Thesis, Department of Mechanical Engineering, State University of New York at Buffalo, Buffalo, NY, May 1980.

45. Roache, Patrick J., Computational Fluid Dynamics, Hermosa Publishers, 1972.

46. Ricou, R. P. and Spalding, D. B., Measurements of Entrainment by Axisymmetrical Turbulent Jets, J.F.M., Vol. 11, 21-32, 1961.

APPENDICES

APPENDIX A

PLUME SIMILARITY EQUATIONS

The similarity equations for an axisymmetric turbulent buoyant plume are developed in this section. Closure is obtained using an eddy viscosity model, and the mean flow equations are reduced to two ordinary second order differential equations.

The momentum, energy, and continuity equations describing the mean flow are

$$U \frac{\partial U}{\partial x} + V \frac{\partial U}{\partial r} = \frac{1}{r} \frac{\partial}{\partial r} (-\overline{ruv}) + \frac{\partial}{\partial x} (-\overline{u^2}) - g \frac{\Delta \rho}{\rho_o} \qquad \text{A1}$$

$$U \frac{\partial \Delta T}{\partial x} + V \frac{\partial \Delta T}{\partial r} = \frac{1}{r} \frac{\partial}{\partial r} (-\overline{rv\theta}) + \frac{\partial}{\partial x} (-\overline{u\theta}) \qquad \text{A2}$$

$$\frac{\partial U}{\partial x} + \frac{1}{r} \frac{\partial (rV)}{\partial r} = 0 \, . \qquad \text{A3}$$

If the Boussinesq approximation

$$-g \frac{\Delta \rho}{\rho_o} = - g \frac{(\rho - \rho_o)}{\rho_o} = g\beta(T - T_o) = g\beta\Delta T \qquad \text{A4}$$

is substituted into equation A1, the mean momentum equation becomes

$$U \frac{\partial U}{\partial x} + V \frac{\partial u}{\partial r} = \frac{1}{r} \frac{\partial}{\partial r} (-\overline{ruv}) + g\beta\Delta T. \qquad \text{A5}$$

The vertical heat flux term $-\overline{u\theta}$ in equation A2 cannot be modeled using a simple eddy viscosity assumption. This term is accounted for in the energy integral constraint. The integral constraint is obtained by integrating equation A2 which yields

$$2\pi \int_o^\infty g\beta(U\Delta T + \overline{u\theta}) r dr = F_o \qquad \text{A6}$$

where ρF_o is identified as the rate at which weight deficiency or buoyancy is added at the source. In a neutrally stable environment, ρF_o is the rate at which buoyancy crosses any given plane.

A similarity solution of the following form is sought

$$\eta = r/x \qquad g\beta\Delta T = T_s\, t(\eta)$$

$$U = U_s\, f(\eta) \qquad g\beta\overline{v\theta} = H_s\, h_1(\eta)$$

$$V = U_s\, k(\eta) \qquad g\beta\overline{u\theta} = H_s\, h_2(\eta)$$

$$\overline{uv} = R_s\, S(\eta) \qquad \text{A7}$$

The constant F_o has units of $[L^4/\tau^3]$ and is used to form the similar coefficients along with the axial coordinate x. The following results are obtained for these dimensioned coefficients:

$$U_s = F_o^{1/3}\, x^{-1/3}$$

$$T_s = F_o^{2/3}\, x^{-5/3}$$

$$R_s = F_o^{2/3}\, x^{-2/3}$$

$$H_s = F_o\, x^{-2} \,. \qquad \text{A8}$$

Using relations A7 and A8 in the terms of the mean flow equations the following results are obtained.

$$\frac{\partial U}{\partial x} = f(\eta)\,\frac{\partial U_s}{\partial x} - \frac{U_s}{x}\,\eta f'(\eta) \qquad \text{A9}$$

$$\frac{\partial U}{\partial r} = \frac{U_s^2}{x}\, k(\eta) f'(\eta) \qquad \text{A10}$$

$$\frac{1}{r}\frac{\partial}{\partial r}(-\overline{ruv}) = -\frac{R_s}{x}\frac{S(\eta)}{\eta} - \frac{\partial R_s}{\partial r}S(\eta) - \frac{R_s}{x}S'(\eta) \qquad \text{A11}$$

$$g\beta\frac{\partial \Delta T}{\partial x} = t(\eta)\frac{\partial T_s}{\partial x}\frac{T_s}{x}\eta t'(\eta) \qquad \text{A12}$$

$$g\beta\frac{\partial \Delta T}{\partial r} = \frac{T_s}{x}t'(\eta) \qquad \text{A13}$$

$$g\beta\frac{\partial}{\partial r}(-\overline{rv\theta}) = -H_s\left(\frac{h_1(\eta)}{x\eta} + \frac{h_1'(\eta)}{x}\right) \qquad \text{A14}$$

$$g\beta\frac{\partial}{\partial x}(-\overline{v\theta}) = -\left(h_2(\eta)\frac{\partial H_s}{\partial x} - H_s\frac{\eta}{x}h_2'(\eta)\right) . \qquad \text{A15}$$

Substitution of these relations into equations A2, A3, and A5 along with the relations for U, V, and $g\beta\Delta T$ from A7 gives the following:

momentum:

$$-\frac{1}{3}f^2(\eta) - \eta f(\eta)f'(\eta) = \frac{1}{\eta}\frac{d}{d\eta}(\eta S(\eta)) + t(\eta) \qquad \text{A16}$$

energy:

$$-\frac{5}{3}f(\eta)t(\eta) - \eta f(\eta)t'(\eta) + k(\eta)t'(\eta)$$

$$= -\frac{1}{\eta}\frac{d}{d\eta}(\eta h_1(\eta)) - (2h_2(\eta) + \eta h_2'(\eta)) \qquad \text{A17}$$

continuity:

$$-\frac{1}{3}f(\eta) - \eta f'(\eta) + k'(\eta) + \frac{k(\eta)}{\eta} = 0 . \qquad \text{A18}$$

The continuity equation is integrated to define the radial velocity parameter, $k(\eta)$, in terms of the axial velocity parameter, $f(\eta)$. This relation is substituted into equations A16 and A17 to obtain

$$-\frac{1}{3}f^2(\eta) - \frac{5}{3}\frac{f'(\eta)}{\eta}\int_o^\eta f(\eta)\eta d\eta = -\frac{1}{\eta}\frac{d}{d\eta}(\eta S(\eta)) + t(\eta) \qquad A19$$

$$-\frac{5}{3}f(\eta)t(\eta) - \frac{5}{3}\frac{t'(\eta)}{\eta}\int_o^\eta f(\eta)\eta d\eta = -\frac{1}{\eta}\frac{d}{d\eta}(\eta h_1(\eta)) - (2h_2(\eta)$$

$$+ \eta h_2'(\eta)). \qquad A20$$

These equations are completely characterized by a single length and time scale since all lengths are proportional to x and all time to x/U_s. Consequently, an eddy viscosity model should predict the mean properties of this flow.

On dimensional grounds the eddy viscosity and diffusivity are written as

$$\nu_e = U_s \times \nu(\eta) \qquad A21$$

$$\alpha_e = U_s \times \alpha(\eta) \quad . \qquad A22$$

Since the flow being modeled is a free shear flow which is assumed to be well mixed, it is assumed that

$$\nu(\eta) = \text{constant} = 1/R_T \qquad A23$$

$$\alpha(\eta) = \text{constant} = 1/P_T R_T \quad . \qquad A24$$

Introducing the eddy viscosity relation proposed by Boussinesq

$$-uv = \eta_e \frac{\partial U}{\partial r} \qquad A25$$

$$-v\theta = \alpha_e \frac{\partial \Delta T}{\partial r} \qquad A26$$

the viscosity terms in equation A11 may be written as

$$\frac{1}{r}\frac{\partial}{\partial r}(-\overline{ruv}) = \frac{F_o^{2/3}\, x^{-5/3}}{R_T}\,\frac{1}{\eta}\,[f'(\eta) + \eta f''(\eta)]$$

or

$$\frac{x^{5/3}}{F_o^{2/3}}\frac{1}{r}\frac{\partial}{\partial r}(-\overline{ruv}) = \frac{1}{R_T\eta}\,[f'(\eta) + \eta f''(\eta)]. \qquad \text{A27}$$

This eddy viscosity model is substituted into equation A16 in place of the viscosity term since

$$-\frac{1}{\eta}\frac{d}{d\eta}[\eta S(\eta)] = \frac{x^{5/3}}{F_o^{2/3}} \cdot \frac{1}{r}\frac{\partial}{\partial r}[-\overline{ruv}]. \qquad \text{A28}$$

The radial heat flux term in equation A17 may be written as

$$\frac{g\beta}{r}\frac{\partial}{\partial r}[-\overline{rv\theta}] = \frac{F_o x^{-3}}{P_T R_T} \cdot \frac{1}{\eta}\,[t'(\eta) + \eta t''(\eta)]$$

or

$$\frac{x^3}{F_o r}\frac{\partial}{\partial r}[-\overline{rv\theta}] = \frac{1}{P_T R_T} \cdot \frac{1}{\eta}\,[t'(\eta) + \eta t''(\eta)]. \qquad \text{A29}$$

This eddy diffusivity model is substituted into equation A17 in place of the radial heat flux term since

$$-\frac{1}{\eta}\frac{d}{d\eta}[h_1(\eta)] = \frac{x^3}{F_o}\, g\beta\,\frac{1}{r}\frac{\partial}{\partial r}[-\overline{rv\theta}]. \qquad \text{A30}$$

Performing these substitutions the similarity velocity and temperature equations A19 and A20 assume the form

$$f''(\eta) + \left[1 + \frac{5}{3} R^T \int_o^\eta f(\eta)\eta d\eta\right] \frac{f'(\eta)}{\eta} + \frac{R_T}{3} f^2(\eta) + R_T\, t(\eta) = 0 \qquad \text{A31}$$

$$t''(\eta) + \left[1 + \frac{5}{3} P_T R_T \int_o^\eta f(\eta)\eta d\eta\right] \frac{t'(\eta)}{\eta} + \frac{5}{3} P_T R_T\, f(\eta) f(\eta) = 0 \,. \qquad \text{A32}$$

This system of coupled ordinary differential equations can be solved for $f(\eta)$ and $t(\eta)$ if R_T and P_T are determined from experimental data, and the boundary conditions are specified. The boundary conditions are

$$f'(0) = 0 \qquad f(\infty) = f'(\infty) = 0$$

$$t'(0) = 0 \qquad t(\infty) = t'(\infty) = 0. \qquad \text{A33}$$

The integral constraint, A6, assumes the form

$$2\pi \int_o^\infty f(\eta) t(\eta) \eta d\eta = Q. \qquad \text{A34}$$

No attempt has been made to model the vertical heat flux term in equation A32, but the Q factor included in equation A34 does account for this term. The Q factor is defined by

$$2\pi \int_o^\infty f(\eta) t(\eta) \eta d\eta = 1 - 2\pi \int_o^\infty h_1(\eta) \eta d\eta \,. \qquad \text{A35}$$

The experimentally determined constant R_T can be eliminated from equations A31 and A32 by the following transformation:

$$\rho = \sqrt{R_T}\, \eta$$

$$f(\eta) \rightarrow f(\rho), \quad t(\eta) \rightarrow t(\rho), \quad k(\eta) \rightarrow k(\rho)/\sqrt{R_T} \,. \qquad \text{A36}$$

For this case equations A31 and A32 become

$$f''(\rho) + \left[1 + \frac{5}{3}\int_o^\rho f(\rho)\rho d\rho\right]\frac{f'(\rho)}{\rho} + \frac{f^2(\rho)}{3} + t(\rho) = 0 \qquad \text{A37}$$

$$t''(\rho) + \left[1 + P_T\frac{5}{3}\int_o^\rho f(\rho)\rho d\rho\right]\frac{t'(\rho)}{\rho} + \frac{5}{3}P_T f(\rho)t(\rho) = 0\ . \qquad \text{A38}$$

The integral constraint A34 assumes the form

$$2\pi\int_o^\infty f(\rho)t(\rho)\rho d\rho = R_T Q. \qquad \text{A39}$$

In this form equations A37 and A38 depend on the parameters R_T and Q only through the integral constraint A39.

APPENDIX B

ANALYTICAL SOLUTION FOR AXISYMMETRIC TURBULENT PLUME

An exact solution for the similarity equations which describe a turbulent buoyant plume was presented by Yih (15). This solution assumes a buoyancy source located at the origin of the flow, and the buoyancy forces are much greater than the inertial forces. The plume is assumed to be incompressible fully developed turbulent flow, stationary in the mean and $\mu << V_T$. The momentum, energy, and continuity equations describing the mean flow are

$$U \frac{\partial U}{\partial x} + V \frac{\partial U}{\partial r} = \frac{1}{r} \frac{\partial}{\partial r} (-\overline{ruv}) - g\Delta\gamma/\gamma_o \qquad B1$$

$$U \frac{\partial \Delta\gamma}{\partial x} + V \frac{\partial \Delta\gamma}{\partial r} = - \frac{1}{r} \frac{\partial}{\partial r} (-\overline{rv\theta}) \qquad B2$$

$$\frac{\partial U}{\partial x} + \frac{1}{r} \frac{\partial (rv)}{\partial r} = 0 \ . \qquad B3$$

Stokes stream function given by

$$U = \frac{1}{r} \frac{\partial \psi}{\partial r} \qquad V = - \frac{1}{r} \frac{\partial \psi}{\partial x} \qquad B4$$

satisfies the continuity equation. The boundary conditions are

$$\frac{\partial U}{\partial r} = \frac{\partial \Delta\gamma}{\partial r} = V = 0 \qquad r = 0$$

$$\psi \text{ is finite; } \Delta\gamma = 0 \qquad r \to \infty.$$

A constant density flux for this flow is defined by the relation

$$G = -2\pi \int_o^\infty u\Delta\gamma r dr \qquad B5$$

where $\Delta\gamma$ is the difference in the plume specific weight γ and specific weight at ambient conditions γ_o.

For modest temperature differences the Boussinesq approximation can be used to relate $\Delta\gamma$ to ΔT as follows:

$$g\beta\Delta T = \frac{\Delta\gamma}{\gamma_o} \quad .$$

The constant flux G has units of $[\ \frac{L-m}{T^3}\ ]$ which are used to form the similarity parameters in this flow. A similarity solution can be developed for equations B1, B2, and B3 using the transformation

$$\psi = 3\lambda\ (\ \frac{Gx^5}{\rho}\ )^{1/3}\ f(\eta) \qquad \text{B6}$$

$$-\Delta\gamma = 3\lambda^2\ (\ \frac{\rho G}{x^5}\ )^{1/3}\ t(\eta) \qquad \text{B7}$$

$$\eta = r/x\ . \qquad \text{B8}$$

Applying transformation B6 to equation B4 provides the relations

$$U = 3\lambda\ (\ \frac{G}{\rho x}\ )^{1/3}\ \frac{f'(\eta)}{\eta} \qquad \text{B9}$$

$$V = \lambda(\ \frac{G}{\rho x}\ )^{1/3}(3f'(\eta) - \frac{5f(\eta)}{\eta}\ )\ . \qquad \text{B10}$$

Relations B9 and B10 are used to find the derivatives required to reduce B1 to a similarity form. Using These U and V velocity relations provides the following results:

$$\frac{\partial U}{\partial x} = 3\lambda(\ \frac{G}{\rho x^4}\ )^{1/3}(\ \frac{2f'(\eta)}{3\eta} - f''(\eta)\ ) \qquad \text{B11}$$

$$\frac{\partial U}{\partial r} = 3\lambda(\ \frac{G}{\rho x^4}\ )^{1/3}(\ \frac{f''(\eta)}{\eta} - \frac{f'(\eta)}{\eta}\ )\ . \qquad \text{B12}$$

If the flux G is used to define an eddy viscosity

$$\nu_T = \lambda \left(\frac{Gx^2}{\rho} \right)^{1/3} \qquad \text{B13}$$

and the Boussinesq relation given by A25 is used to define the turbulent transport

$$-\overline{uv} = \nu_T \frac{\partial U}{\partial r} \qquad \text{B25}$$

the Reynolds stress term in equation B1 becomes

$$\frac{\nu_T}{r} \frac{\partial}{\partial r} (-r\overline{uv}) = \frac{3\lambda^2}{\eta} \left(\frac{G}{\rho^2 x^5} \right)^{1/3} \left(f'''(\eta) + \frac{f'(\eta)}{\eta^2} - \frac{f''(\eta)}{\eta} \right) . \qquad \text{B14}$$

If relations B7, B9, B10, B11, B12, and B14 are substituted into equation B1, the following similarity equation is obtained for the momentum equation:

$$(1 + 5f(\eta)) \left(\frac{f'(\eta)}{\eta} \right)' = f'''(\eta) + \eta t(\eta) . \qquad \text{B15}$$

The boundary conditions for the momentum equation become

$$f(0) = f'(0) = 0 \qquad f(\infty) \text{ is finite } t(\infty) = 0 . \qquad \text{B16}$$

The transformation B7 is used to obtain the relations:

$$\frac{\partial \Delta\gamma}{\partial x} = \frac{3\lambda^2}{x^{4/3}} \left(\frac{G^2\rho}{x^6} \right)^{1/3} (5t(\eta) + 3\eta t'(\eta)) \qquad \text{B17}$$

$$\frac{\partial \Delta\gamma}{\partial r} = -\frac{3\lambda^2}{x^{2/3}} \left(\frac{G^2\rho}{x^6} \right)^{1/3} t'(\eta) . \qquad \text{B18}$$

If Reynolds' analogy A35 is used to define the radial heat flux term it can be shown that

$$\frac{1}{r}\frac{\partial}{\partial r}(-r\overline{v\theta}) = -\frac{3\lambda^3}{\sigma}\left(\frac{G^2\rho}{6}\right)^{1/3}\cdot\frac{1}{x^{2/3}\eta}(\eta t'(\eta))' \quad . \qquad B19$$

Relations B9, B10, B17, B18, and B19 are used in equation B2 to obtain the following similarity equation:

$$-5\,(t(\eta)\cdot f(\eta))' = (\eta t'(\eta))' \quad . \qquad B20$$

The boundary conditions are given by

$$f(0) = f'(0) = t'(0) = 0$$

$$f(\infty) \text{ is finite and } t(\infty) = 0 \quad . \qquad B21$$

The integral constraint B5 in similarity form becomes:

$$18\pi\lambda^3 \int_0^\infty f'(\eta)t(\eta)d\eta = 1 \quad . \qquad B22$$

Equations B15 and B20 along with the respective boundary conditions can be satisfied with solutions of the form

$$f(\eta) = B(1 - (1+A\eta^2)^{-1}) \qquad B23$$

$$t(\eta) = C(1 + A\eta^2)^{-m} \quad . \qquad B24$$

Substitution of the above solutions into the similarity momentum equation B15 provides the following

$$(1 + A\eta^2)^{-3}(16A^2B\eta + 40A^2B^2\eta) + 1 + A\eta^2)^{-4}$$

$$\cdot\,(-44A^2B^2\eta - 48A^3B\eta^3) = \eta C(1 + A\eta^2)^{-m} \quad . \qquad B25$$

Relation B25 has a solution for m = 3,4. Equating the coefficients for like powers of η provides:

m = 3	m = 4
B = 12/11	B = 4/5
$C = 1536A^2/121$	$C = 256A^2/25$.

The constant A is related to the free constant λ through the integral constraint B22 which provides upon substitution of B23 and B24 and integration the relation

$$A^2 = 1331/82942\pi\ \lambda_0^3 \quad \text{for } m = 3$$

$$A^2 = 625/18432\pi\ \lambda^3 \quad \text{for } m = 4 \ .$$

Substitution of the solutions B23 and B24 into the similarity density equation B20 results in

$$-10\sigma ABC\eta(1 + A\eta^2)^{-(m+1)} + 10\sigma ABCm\eta(1 + A\eta^2)^{-(m+2)} - 10\sigma ABCm\eta(1 + A\eta^2)^{-(m+1)} = -4ACm\eta(1 + A\eta^2)^{-(m+1)} + 4ACm(m+1)\eta^3(1 + A\eta^2)^{-(m+2)} \ . \qquad \text{B26}$$

Equating coefficients for same powers in η provides the result

$$M = \frac{5\ B}{2}$$

therefore for

m = 3	$\sigma = 1.1$
m = 4	$\sigma = 2.0$.

Summary:

Similarity Equations:

$$(1 + 5f(\eta))\left(\frac{f'(\eta)}{\eta}\right)' = f'''(\eta) + \eta t(\eta) \qquad \text{B15}$$

$$-5\sigma(t(\eta)\cdot f(\eta))' = (\eta t'(\eta))' \qquad \text{B20}$$

Boundary Conditions:

$$f(0) = f'(0) = t'(0) = 0$$

$$f(\infty) \text{ is finite, } t(\infty) = 0$$

Integral Constraint:

$$18\pi\lambda^3 \int_0^\infty f'(\eta)t(\eta)d\eta = 1$$

Solution:

$$f(\eta) = B(1 - (1 + A\eta^2)^{-1}) \qquad \text{B23}$$

$$t(\eta) = C(1 + A\eta^2)^{-m} \qquad \text{B24}$$

for

$m = 3$	$m = 4$
$B = \frac{12}{11}$	$B = \frac{4}{5}$
$C = \frac{1536A^2}{121}$	$C = \frac{256A^2}{25}$
$A^2 = \frac{1331}{82942\pi\lambda^3}$	$A^2 = \frac{625}{18432\pi\lambda^3}$

$$m = \frac{5\sigma B}{2}$$

$\sigma = 1.1$	$\sigma = 2.0$

It is important to note that this solution is applicable only for Prandtl numbers of 1.1 and 2.0. The general similarity solution for all Prandtl numbers is developed in Appendix D.

APPENDIX C

JET INTEGRAL CONSTRAINTS

Although the jet similarity equations are well known, a brief summary of the jet equations is required to introduce the integral technique used to account for the turbulence contribution to the axial transport. The mean momentum equations for an axisymmetric turbulent jet are given by:

r-direction:

$$\frac{DV}{Dt} - \frac{W^2}{r} = -\frac{1}{\rho}\frac{\partial p}{\partial r} - \frac{1}{r}\frac{\partial}{\partial r}\left(\overline{rv^2}\right) - \frac{1}{r}\frac{\partial}{\partial \phi}\left(\overline{vw}\right) - \frac{\partial}{\partial x}\left(\overline{uv}\right) + \frac{\overline{w^2}}{r} \qquad C1$$

ϕ-direction:

$$\frac{DW}{Dt} + \frac{VW}{r} = -\frac{1}{\rho}\frac{\partial p}{\partial \phi} - \frac{1}{r}\frac{\partial}{\partial \phi}\left(\overline{w^2}\right) - \frac{\partial}{\partial x}\left(-\overline{uw}\right) - 2\frac{\overline{vw}}{r} \qquad C2$$

x-direction:

$$\frac{DU}{Dt} = -\frac{1}{\rho}\frac{\partial p}{\partial r} - \frac{\partial}{\partial x}\left(\overline{u^2}\right) - \frac{1}{r}\frac{\partial}{\partial r}\left(\overline{ruv}\right) - \frac{1}{r}\frac{\partial}{\partial \phi}\left(\overline{uw}\right) . \qquad C3$$

The r-direction momentum equation can be integrated to obtain:

$$\frac{p_\infty - p}{\rho} = \overline{v^2} - \int_r^\infty \frac{\partial}{\partial x}\overline{uv}\, dr + \int_r^\infty \frac{\overline{w^2}}{r}\, dr . \qquad C4$$

Equation C4 is differentiated with respect to x to obtain:

$$-\frac{1}{\rho}\frac{\partial p}{\partial x} = \frac{\partial}{\partial x}\overline{v^2} - \frac{\partial}{\partial x}\int_r^\infty \frac{\partial}{\partial x}\left(\overline{uv}\right) dr + \frac{\partial}{\partial x}\int_r^\infty \frac{\overline{w^2}}{r}\, dr . \qquad C5$$

Substituting this result into the x-direction momentum equation and using the continuity relation equation, C3 assumes the form

$$\frac{\partial U^2}{\partial x} + \frac{1}{r}\frac{\partial}{\partial r}(rUV) = -\frac{\partial}{\partial x}\overline{u^2} - \frac{1}{r}\frac{\partial}{\partial r}(\overline{ruv})$$

$$+ \frac{\partial}{\partial x}\overline{v^2} - \frac{\partial}{\partial x}\int_r^\infty \frac{\partial}{\partial x}(\overline{uv})\,dr + \frac{\partial}{\partial x}\int_r^\infty \frac{\overline{w^2}}{r}\,dr\,. \qquad C6$$

Equation C6 is integrated over the limits of 0 to ∞ to obtain:

$$\frac{\partial}{\partial x}\int_o^\infty U^2 r dr + \int_o^\infty \frac{1}{r}\frac{\partial rUV}{\partial r}\,rdr = \frac{\partial}{\partial x}\int_o^\infty -\overline{u^2} r dr$$

$$+ \int_o^\infty \frac{1}{r}\frac{\partial}{\partial r}(-\overline{ruv})rdr + \frac{\partial}{\partial x}\int_o^\infty \overline{v^2}\,rdr - \frac{\partial}{\partial x}\int_o^\infty\int_r^\infty \frac{\partial\overline{uv}}{\partial x}\,rdr$$

$$+ \frac{\partial}{\partial x}\int_o^\infty \left(\int_r^\infty \frac{\overline{w^2}}{r}\,dr\right)rdr. \qquad C7$$

The term $\frac{\partial(\overline{uv})}{\partial x}$ is of lower order than all other terms in equation C7. Consequently it is ignored. Performing the integration yields

$$\frac{\partial}{\partial x}\int_o^\infty U^2 r dr + rUV\Big|_o^\infty = \frac{\partial}{\partial x}\int_o^\infty -\overline{u^2} r dr - \overline{ruv}\Big|_o^\infty$$

$$+ \frac{\partial}{\partial x}\int_o^\infty \overline{v^2} r dr - \frac{\partial}{\partial x}\left(\frac{r^2}{2}\int_r^\infty \frac{\overline{w^2}}{r}\,dr\Big|_o^\infty - \int_o^\infty \frac{\overline{w^2}}{2}\,rdr\right).$$

The above relation reduces to the following:

$$\int_o^\infty \left(U^2 + \overline{u^2} - \overline{v^2} + \frac{\overline{w^2}}{2}\right)rdr = 0. \qquad C8$$

This integral constraint is used to account for the turbulence contribution to the axial transport of momentum. The technique used to account for the turbulence contribution to the axial transport of energy is developed in Appendix A.

APPENDIX D

ANALYTICAL SOLUTION FOR AXISYMMETRIC TURBULENT JET

In this section the exact similarity solution for a hot axisymmetric jet is summarized. This solution assumes a bouyancy and momentum source located at the origin of the flow, and the inertial forces are much greater than the bouyancy forces. The jet is assumed to be incompressible fully developed turbulent flow, stationary in the mean and $\mu << \nu_e$. The momentum, energy, and continuity equations describing the mean flow are

$$U \frac{\partial U}{\partial X} + V \frac{\partial U}{\partial r} = \frac{1}{r} \frac{\partial}{\partial r} (-r \overline{uv}) \qquad D1$$

$$U \frac{\partial \Delta T}{\partial X} + V \frac{\partial \Delta T}{\partial r} = \frac{1}{r} \frac{\partial}{\partial r} (-r \overline{v\theta}) \qquad D2$$

$$\frac{\partial U}{\partial X} + \frac{1}{r} \frac{\partial (rV)}{\partial r} = 0 \ . \qquad D3$$

The momentum equation is written in the form

$$\frac{\partial U^2}{\partial x} - U \frac{\partial U}{\partial x} + V \frac{\partial U}{\partial r} = \frac{1}{r} \frac{\partial}{\partial r} (-r \overline{uv}) \qquad D4$$

and integrated over the limits shown

$$2\pi \int_o^\infty \frac{\partial U^2}{\partial x} r \, dr + 2\pi \int_o^\infty U \frac{\partial U}{\partial X} r \, dr + 2\pi \int_o^\infty V \frac{\partial U}{\partial r} r \, dr$$

$$= 2\pi \int_o^\infty \partial (-r \overline{uv}) \ . \qquad D5$$

This integration is accomplished using the continuity relation D3 in D5 to obtain

$$2\pi \int_o^\infty \frac{\partial U^2}{\partial x} r \, dr + 2\pi \int_o^\infty \frac{1}{r} \frac{\partial rVU}{\partial r} r \, dr = 2\pi \int_o^\infty \partial (-r \overline{uv}) \ . \qquad D6$$

Integration yields

$$M_o = 2\pi \int_o^\infty U^2 r \, dr \quad . \qquad D7$$

This equation indicates that the momentum of a pure jet flow is constant and imposes an integral constraint on the flow field. Relation D7 has dimensions of $\left[\frac{L^4}{\tau^2} \right]$ and will be used to define the similarity parameters of this flow.

The temperature diffusion equation can be integrated in a similar manner to provide the energy integral constraint.

$$F_o = 2\pi \int_o^\infty g \, \beta U \, \Delta T \, r \, dr \quad . \qquad D8$$

This is a statement of energy conservation and also will be used to define similarity parameters for the mean temperature field. The quantity F_o has units of $[L^4/\tau^3]$.

The continuity equation D3 satisfies Stokes stream function ψ of the form

$$U = \frac{1}{r} \frac{\partial \psi}{\partial r} \qquad V = - \frac{1}{r} \frac{\partial \psi}{\partial x} \quad . \qquad D9$$

The boundary conditions for equations D1, D2, and D9 are

$$\frac{\partial U}{\partial r} = \frac{\partial \Delta T}{\partial r} = V = 0 \text{ at } r = 0 \qquad D10$$

and

$$\Delta T = U = V = 0; \; \frac{\partial U}{\partial r} = \frac{\partial V}{\partial r} = 0, \text{ as } r \to \infty$$

$$\psi \text{ is finite as } r \to \infty \quad . \qquad D11$$

A similarity solution is sought for the system of equations D1, D2, and D3 which satisfy the integral constraint D7 and D8 and the boundary conditions D9 and D10. A similarity solution is implemented using the following transformations

$$\psi = \lambda(M_o^2)^{1/2} f(\eta) \qquad \text{D12}$$

$$gB\Delta T = -\frac{\lambda^2 F_o}{M_o^{1/2} x} t(\eta) \qquad \text{D13}$$

$$\eta = r/x \qquad \text{D14}$$

NOTE: $(M_o x^2)^{1/2} = [L^3/\tau]$

$F_o/M_o^{1/2} x = [L/\tau^2]$

λ - free constant which must be determined from experimental data.

Substitution of relation D12 into D9 the definition of ψ provides the following relations:

$$U = \lambda \frac{M_o^{1/2}}{X} \frac{f'(\eta)}{\eta} \qquad \text{D15}$$

$$V = -\frac{\lambda M_o^{1/2}}{r} [f(\eta) - \eta f'(\eta)] \; . \qquad \text{D16}$$

Furthermore these relations are used to determine

$$\frac{\partial U}{\partial r} = \frac{\lambda M_o^{1/2}}{X^2 \eta} [f''(\eta) - \frac{f'(\eta)}{\eta}] \qquad \text{D17}$$

$$\frac{\partial U}{\partial x} = - \frac{\lambda M_o^{1/2}}{X^2} f''(\eta) \quad . \qquad \text{D18}$$

The simple proportionality correlation proposed by Boussinesq -- between the turbulent transport and mean gradient -- is used to define eddy viscosity as follows

$$- \overline{uv} = \nu_e \frac{\partial U}{\partial r} \quad . \qquad \text{D19}$$

Using this relation to define the Reynolds stress term in equation D1 provides the following results

$$\frac{\nu_e}{r} \frac{\partial}{\partial r} \left(r \frac{\partial U}{\partial r}\right) = \frac{\lambda^2 M_o}{r x^2} \left[f''' - \frac{f''}{\eta} + \frac{f'}{\eta^2}\right] \quad . \qquad \text{D20}$$

Substitution of relations D15, D16, D17, D18, and D19 into D1 reduces the momentum equation D1 to the form

$$[1 - f(\eta)] \left[\frac{f'(\eta)}{\eta}\right]' - \frac{f'(\eta)^2}{\eta} = f'''(\eta) \quad . \qquad \text{D21}$$

This equation is satisfied by the solution

$$f(\eta) = B[1 - (1+A\eta^2)^{-m}] \quad . \qquad \text{D22}$$

If relation D28 is substituted into D27, the following results:

$$\begin{aligned} &- 4A^2B\, m(m+1)\eta(1+A\eta^2)^{-(m+2)} + 4A^2B^2 m(m+1)\eta(1+A\eta^2)^{-(m+2)} \\ &- 4A^2B^2 m(m+1)\eta(1+A\eta^2)^{-2(m+1)} - 4A^2B^2 m^2 \eta(1+A\eta^2)^{-2(m+1)} \\ &+ 4A^2Bm(m+1)\eta(1+A\eta^2)^{-(m+2)} + 8A^2Bm(m+1)\eta(1+A\eta^2)^{-(m+2)} \\ &+ 8A^3Bm(m+1)(m+2)\eta^3(1+A\eta^2)^{-(m+3)} = 0 \quad . \end{aligned} \qquad \text{D22}$$

The above is satisfied for M-1 for which case it is reduced to

$$-8A^2B\eta(1+A\eta^2)^{-3} + 8A^2B^2\eta(1+A\eta^2)^{-3} - 12A^2B^2\eta(1+A\eta^2)^{-4}$$

$$+ 24A^2B^2\eta(1+A\eta^2)^{-3} - 48A^3B^3\eta(1+A\eta^2)^{-4} = 0 \ .$$

If this equation is multiplied by $(1+A\eta^2)^4$ and like powers of η equated, the equation is satisfied for

$$B = 4.0 \ . \qquad \text{D23}$$

The integral constraint D7 is used to evaluate the constant A. In similarity form this constraint assumes the form

$$\int_o^\infty \lambda^2 \left(\frac{f(\eta)}{\eta} \right)^2 \eta \, d\eta = 1/2\pi \ . \qquad \text{D24}$$

In terms of the assumed solution this integral is

$$\int_o^\infty 16A^2B^2\lambda^2(1+A\eta^2)^{-4}\eta \, d\eta = 1/2\pi$$

and the evaluation of the integral provides the following:

$$A = \frac{3}{64\pi \lambda^2} \ . \qquad \text{D25}$$

It is also noted that the assumed solution p results in a dimensionless velocity obtained from D15 of the form

$$\frac{x}{M_o^{1/2}} U = 2AB\lambda(1+A\eta^2)^{-2} \ . \qquad \text{D26}$$

This development provides a similarity solution for the mean flow momentum equation with one free parameter to be determined from the

experimental data. Next the conditions required for the temperature equation to satisfy the assumed velocity solution will be developed.

The similarity relation D13 is used to determine the temperature derivatives required for the energy equation D2. Using D13 it can be shown that

$$\frac{\partial(g\beta\Delta T)}{\partial x} = \frac{\lambda^2 F_o}{M_o^{1/2} x^2} [g(\eta) + \eta t'(\eta)] \qquad D27$$

$$\frac{\partial(g\beta\Delta T)}{\partial r} = -\frac{\lambda^2 F_o}{M_o^{1/2} x^2} t'(\eta) \quad . \qquad D28$$

Reynolds' analogy is used to express the turbulent radial heat flux as a function of the temperature gradient. This analogy states

$$-\overline{v\theta} = \alpha_e \frac{\partial T}{\partial r} \qquad D29$$

where α_e - thermal diffusivity.

Relation D35 is used in equation D2 to model the turbulent radial heat flux term. This substitution provides the following results:

$$\frac{1}{r}\frac{\partial}{\partial r}(-r\,\overline{v\theta}) = -\frac{\lambda^3}{\sigma}\frac{F_o}{x^2 r}[\eta t'(\eta)]' \quad . \qquad D30$$

Equation D2 is reduced to the following similarity form using D30, D28, D15, and D16,

$$-\sigma[f(\eta)t(\eta)]' = [\eta t(\eta)]' \quad . \qquad D31$$

Equation D31 is satisfied by a solution of the form

$$t(\eta) = C(1+A\eta^2)^{-m} \quad . \qquad A32$$

Using equations D32 and D22 in D31 provides the following

$$-2ABC\sigma\eta(1+A\eta^2)^{-(m+2)} + 2ABC\sigma m\eta(1+A\eta^2)^{-(m+1)}$$

$$-2ABC\sigma m\eta(1+A\eta^2)^{-(m+2)} + 4ACm\eta(1+A\eta^2)^{-(m+1)}$$

$$-4A^2C\eta^3 m(m+1)(1+A\eta^2)^{-(m+2)} = 0 \ .$$

Equating the coefficients for like powers of η in the above relation yields

$$m = \frac{B\sigma}{2} \ . \qquad \text{D33}$$

Since B = 4 from the solution for the momentum equation, equation D32 becomes

$$t(\eta) = C(1+A\eta^2)^{-2} \ . \qquad \text{D34}$$

Substitution of D34 into the similarity form for the energy integral constraint

$$\int_o^\infty \lambda^3 \frac{f'(\eta)}{\eta} t \ \eta d\eta = 1/2\pi \qquad \text{D35}$$

results in the following integral relation

$$\int_o^\infty 2\lambda^3 ABC\eta(1+A\eta^2)^{-(2\sigma+2)} d\eta = 1/2\pi \ . \qquad \text{D36}$$

Evaluation of this integral relates C to the known constants and the free parameter λ which is determined from experimental results. The value of C is given by

$$C = \frac{2\sigma+1}{8\pi\lambda^3} \ . \qquad \text{D37}$$

Summary:

Similarity Form of Momentum Equation:

$$[1-f(\eta)]\left[\frac{f'(\eta)}{\eta}\right]' - \frac{f'(\eta)^2}{\eta} = f''(\eta) \qquad \text{D21}$$

Solution:

$$f(\eta) = B[1 - (1+A\eta^2)^{-m}] \qquad \text{D22}$$

Boundary Conditions:

$$f(0) = f'(0) = 0 \qquad f(\infty) \text{ is finite}$$

Integral Constraint:

$$\int_o^\infty \sigma^2 \left[\frac{f'(\eta)}{\eta}\right]^2 \eta d\eta = 1/2\pi \qquad \text{D24}$$

Constants:

$$B = 4.0 \quad A = \frac{3}{64\pi\lambda^2}$$

Similarity Form of Temperature Equation:

$$-\sigma[f(\eta)t(\eta)]^1 = [\eta t(\eta)]^1 \qquad \text{D31}$$

Solution:

$$t(\eta) = C(1+A\eta^2)^{-2\sigma} \qquad \text{D34}$$

Boundary Conditions:

$$t(0) = 0 \qquad t(\infty) = 0$$

Integral Constraint:

$$\int_o^\infty \lambda^3 \frac{f'(\eta)}{\eta} t\, \eta d\eta = 1/2\pi \qquad \text{D35}$$

Constants:

$$C = \frac{2\sigma+1}{8\pi\lambda^3}$$

APPENDIX E

BUOYANT JET EQUATIONS

A set of dimensionless equations is derived which describe a fully developed hot jet evolving into a fully developed plume. It is assumed that the momentum forces are much greater than the buoyancy forces. The buoyancy term is included in the momentum equation, and it is shown that a characteristic length scale can be defined from the initial momentum and buoyancy flux which controls the buoyancy. As this length scale becomes large relative to the distance from the source the mean equations are reduced to the jet case. Eddy viscosity and diffusivity models are introduced which are functions of the characteristic length scale and axial distance from the flow source.

Consider the fully developed turbulent hot jet shown in Figure 20. In the fully developed jet region both the momentum flux and energy flux and constant. As the jet evolves beyond the fully developed region, the momentum decreases as a result of entrained air from the ambient, but the energy remains essentially constant. The momentum flux is defined by

$$M_o = 2\pi \int_o^\infty U^2 r dr = \left[\frac{\ell^4}{\tau^2} \right] \qquad \text{E1}$$

and the energy flux is defined by

$$F_o = 2\pi \int_o^\infty g\beta\Delta T U r dr = \left[\frac{\ell^4}{\tau^3} \right] \qquad \text{E2}$$

where: [ ] are the dimensions of the respective quantities

ℓ - designates length dimension

τ - designates time dimension.

The mean flow equations of momentum, energy, and continuity are

$$U \frac{\partial U}{\partial x} + V \frac{\partial U}{\partial r} = \frac{1}{r} \frac{\partial}{\partial r} (-r\overline{uv}) + g\beta\Delta T \qquad \text{E3}$$

$$U \frac{\partial \Delta T}{\partial x} + V \frac{\partial \Delta T}{\partial r} = \frac{1}{r} \frac{\partial}{\partial r} (-r\overline{v\theta}) \qquad \text{E4}$$

$$\frac{\partial U}{\partial x} + \frac{1}{r} \frac{\partial (rV)}{\partial r} = 0. \qquad \text{E5}$$

For a turbulent buoyant jet the only parameters which can govern the evolution of the flow are either those occurring in the equations of motion or those imposed at the source of the flow. The only parameter in the equations of motion is gB and at the source M_o and F_o. At any given cross-section the radial distribution of the mean flow must be considered a function of the distance from the source. From this basic set of parameters two independent dimensionless ratios can be formed. These ratios assume the form

$$\xi = \frac{x \, F_o^{1/2}}{M_o^{3/4}} = \frac{x}{L} \qquad \text{E6}$$

$$\eta = r/x \quad . \qquad \text{E7}$$

The equations describing this flow must include the two dimensionless length scales ξ and η. This solution is of the form

$$\eta = r/x$$

$$\xi = x/L$$

$$U = U_s(x) f(\eta, \xi)$$

$$V = U_s(x) k(\eta, \xi)$$

$$\overline{uv} = R_s(x) S(\eta, \xi)$$

$$g\beta\Delta T = T_s(x) t(\eta, \xi)$$

$$g\beta\overline{v\theta} = H_s(x) h(\eta, \xi) \qquad \text{E8}$$

Using the momentum flux M_o and energy flux F_o the coefficients in E8 are defined as follows:

$$\begin{aligned} U_s(x) &= M_o^{1/2} x^{-1} \\ R_s(x) &= M_o x^{-2} \\ T_s(x) &= F_o M_o^{-1/2} x^{-1} \\ H_s(x) &= F_o x^{-2} \quad . \end{aligned} \tag{E9}$$

Initially consider the results obtained if relations E8 and E9 are used in the momentum and continuity equations E3 and E5. For these relations

$$\frac{\partial U}{\partial x} = \frac{\partial U_s}{\partial x} f(\eta,\xi) + U_s \frac{\partial f(\eta,\xi)}{\partial \xi} \frac{\partial \xi}{\partial x} + U_s \frac{\partial f(\eta,\xi)}{\partial \eta} \frac{\partial \eta}{\partial x}$$

$$\frac{\partial U}{\partial x} = f(\eta,\xi) \frac{\partial U_s}{\partial x} + \frac{U_s}{L} \frac{\partial f(\eta,\xi)}{\partial \xi} - \frac{U_s}{x} \eta \frac{\partial f(\eta,\xi)}{\partial \eta}$$

or

$$\frac{\partial U}{\partial x} = f \frac{\partial U_s}{\partial x} + \frac{U_s}{L} \frac{\partial f}{\partial \xi} - \frac{U_s}{x} \eta f' \tag{E10}$$

where: $f' = \dfrac{\partial f(\eta,\xi)}{\partial \eta}$

and it is understood that $f = f(\eta,\xi)$.

$$\frac{\partial U}{\partial r} = U_s \frac{\partial f(\eta,\xi)}{\partial \eta} \frac{\partial \eta}{\partial r} = \frac{U_s}{x} f' \quad . \tag{E11}$$

The continuity equation E5 is used to obtain a relation for V in terms of U. Equation E5 may be written as

$$rv = - \int_o^\eta \frac{\partial U}{\partial x} r dr = - x^2 \int_o^\eta \frac{\partial U}{\partial x} \eta d\eta$$

$$= - x^2 [\int_o^\eta \frac{\partial U_s}{\partial x} f\eta d\eta + \frac{U_s}{L} \int_o^\eta \frac{\partial f}{\partial \xi} \eta d\eta - \frac{U_s}{x} \int_o^\eta \eta^2 f' d\eta] . \quad E12$$

The extreme term on the r.h. side of the above equation may be integrated by parts to provide

$$\int_o^\eta \eta^2 f' d\eta = \eta^2 f - 2 \int_o^\eta f\eta d\eta$$

which is substituted into E12 to obtain

$$V = - \frac{x}{\eta} [(\frac{2U_s}{x} + \frac{\partial U_s}{\partial x}) \int_o^\eta f\eta d\eta - \frac{U_s}{x} \eta^2 f + \frac{U_s}{L} \int_o^\eta \frac{\partial f}{\partial \xi} \eta d\eta]. \quad E13$$

An eddy viscosity for this flow is defined by the relation

$$-\overline{uv} = \nu_e \frac{\partial U}{\partial r} = \frac{\nu_e U_s}{x} f' . \quad E14$$

Substitution of relation E14 into the Reynolds stress term of equation E3 yields

$$\frac{1}{r} \frac{\partial}{\partial r} (-\overline{ruv}) = \frac{U_s^2}{R_T x} \frac{(\eta f')'}{\eta} . \quad E15$$

If the various derivative relations in the η, ξ coordinate system are substituted into equation E3, the momentum equation becomes

$$f^2 + \frac{f'}{\eta} \int_o^\eta f\eta d\eta + \frac{1}{R_T} \frac{(\eta f')'}{\eta} = -\xi^2 t$$

$$+ \xi [f \frac{\partial f}{\partial \xi} - \frac{f'}{\eta} \int_o^\eta \frac{\partial f}{\partial \xi} \eta d\eta]. \quad E16$$

Equation E16 is a dimensionless momentum equation in two length scales η and ξ.

The relations E8 and E9 are used with the energy equation E4 to develop the following:

$$\frac{\partial \Delta T}{\partial x} = \frac{\partial T_s}{\partial x} t(\eta,\xi) + T_s \frac{\partial t(\eta,\xi)}{\partial \eta} \frac{\partial \eta}{\partial x} + T_s \frac{\partial t(\eta,\xi)}{\partial \xi} \frac{\partial \xi}{\partial x}$$

letting

$$\frac{\partial t(\eta,\xi)}{\partial \eta} = t' \qquad \frac{\partial t(\eta,\xi)}{\partial \xi} = \frac{\partial t}{\partial \xi}$$

then

$$\frac{\partial \Delta T}{\partial x} = t \frac{\partial T_s}{\partial x} - \frac{T_s}{x} \eta t' + \frac{T_s}{L} \frac{\partial t}{\partial \xi} \qquad \text{E17}$$

$$\frac{\partial \Delta T}{\partial r} = T_s \frac{\partial t}{\partial \eta} \frac{\partial \eta}{\partial r} = \frac{T_s}{x} t' \ . \qquad \text{E18}$$

Defining an eddy diffusivity of the form

$$-\overline{v\theta} = \alpha_e \frac{\partial \Delta T}{\partial r} = \alpha_e \frac{T_s}{x} t'$$

it follows that

$$\frac{1}{r} \frac{\partial}{\partial r} (-\overline{rv\theta}) = \frac{1}{P_T R_T} \frac{U_s T_s}{x} \frac{(\eta t')'}{\eta} \ . \qquad \text{E19}$$

Substituting the above derivative relations into equation E4 yields

$$tf + \frac{t'}{\eta} \int_o^\eta f\eta d\eta + \frac{1}{p_T R_T} \frac{(\eta t')'}{\eta} = \xi [f \frac{\partial t}{\partial \xi} - \frac{t'}{\eta} \int_o^\eta \frac{\partial f}{\partial \eta} \eta d\eta]. \qquad \text{E20}$$

If the momentum equation E3 is integrated over the limits of 0 to ∞, the resulting integral constraint is given by

$$\frac{d}{dx}\int_o^\infty U^2 r dr = \int_o^\infty gB\Delta T r dr$$

and in dimensionless parameters the above becomes

$$\frac{d}{d\xi}\int_o^\infty f^2(\eta,\xi)\eta d\eta = \xi\int_o^\infty t(\eta,\xi)\eta d\eta \ . \qquad \text{E21}$$

The energy integral constraint for this flow assumes the form

$$2\pi\int_o^\infty t(\eta,\xi)f(\eta,\xi)\eta d\eta = 1. \qquad \text{E22}$$

In addition to the integral constraints the boundary conditions for equations E16 and E20 are

$$\frac{\partial f(0,\xi)}{\partial\eta} = \frac{\partial t(0,\xi)}{\partial\eta} = 0$$

$$\frac{\partial f(\infty,\xi)}{\partial\eta} = \frac{\partial t(\infty,\xi)}{\partial\eta} = 0$$

$$f(\infty,\xi) = t(\infty,\xi) = 0. \qquad \text{E23}$$

APPENDIX F

BUOYANT JET PERTURBATION EQUATIONS

The buoyant jet equations will be expanded in powers of the dimensionless length ξ to obtain a set of perturbation equations. Unfortunately, this expansion results in two additional unknown coefficients for each order in ξ. The number of equations are reduced by assuming a trivial solution for the equations for odd order in ξ and a set of equations are presented for an eddy viscosity independent of ξ.

The buoyant jet equations developed in Appendix E are

$$f^2 + \frac{f'}{\eta}\int_o^\eta f\eta d\eta + \frac{1}{R_T}\frac{(\eta f')'}{\eta} = -\xi^2 t + \xi\left[f\frac{\partial f}{\partial \xi} - \frac{f'}{\eta}\int_o^\eta \frac{\partial f}{\partial \xi}\eta d\eta\right] \qquad \text{E16}$$

$$tf + \frac{t'}{\eta}\int_o^\eta f\eta d\eta + \frac{1}{P_T R_T}\frac{(\eta t')'}{\eta} = \xi\left[f\frac{\partial t}{\partial \xi} - \frac{t'}{\eta}\int_o^\eta \frac{\partial f}{\partial \xi}\eta d\eta\right] \qquad \text{E20}$$

$$\frac{d}{d\xi}\int_o^\infty f^2\eta d\eta = \xi\int_o^\infty t\eta d\eta \qquad \text{E21}$$

$$2\pi\int_o^\infty f\cdot t\eta d\eta = 1 \qquad \text{E22}$$

where: $f = f(\eta,\xi)$; $f' = \dfrac{\partial f(\eta,\xi)}{\partial \xi}$

$t = t(\eta,\xi)$; $t' = \dfrac{\partial t(\eta,\xi)}{\partial \xi}$

$\lambda = 1/R_T$.

Assuming P_T is constant and the velocity, temperature, and eddy viscosity functions are expanded in terms of η and ξ as follows:

$$f(\eta,\xi) = f_j(\eta) + \xi f_{j1}(\eta) + \xi^2 f_{j2}(\eta) + \xi^3 f_{j3}(\eta) + \cdots$$

$$t(\eta,\xi) = t_j(\eta) + \xi t_{j1}(\eta) + \xi^2 t_{j2}(\eta) + \xi^3 t_{j3}(\eta) + \cdots \qquad \text{F1}$$

$$\eta_e(\xi) = \frac{1}{R_T}\,(1 + \xi\nu_1 + \xi^2\nu_2 + \xi^3\nu_3 + \cdots)$$

$$\alpha_e(\xi) = \frac{1}{P_T R_T}\,(1 + \xi\alpha_1 + \xi^2\alpha_2 + \xi^3\alpha_3 + \cdots)\ .$$

The momentum integral constraint, equation E21, is written in terms of the expansions F1 to obtain the following

$$\frac{d}{d\xi}\int_o^\infty [f_j^{\,2} + 2\xi f_j f_{j1} + \xi^2(2f_j f_{j2} + f_{j1}^{\,2}) + 2\xi^3(f_j f_{j3} + f_{j1} f_{j2})$$

$$+ \xi^4(2f_j f_{j4} + f_{j2}^{\,2} + 2f_{j1} f_{j3}) + \cdots]\eta d\eta$$

$$= \xi\int_o^\infty [t_j + \xi t_{j1} + \xi^2 t_{j2} + \xi^3 t_{j3} + \xi^4 t_{j4} + \cdots]\eta d\eta\ . \qquad \text{F2}$$

For the above relation to be valid terms of the same order in ξ must satisfy the equality. This requirement gives the following relations

order ξ^{-1}:

$$2\pi\int_o^\infty f_j^{\,2}\eta d\eta = 1 \qquad \text{F3}$$

order 1:

$$\int_o^\infty f_j f_{j1}\eta d\eta = 0 \qquad \text{F4}$$

order ξ:

$$2\int_o^\infty (2f_j f_{j2} + f_{j1}^{\,2})\eta d\eta = \int_o^\infty t_j\eta d\eta \qquad \text{F5}$$

order ξ^2:

$$6\int_o^\infty (f_j f_{j3} + f_{j1} f_{j2})\eta d\eta = \int_o^\infty t_{j1}\eta d\eta \qquad \text{F6}$$

order ξ^3:

$$4\int_o^\infty (2f_j f_{j4}+f_{j2}^2+2f_{j1}f_{j3})\eta d\eta = \int_o^\infty t_{j2}\eta d\eta \qquad \text{F7}$$

order ξ^4:

$$10\int_o^\infty (f_j f_{j5}+f_{j1}f_{j4}+f_{j2}f_{j3})\eta d\eta = \int_o^\infty t_{j3}\eta d\eta \ . \qquad \text{F8}$$

Expanding the energy integral constraint E22 in a similar manner the following relations are obtained:

order 1:

$$2\pi \int_o^\infty f_j t_j \eta d\eta = 1 \qquad \text{F9}$$

order ξ^1:

$$\int_o^\infty (f_j t_{j1}+f_{j1}t_j)\eta d\eta = 0 \qquad \text{F10}$$

order ξ^2:

$$\int_o^\infty (f_j t_{j2}+f_{j1}t_{j1}+f_{j2}t_j)\eta d\eta = 0 \qquad \text{F11}$$

order ξ^3:

$$\int_o^\infty (f_j t_{j3}+f_{j1}t_{j2}+f_{j2}t_{j1}+f_{j3}t_j)\eta d\eta = 0 \qquad \text{F12}$$

order ξ^4:

$$\int_o^\infty (f_j t_{j4}+f_{j1}t_{j3}+f_{j2}t_{j2}+f_{j3}t_{j1}+f_{j4}t_j)\eta d\eta = 0 \ . \qquad \text{F13}$$

Equations F3 through F13 are the momentum and energy integral constraints for velocity and temperature equations to be developed in this perturbation analysis.

If the various terms of equation E16 are expanded in terms of the relations given by F1, the following expansions are obtained:

$$f^2 = f_j^2 + \xi f_j f_{j1} + \xi^2(2f_j f_{j2}+f_{j1}^2) + \xi^3(2f_j f_{j3}+2f_{j1}f_{j2}) +\cdots$$

$$\frac{f'}{\eta}\int_o^\eta f\eta d\eta = \frac{f_j'}{\eta}\int_o^\eta f_j\eta d\eta + \xi\left(\frac{f_j'}{\eta}\int_o^\eta f_{j1}\eta d\eta + \frac{f_{j1}'}{\eta}\int_o^\eta f_j\eta d\eta\right)$$

$$+ \xi^2\left(\frac{f_j'}{\eta}\int_o^\eta f_{j2}\eta d\eta + \frac{f_{j1}'}{\eta}\int_o^\eta f_{j1}\eta d\eta + \frac{f_{j2}'}{\eta}\int_o^\eta f_j\eta d\eta\right)$$

$$+ \xi^3\left(\frac{f_j'}{\eta}\int_o^\eta f_{j3}\eta d\eta + \frac{f_{j1}'}{\eta}\int_o^\eta f_{j2}\eta d\eta + \frac{f_{j2}'}{\eta}\int_o^\eta f_{j1}\eta d\eta\right.$$

$$\left. + \frac{f_{j3}'}{\eta}\int_o^\eta f_j\eta d\eta\right) +\cdots$$

$$\frac{1}{R_T}\frac{(\eta f')'}{\eta} = \frac{1}{R_T\eta}\left[(\eta f_j')' + \xi[\nu_1(\eta f_j')' + (\eta f_{j1}')']\right.$$

$$+ \frac{\xi^2}{R_T}\left[\nu_2(\eta f_j')' + \nu_1(\eta f_{j1}')' + (\eta f_{j2}')'\right]$$

$$+ \frac{\xi^2}{R_T}\left[\nu_3(\eta f_j')' + \nu_2(\eta f_{j1}')' + \nu_1(\eta f_{j2}')' + (\eta f_{j3}')' +\cdots\right]$$

$$- \xi^2 t = \xi^2 t_j + \xi^3 t_{j1} + \xi^4 t_{j2} +\cdots$$

$$\xi\, f\frac{\partial f}{\partial \xi} = \xi f_j f_{j1} + \xi^2(2f_j f_{j2}+f_{j1}^2) + \xi^3(3f_j f_{j3}+3f_{j1}f_{j2}) +\cdots$$

$$- \frac{f'}{\eta}\int_o^\eta \frac{\partial f}{\partial \xi}\eta d\eta = \frac{f_j'}{\eta}\int_o^\eta f_{j1}\eta d\eta + \xi^2\left(2\frac{f_j'}{\eta}\int_o^\eta f_{j2}\eta d\eta\right.$$

$$\left. + \frac{f_{j1}'}{\eta}\int_o^\eta f_{j1}\eta d\eta\right) + \xi^3\left(3\frac{f_j'}{\eta}\int_o^\eta f_{j3}\eta d\eta\right.$$

$$+ 2\frac{f_{j1}'}{\eta}\int_o^\eta f_{j2}\eta d\eta + \frac{f_{j2}'}{\eta}\int_o^\eta f_{j1}\eta d\eta) + \cdots \quad .$$

The various terms of equation E20 are expanded also to obtain

$$t\,f = t_j f_j + \xi(t_j f_{j1}+t_{j1}f_j) + \xi^2(t_j f_{j2}+t_{j1}f_{j1} + t_{j2}f_j)$$

$$+ \xi^3(t_j f_{j3}+t_{j1}f_{j2}+t_{j2}f_{j1}+t_{j3}f_j) + \cdots$$

$$\frac{t'}{\eta}\int_o^\eta f\eta d\eta = \frac{t_j'}{\eta}\int_o^\eta f_j\eta d\eta + \xi(\frac{t_j'}{\eta}\int_o^\eta f_{j1}\eta d\eta$$

$$+ \frac{t_{j1}'}{\eta}\int_o^\eta f_j\eta d\eta) + \xi^2(\frac{t_j'}{\eta}\int_o^\eta f_{j2}\eta d\eta + \frac{t_{j1}'}{\eta}\int_o^\eta f_j\eta d\eta$$

$$+ \frac{t_{j2}'}{\eta}\int_o^\eta f_j\eta d\eta) + \xi^3(\frac{t_j'}{\eta}\int_o^\eta f_{j3}\eta d\eta + \frac{t_{j1}'}{\eta}\int_o^\eta f_{j2}\eta d\eta$$

$$+ \frac{t_{j2}'}{\eta}\int_o^\eta f_{j1}\eta d\eta + \frac{t_{j3}'}{\eta}\int_o^\eta f_j\eta d\eta) + \cdots$$

$$\frac{1}{P_T R_T}\frac{(\eta t')'}{\eta} = \frac{1}{P_T R_T \eta}[(\eta t_j')'+\xi[\nu_1(\eta t_j')'+(\eta t_{j1}')']$$

$$+ \xi^2[\nu_2(\eta t_j')'+\nu_1(\xi t_{j1}')'+(\eta t_{j2}')'] + \cdots$$

$$\xi f\frac{\partial t}{\partial \xi} = \xi f_j t_{j1} + \xi^2(2f_j t_{j2}+f_{j1}t_{j1}) + \xi^3(3f_j t_{j3}+2f_{j1}t_{j2}+f_{j2}t_{j1}) + \cdots$$

$$- \xi\frac{t'}{\eta}\int_o^\eta \frac{\partial f}{\partial \xi}\eta d\eta = - \xi\frac{t_j'}{\eta}\int_o^\eta f_{j1}\eta d\eta - \xi^2(2\frac{t_j'}{\eta}\int_o^\eta f_{j2}\eta d\eta$$

$$+ \frac{t_{j1}'}{\eta}\int_o^\eta f_{j1}\eta d\eta) - \xi^3(3\frac{t_j'}{\eta}\int_o^\eta f_{j3}\eta d\eta + 2\frac{t_{j1}'}{\eta}\int_o^\eta f_{j2}\eta d\eta$$

$$+ \frac{t_{j2}'}{\eta}\int_o^\eta f_{j1}\eta d\eta) + \cdots \quad .$$

If these expansions are substituted into equations E16, E20, E21, and E22, equating like powers of ξ yield the following sets of equations:

order 1:

$$f_j^2 + \frac{f_j'}{\eta}\int_o^\eta f_j \eta d\eta + \frac{1}{R_T}\frac{(\eta f_j')'}{\eta} = 0$$

$$f_j t_j + \frac{t_j'}{\eta}\int_o^\eta f_j \eta d\eta + \frac{1}{P_T R_T}\frac{(\eta t_j')'}{\eta} = 0$$

$$2\pi \int_o^\infty f_j \eta d\eta = 1$$

$$2\pi \int_o^\infty t_j f_j \eta d\eta = 1 \ , \qquad \text{F13}$$

order ξ:

$$f_j f_{j1} + \frac{f_{j1}'}{\eta}\int_o^\eta f_j \eta d\eta + 2\frac{f_j'}{\eta}\int_o^\eta f_{j1}\eta d\eta + \frac{1}{R_T}\frac{(\eta f_{j1}')'}{\eta} = -\frac{\nu_1}{R_T}\frac{(\eta f_j')'}{\eta}$$

order ξ^1:

$$f_{j1} t_j + \frac{t_{j1}'}{\eta}\int_o^\eta f_j \eta d\eta + 2\frac{t_j'}{\eta}\int_o^\eta f_{j1}\eta d\eta + \frac{1}{P_T R_T}\frac{(\eta t_{j1}')'}{\eta} =$$

$$= -\frac{\alpha}{P_T R_T}\frac{(\eta t_j')'}{\eta} \qquad \text{F14}$$

$$\int_o^\infty f_j f_{j1} \eta d\eta = 0$$

$$\int_o^\infty (f_j t_{j1} + f_{j1} t_j)\eta d\eta = 0,$$

order ξ^2:

$$3\frac{f_j'}{\eta}\int_o^\eta f_{j2}\eta d\eta + \frac{f_{j2}}{\eta}\int_o^\eta f_j\eta d\eta + \frac{1}{R_T}\frac{(\eta f_{j2}')'}{\eta}$$

$$= - t_j - 2\frac{f_{j2}'}{\eta}\int_o^\eta f_{j1}\eta d\eta - \frac{\nu_1}{R_T}\frac{(\eta f_{j1}')'}{\eta} - \frac{\nu_2}{R_T}\frac{(\eta f_j')'}{\eta}$$

$$- f_j t_{j2} + f_{j2} t_j + 3\frac{t_j'}{\eta}\int_o^\eta f_{j2}\eta d\eta + \frac{t_{j2}'}{\eta}\int_o^\eta f_j\eta d\eta$$

$$+ \frac{1}{P_T R_T}\frac{(\eta t_{j2}')'}{\eta} = - 2\frac{t_{j1}'}{\eta}\int_o^\eta f_{j1}\eta d\eta - \frac{\alpha_1}{P_T R_T}\frac{(\eta t_{j1}')'}{\eta}$$

$$- \frac{\alpha_2}{P_T R_T}\frac{(\eta t_j')'}{\eta} \qquad \text{F15}$$

$$2\int_o^\infty (2f_j f_{j2} + f_{j1}^2)\eta d\eta = \int_o^\infty t_j \eta d\eta$$

$$\int_o^\infty (f_j t_{j2} + f_{j1} t_{j1} + f_{j2} t_j)\eta d\eta = 0 .$$

The boundary conditions for equations F13 through F15 are

$$f_j' = f_{j1}' = f_{j2}' = t_j' = t_{j1}' = t_{j2}' = 0 \quad \text{for } \eta = 0$$

$$f_j = f_{j1} = f_{j2} = t_j = t_{j1} = t_{j2} = 0 \quad \text{for } \eta \to \infty$$

$$f_j' = f_{j1}' = f_{j2}' = t_j' = t_{j1}' = t_{j2}' = 0 \quad \text{for } \eta \to \infty.$$

If the odd coefficients of the eddy viscosity and eddy diffusivity expansion are set equal to zero the solutions to the equations for odd powers of ξ are identically zero and homogeneous. Consequently, both

the odd order equations and the integral constraints are satisfied by the trivial solutions. For this case the perturbation equations to fourth order in ξ are:

order 1:

$$f_j^{\,2} + \frac{f_j'}{\eta}\int_o^\eta f_j \eta d\eta + \frac{1}{R_T}\frac{(\eta f_j')'}{\eta} = 0$$

$$f_j t_j + \frac{t_j'}{\eta}\int_o^\eta f_j \eta d\eta + \frac{1}{P_T R_T}\frac{(\eta t_j')'}{\eta} = 0 \qquad \text{F16}$$

order 1:

$$2\pi \int_o^\infty f_j^{\,2} \eta d\eta = 1$$

$$2\pi \int_o^\infty f_j t_j \eta d\eta = 1$$

order ξ^2:

$$3\frac{f_j'}{\eta}\int_o^\eta f_{j2}\eta d\eta + \frac{f_{j2}'}{\eta}\int_o^\eta f_j \eta d\eta + \frac{1}{R_T}\frac{(\eta f_{j2}')'}{\eta}$$

$$= - t_j - \frac{\nu_2}{R_T}\frac{(\eta f_j')'}{\eta}$$

$$- f_j t_{j2} + f_{j2} t_j + 3\frac{t_j'}{\eta}\int_o^\eta f_{j2}\eta d\eta + \frac{t_{j2}'}{\eta}\int_o^\eta f_j \eta d\eta$$

$$+ \frac{1}{P_T R_T}\frac{(\eta t_{j2}')'}{\eta} = - \frac{\alpha_2}{P_T R_T}\frac{(\eta t_j')'}{\eta} \qquad \text{F16}$$

$$4\int_o^\infty f_j f_{j2}\eta d\eta = \int_o^\infty t_j \eta d\eta$$

$$\int_o^\infty (f_j t_{j2} + f_{j2} t_j)\eta d\eta = 0 \quad .$$

order ξ^4:

$$-2f_j f_{j4} + \frac{f_{j4}'}{\eta}\int_o^\eta f_j \eta d\eta + 5\frac{f_j'}{\eta}\int_o^\eta f_{j4}\eta d\eta$$

$$+\frac{1}{R_T}\frac{(\eta f_{j4}')'}{\eta} = -t_{j2} + f_{j2}^2 - 3\frac{f_{j2}'}{\eta}\int_o^\eta f_{j2}\eta d\eta$$

$$-\frac{\nu_2}{\eta}\frac{(\eta f_{j2}')'}{\eta} - \frac{\nu_4}{R_T}\frac{(\eta f_j')'}{\eta}$$

$$-3f_j t_{j4} + \frac{t_{j4}'}{\eta}\int_o^\eta f_j \eta d\eta + \frac{1}{P_T R_T}\frac{(\eta t_{j4}')'}{\eta}$$

$$= f_{j2}t_{j2} - f_{j4}t_j - 5\frac{t_j'}{\eta}\int_o^\eta f_{j4}\eta d\eta - 3\frac{t_{j2}'}{\eta}\int_o^\eta f_{j2}\eta d\eta$$

$$-\frac{\alpha_2}{P_T R_T}\frac{(\eta t_{j2}')'}{\eta} - \frac{\alpha_4}{P_T R_T}\frac{(\eta t_j')'}{\eta} \qquad \text{F17}$$

$$4\int_o^\infty (2f_j f_{j4} + f_{j2}^2)\eta d\eta = \int_o^\infty t_{j2}\eta d\eta$$

$$\int_o^\infty (t_j f_{j4} + t_{j2}f_{j2} + t_{j4}f_j)\eta d\eta = 0.$$

The boundary conditions for equations F16 through F17 are

$$f_j' = f_{j2}' = f_{j4}' = t_j' = t_{j2}' = t_{j4}' = 0 \qquad \text{for } \eta = 0$$

$$f_j = f_{j2} = f_{j4} = t_j = t_{j2} = t_{j4} = 0 \qquad \text{for } \eta \to \infty$$

$$f_j' = f_{j2}' = f_{j4}' = t_j' = t_{j2}' = t_{j4}' = 0 \qquad \text{for } \eta \to \infty \quad .$$

APPENDIX G

ANALYTICAL SOLUTION FOR BUOYANT JET

The analytical eddy viscosity solutions for the jet and plume give the following relations for the mean profiles.

$$f_j(\eta) = 2A_jB_j\lambda_j(1+A_j\eta^2)^{-2}$$

$$t_j(\eta) = C_j\lambda_j{}^2(1+A_j\eta^2)^{-2\sigma}$$

$$f_p(\eta) = 2A_pB_p\lambda_p(1+A_p\eta^2)^{-2}$$

$$t_p(\eta) = C_p\lambda_p{}^2(1+A_p\eta^2)^{-4} \qquad \text{G1}$$

where the plume solution is that obtained by Yih for a Prandtl number of 2.0, and the jet solution is applicable for all Prandtl numbers. For a Prandtl number of 2.0, the jet and plume velocity and temperature profiles have the same dependence on η, $(1+A\eta^2)^{-2}$ and $(1+A\eta^2)^{-4}$ respectively. Although the A's are not the same for the jet and plume, analytical solutions can be developed for the perturbation equations.

For this development it is assumed that α_1, α_3,... and ν_1, ν_3,... are zero and the even values are simply related to R_T. The dimensionless momentum and temperature equations, E16 and E20 respectively may be written in the form:

$$\lambda f'' + [\lambda + \int_o^\eta f\eta d\eta]\frac{f'}{\eta} + f^2 + \xi[\frac{f'}{\eta}\int_o^\eta \frac{\partial f}{\partial \xi}\eta d\eta - f\frac{\partial f}{\partial \xi}]$$

$$+ \xi^2 t = 0 \qquad \text{G2}$$

$$\frac{\lambda}{\sigma}t'' + [\frac{\lambda}{\sigma} + \int_o^\eta f\eta d\eta]\frac{t'}{\eta} + ft + \xi[\frac{t'}{\eta}\int_o^\eta \frac{\partial f}{\partial \xi}\eta d\eta - f\frac{\partial t}{\partial \xi}] = 0 \qquad \text{G3}$$

where:

$$\lambda = 1/R_T \qquad \sigma = P_T$$

$$f = f(\eta,\xi) \qquad t = t(\eta,\xi)$$

$$f' = \frac{\partial f(\eta,\xi)}{\partial \eta} \qquad t' = \frac{\partial t(\eta,\xi)}{\partial \eta}$$

$$f'' = \frac{\partial^2 f(\eta,\xi)}{\partial^2 \eta} \qquad t'' = \frac{\partial^2 t(\eta,\xi)}{\partial \eta^2}$$

and the integral constraints are given by

$$\frac{d}{d\xi}\int_o^\infty f^2 \eta d\eta = \xi \int_o^\infty t\eta d\eta \qquad \text{E21}$$

$$2\pi \int_o^\infty f t \eta d\eta = 1 \quad . \qquad \text{E22}$$

Assuming a separation of variables solution of the form

$$f(\eta,\xi) = \phi(\eta)F(\xi) \qquad \phi(\eta) = (1+A\eta^2)^{-2}$$

$$t(\eta,\xi) = \phi^2(\eta)T(\xi) \qquad \phi^2(\eta) = (1+A\eta^2)^{-4}$$

$$F(\xi) = B_o + B_2\xi^2 + B_4\xi^4 + \cdots$$

$$T(\xi) = C_o + C_2\xi^2 + C_4\xi^4 + \cdots$$

$$\lambda(\xi) = \lambda_o + \lambda_2\xi^2 + \lambda_4\xi^4 + \cdots$$

the integral constraints become

$$\frac{d}{d\xi}\int_o^\infty F^2(\xi)\phi^2(\eta)\eta d\eta = \xi \int_o^\infty T(\xi)\phi^2(\eta)\eta d\eta \qquad \text{G5}$$

$$2\pi \int_o^\infty T(\xi)F(\xi)\phi^3(\eta)\eta d\eta = 1 \quad . \qquad \text{G6}$$

Substituting the assumed expansions for $F(\xi)$, $T(\xi)$, and $\phi(\eta)$ into the integral constraints and equating the various orders of ξ yields

$$A = \pi B_o^2/3 \qquad C_o = 5A/\pi B_o$$

$$B_2 = C_o/4B_o \qquad C_2 = -C_o B_2/B_o$$

$$B_4 = (C_2 - 4B_2^2)/8B_o \qquad C_4 = -(C_o B_4 + C_2 B_2)/B_o$$

$$B_6 = (C_4 - 12B_2 B_4)/12B_o \; . \qquad \text{G7}$$

If the assumed functional relations for $f(\eta,\xi)$ and $t(\eta,\xi)$ are substituted in equations G2 and G3, the dimensionless momentum and temperature are respectively

Momentum:

$$\lambda F\phi'' + [\lambda F + F^2 \int_o^\eta \phi\eta d\eta] \frac{\phi^1}{\eta} + F^2\phi^2$$

$$+ \xi[FF' \frac{\phi'}{\eta} \int_o^\eta \phi\eta d\eta - FF'\phi^2] + \xi^2 T\phi^2 = 0 \qquad \text{G8}$$

Temperature:

$$\frac{\lambda}{\sigma} T\phi^{2}'' + [\frac{\lambda}{\sigma} T + FT\int_o^\infty \phi\eta d\eta] \frac{\phi^{2}'}{\eta} + FT\phi^3$$

$$+ \xi[F'T \frac{\phi^{2}'}{\eta} \int_o^\eta \phi\eta d\eta - FT'\phi^3] = 0 \; . \qquad \text{G9}$$

Using the definition of ϕ it is easily shown that

$$\phi'' = -4A\phi^{-3/2} + 24A^2\eta^2\phi^{-2}$$

$$\frac{\phi'}{\eta} = -4A\phi^{-3/2}$$

$$\frac{\phi'}{\eta} \int_o^\eta \phi\eta d\eta = +2(\phi^2 - \phi^{-3/2})$$

$$\phi^{2}{}'' = - 8A\phi^{-5/2} + 80A^{2}\eta^{2}\phi^{-3}$$

$$\frac{\phi^{2}{}'}{\eta} = - 8A\phi^{-5/2}$$

$$\frac{\phi^{2}{}'}{\eta} \int_{o}^{\eta} \phi\eta d\eta = + 4(\phi^{3}-\phi^{-5/2})$$

and substituting these results into equations G8 and G9 yields:

Momentum:

$$\lambda F(24A\eta^{2}-8A\phi^{1/2}) + 2F^{2}(1-\phi^{1/2}) + F^{2}$$

$$+ \xi FF'-2\xi FF^{1}\phi^{1/2}+\xi^{2}T = 0 \qquad \text{G10}$$

Temperature:

$$\frac{\lambda}{\sigma} T(80A^{2}\eta^{2}-16A\phi^{1/2}) + 4FT(1-\phi^{1/2}) + FT$$

$$+ 4\xi F'T-4\xi F'T\phi^{1/2}-\xi FT' = 0 \ . \qquad \text{G11}$$

If the assumed expansions for $F(\xi)$, $T(\xi)$, and $\lambda(\xi)$ are substituted into equation G10 and terms to the same order in ξ are equated, the following results are obtained:

order 1:

$$16A^{2}\lambda_{o}\eta^{2}-2AB_{o}\eta^{2}-8A\lambda_{o}+B_{o} = 0 \qquad \text{G12}$$

order ξ^{2}:

$$(\lambda_{o}B_{2}+\lambda_{2}B_{o})(16A^{2}\eta^{2}-8A) - 8AB_{o}B_{2}\eta^{2}+C_{o} = 0 \qquad \text{G13}$$

order ξ^4:

$$(\lambda_o B_4+\lambda_2 B_2+\lambda_4 B_o)(16A^2\eta^2-8A) - 6A\eta^2(2B_o B_4+B_2^2) - (2B_o B_4+B_2^2) + C_2 = 0 \qquad \text{G14}$$

The above equations are solved by equating terms of the same order in η. Using these results and the results imposed by the integral constraints, relations G7, the following values are obtained for the various constants:

$$A = 3/64\pi\lambda_o^2$$

$$B_o = 3/8\pi\lambda_o \qquad C_o = 5/8\pi\lambda_o$$

$$B_2 = 5/12 \qquad C_2 = -25/36$$

$$B_4 = 25\pi\lambda_o/54 \qquad C_4 = 125\pi\lambda_o/3^4$$

$$\lambda_2 = 10\pi\lambda_o^2/3 \qquad \lambda_4 = -500\pi^2\lambda_o^3/3^4 \quad .$$

Solving the temperature equation, G11, in the same manner as the momentum equation, G10, provides a check on the solutions presented above. Substituting the assumed expansions for $F(\xi)$, $T(\xi)$, and $\lambda(\xi)$ into equation G11 and equating terms of the same order in ξ provides the following relations:

order 1:

$$\lambda_o(32A^2\eta^2-8A) - 4AB_o\eta^2+B_o = 0 \qquad \text{G15}$$

order ξ^2:

$$(\lambda_o C_2+\lambda_2 C_o)(32A^2\eta^2-8A) - 4AB_oC_2\eta^2 - 12AB_2C_o\eta^2 - B_oC_2 + B_2C_o = 0 \qquad \text{G16}$$

order ξ^4:

$$(\lambda_o C_4+\lambda_2 C_2+\lambda_4 C_o)(32A^2\eta^2-8A) - 4(B_oC_4+B_2C_2+B_4C_o)A\eta^2 - 8(B_2C_2+2B_4C_o)A\eta^2$$

$$+ B_4C_o - B_2C_2 - 3B_oC_4 = 0 \quad . \qquad \text{G17}$$

The above set of equations is satisfied by the previously derived constants.

Substituting the coefficients into the functional relations for $f(\eta,\xi)$ and $t(\eta,\xi)$ provides the following results:

$$f(\eta,\xi) = (1+A\eta^2)^{-2}\left(\frac{3}{8\pi\lambda_o} + \xi^2\frac{5}{12} - \xi^4\frac{25\pi\lambda_o}{2.3^3} - \cdots\right)$$

$$t(\eta,\xi) = (1+A\eta^2)^{-4}\left(\frac{5}{8\pi\lambda_o} - \xi^2\frac{25}{36} + \xi^4\frac{125\pi\lambda_o}{3^4} - \cdots\right) .$$

The above series can be extended by using only the integral constraints to evaluate the coefficients for higher order terms in ξ. The values of B_6 and C_6 were obtained using the integral constraints. These values are given by

$$B_6 = \frac{125\pi\lambda_o^2}{3^6} \qquad C_6 = -\frac{6250\pi^2\lambda_o^2}{3^7} \quad .$$

Recall that the solutions presented here are valid only for a Prandtl number of 2.0.

VITA

Clifford Bruce Baker was born to Dave Clifford and Elsie Maria Baker in Clinchco, Virginia, on January 6, 1930. In 1948 he was graduated from Hamilton High School, Mendota, Virginia. He received a Bachelor of Science degree with a major in Mechanical Engineering from Virginia Polytechnic Institute in 1958 and a Master of Science degree from the University of Maryland with a major in Mechanical Engineering in 1964.

He has held various positions with several research and development laboratories. These include Research Associate with The Johns Hopkins University Applied Physics Laboratory in Laurel, Maryland; Research Engineer with the Cummins Engine Company in Columbus, Indiana; and Research Assistant with The Pennsylvania State University Applied Research Laboratory. Presently he is employed as an Assistant Professor with the University of Pittsburgh at Johnstown, in the Engineering Technology Division.

During his professional career he has worked and published papers in the areas of subsonic, supersonic and hypersonic flow, hydrodynamics, cavitation, turbulence, thermodynamics, and instrumentation.

He is an associate member of Sigma Xi and Pi Tau Sigma.